Ethereal oxygen effects on structure and reactivity
by David Kent Johnson

A thesis submitted in partial fulfillment of the requirements for the degree Doctor of Philosophy in Chemistry
Montana State University
© Copyright by David Kent Johnson (1988)

Abstract:
The role the oxygen atom plays in influencing the stereochemistry of electrophilic additions to cis-8-oxabicyclo[4.3.0]non-3-ene, [1] and 8- oxatricylo[4.3.3.0]undec-3-ene, [7], was examined. A complete absence of stereoselectivity was observed in [7], This was consistent with calculations completed on the olefin that suggest: (1) there are two boat conformers existing for the alkene in approximate equilibrium abundances, (2) the conformers have HOMOs of equal energy and as a. result should have equal reactivity, and (3) there is no contribution by the oxygen atom in the HOMOs of either conformer which could possibly have directed the addition. The modest stereoselectivity observed in [1] was attributed to simple steric effects.

The role of the oxygen atom in imparting reactivity during solvolysis on the syn- and anti-tosylates derived from [1] and [7] was examined. Identical reactivities and products were observed in the solvolysis of the syn and anti-tosylates of [1]. This was interpreted to mean oxygen does not influence reactivity in these compounds. A slight rate enhancement (1.53) was observed for the anti tosylate of [7] relative to the syn-isomer. A stabilized hydrogen bonded intimate ion pair (IIP) was used to rationalize this increased reactivity.

The role of the oxygen atom to influence the stereochemistry of catalytic hydrogenation in 3-methyl-8-oxabicylo[4.3.3.0]undec-3-ene, [35], was studied and modest stereoselectivity was observed (3:1). This is suggestive of an oxygen/catalysts interaction (haptophilicty).

The olefins resulting from the palladium induced bond isomerization of [1] were characterized and examined by the MM2 and MNDO methods. These olefins were found to exhibit increasing thermodynamic stability as measured by heats of formation and hyperstability. This stability was used to rationalize the bond isomerization on the basis of the Polanyi mechanism. A correlation between hyperstability and HOMO n bond order was observed in this system.

The major ions in the EI mass spectrum of [1] were determined from an examination of the mass spectra of a series of deuterium labelled analogues of [1] which were prepared. Fragmentation mechanisms were proposed for the formation of these ions.

ETHEREAL OXYGEN EFFECTS ON STRUCTURE AND REACTIVITY

by

David Kent Johnson

A thesis submitted in partial fulfillment
of the requirements for the degree

of

Doctor of Philosophy

in

Chemistry

MONTANA STATE UNIVERSITY
Bozeman, Montana

May 1988

D378
J6307

APPROVAL

of a thesis submitted by

David Kent Johnson

This thesis has been read by each member of the thesis committee and has been found to be satisfactory regarding content, English usage, format, citations, bibliographic style, and consistency, and is ready for submission to the College of Graduate Studies.

May 31, 1988 — Date

Bradford P. Mundy — Chairperson, Graduate Committee

Approved for the Major Department

_____ — Date

Edwin H [illegible] — Head, Major Department

Approved for the College of Graduate Studies

June 1, 1988 — Date

Henry L Parsons — Graduate Dean

STATEMENT OF PERMISSION TO USE

In presenting this thesis in partial fulfillment of the requirements for a doctoral degree at Montana State University, I agree that the Library shall make it available to borrowers under rules of the Library. I further agree that copying of this thesis is allowable only for scholarly purposes, consistent with "fair use" as prescribed in the U.S. Copyright Law. Requests for extensive copying or reproduction of this thesis should be referred to University Microfilms International, 300 North Zeeb Road, Ann Arbor, Michigan 48106, to whom I have granted "the exclusive right to reproduce and distribute copies of the dissertation in and from microfilm and the right to reproduce and distribute by abstract in any format."

Signature David Kent Johnson

Date 5/20/1988

To my mom and dad for their constant love and support.

"The real cycle you're working on
is a cycle called 'yourself'."

"The study of the art of motorcycle maintenance [or chemistry] is really a miniature study of the art of rationality itself. Working on a motorcycle [or in chemistry], working well, caring, is to become part of a process, to achieve an inner peace of mind. The motorcycle [The chemistry] is primarily a mental phenomenon."

- Robert M. Pirsig
Zen and the Art of Motorcycle Maintenance

ACKNOWLEDGEMENTS

This endeavor could not have been completed without the help of a number of people. Special thanks are extended to Joe Sears, Dave Theiste, and Tim Schram for their unselfish assistance, respectively, on the mass spectrometer, the computer, and the NMR; to Ray Larson and Dr. Fitzgerald for their assistance with x-ray crystallography; and to Montana Interface and especially Dr. Howald for their assistance with our kinetic experiments. Special thanks is also extended to Dr. Craig for his helpful discussions on physical-organic chemistry and for the interest and enthusiasm he has shown in my career; and to Dr. Mundy for his integrity, his support of students, and for his deep devotion and love of chemistry that he has openly exhibited during my graduate years. Lastly my deepest appreciation is extended to my dear wife, Andrea, for her assistance with word processing and her everpresent love and companionship.

TABLE OF CONTENTS

LIST OF TABLES.....vii

LIST OF FIGURES.....ix

ABSTRACT.....xiv

1. INTRODUCTION.....1

Neighboring Group Participation by Oxygen.....1
Oxygen Effects on Hydrogenation.....12
Palladium Promoted Bond Isomerization in Cyclic Systems.....17
Scope and Goals of this Investigation.....19

2. RESULTS AND DISCUSSION.....21

Oxygen's Effect in Influencing Stereochemistry.....21
Oxygen's Effect in Influencing Reactivity.....37
A Search for an Oxygen/Catalyst Interaction.....56
An Examination of the Palladium Induced Bond Isomerization of cis-8-oxabicylo[4.3.0]non-3-ene.....59
An Examination of the Mass Spectrum of cis-8-oxabicyclo[4.3.0]non-3-ene.....69

3. CONCLUSIONS.....78

Summary of this Research.....78
Suggested Future Work.....80

4. EXPERIMENTAL.....82

REFERENCES.....129

LIST OF TABLES

Table		Page
1.	Solvolytic rate influences by oxygen and sulfur	2
2.	Relative rates of solvolysis of p-bromobenzenesulfonates in acetic acid at 50°C	3
3.	Acetolysis of arenesulfonates	6
4.	Oxygen's inductive effect on carbon-carbon bond participation	7
5.	Oxymercuration competition results	8
6.	Relative rates of catalytic hydrogenation	12
7.	Relative substrate/catalyst affinities	13
8.	Product studies on cis-8-oxabicyclo[4.3.0]non-3-ene	22
9.	Product studies on 8-oxatricyclo[4.3.3.0] undec-3-ene	22
10.	Ground state conformational energies for 8-oxabicyclo[4.3.0]non-3-ene, [1]	29
11.	Ground state conformational energies for 8-oxatricyclo[4.3.3.0]non-3-ene, [7]	30
12.	HOMO conformational energies of cis-8-oxabicyclo[4.3.0] non-3-ene	32
13.	HOMO conformational energies of 8-oxatricyclo[4.3.3.0]undec-3-ene	32
14.	Kinetic results of the 50% aqueous methanolysis of [19] and [31]	43
15.	Kinetic results of the 50% aqueous methanolysis of [24] and [32]	44
16.	Activation parameters of the 50% aqueous methanolysis of [19], [31], [24] and [32]	44
17.	Modelled bicyclic tosylate energies	48
18.	Calculated olefinic energies (Kcal/mole)	50

LIST OF TABLES - Continued

19. Modelled tricyclic tosylate stabilities (Kcal/mole).....53

20. Calculated carbocation stabilities (Kcal/mole).....54

21. MM2 calculated energies (Kcal/mole).....64

22. MNDO calculated heats of formation (Kcal/mole).....66

23. HOMO P_Z atomic orbital coefficients of olefinic carbons and HOMO π bond orders.....66

24. Atomic coordinates ($x10^4$) and isotropic thermal parameters ($A°x10^3$) of [19].....112

25. Bond lengths (A°) of [19].....113

26. Bond angles (°) of [19].....114

27. Atomic coordinates ($x10^4$) and isotropic thermal parameters ($A°x10^3$) for [24].....118

28. Bond lengths (A°) for [24].....119

29. Bond angles (°) of [24].....120

LIST OF FIGURES

Figure — Page

1. Heteroatom stabilization in a norobornyl system....3
2. Oxygen intermediate stabilization....4
3. Oxygen participation in endo-9-oxabicyclo[4.2.1]-2-yl-p-bromobenzenesulfonate....4
4. Oxygen participation in 2-ethoxybenzl-3-cyclohexyl-p-nitrobenzoate....5
5. Transannular dipole effect....6
6. Predicted conformation of cis-8-oxabicyclo [4.3.0]non-3-ene....9
7. Oxymercuration of cis-8-oxabicyclo[4.3.0]non-3-ene....9
8. Proposed oxygen participation in the oxymercuration of cis-8-oxabicyclo[4.3.0]non-3-ene....10
9. Steric bias in cis-8-oxabicyclo[4.3.0]non-3-ene....10
10. Absence of oxygen participation in 8-oxatricyclo [4.3.0]undec-3-ene....11
11. Complexation if cis-8-oxabicyclo[4.3.0]non-3-ene, [1], to platinum....14
12. Effect of tetrahydrofuran on the reduction of cyclohexene....14
13. Effect of cis-8-oxabicyclo[4.3.0]nonane on the reduction of cyclohexe....15
14. Haptophilicity involving the methoxy group....16
15. Haptophilicity involving the ester group....16
16. Stereospecific hydrogenation of 2-methylene-cis-1,5 dicarboxymethyl[4.3.0]octane....17
17. Palladium promoted bond isomerization in the methylcyclohexene system....18
18. Palladium induced bond isomerization of cis-8-oxabicyclo[4.3.0]non-3-ene....18

LIST OF FIGURES - continued

19. Synthesis of cis-8-oxabicyclo[4.3.0]non-3-ene, [1], and 8-oxatricyclo[4.3.3.0]undec-3-ene, [7].....21

20. Determination of the stereochemistry of the syn-alcohol of [1].....23

21. % enhancement of NOE experiment on syn-methoxy derivative of [1].....25

22. Determination of the stereochemistry of the syn-alcohol of [7].....26

23. Equilibrium conformations of 8-oxabicyclo[4.3.0]non-3-ene.....30

24. Equilibrium conformations of 8-oxatricyclo[4.3.3.0]undec-3-ene.....31

25. HOMO contour plots of 8-cis-bicyclo[4.3.0] non-3-ene.....34

26. HOMO contour polots of 8-oxatricyclo[4.3.3.0] undec-3-ene.....34

27. Does the oxygen atom influence reactivity in the solvolysis of these tosylates?.....38

28. Boat conformations of anti-isomers, [A] and [C].....38

29. Boat conformations of syn-isomers, [B] and [D].....38

30. Syntheses of syn-and anti-tosylates dervived from [1].....40

31. Syntheses of syn- and anti-tosylates derived from [7].....41

32. ORTEP drawings of the x-ray structures of [19] and [24].....42

33. Product studies of 50% aqueous methanolysis of [19].....45

34. Product studies of 50% aqueous methanolysis of [31].....46

35. Product studies of 50% aqueous methanolysis of [24].....46

36. Product studies of 50% aqueous methanolysis of [32].....47

37. Reaction scheme for the solvolysis of [19], [24], and [31].....49

38. Proposed reaction scheme for the solvolysis of [32].....54

LIST OF FIGURES - continued

39. Proposed oxygen/catalyst interaction.....57

40. Synthesis of 3-methyl-8-oxatricyclo[4.3.3.0] dodec-3-ene, [35].....58

41. GC traces of the palladium induced bond isomerization of cis-8-oxabicyclo[4.3.0]non-3-ene.....59

42. Bond migrations and olefinic reductions of cis-8-oxabicyclo[4.3.0]non-3-ene.....60

43. Preparation of cis-8-oxabicyclo[4.3.0]non-2-ene.....61

44. Synthesis of -1,6-8-oxabicyclo[4.3.0]nonene.....61

45. Reaction composition of the hydrogenation (Pd/C) of cis-bicyclo[4.3.0]non-3-ene at 3 minutes (a) and 15 minutes (b).....62

46. Polanyi's hydrogenation mechanism.....63

47. Hyperstable olefins.....65

48. HOMO contour plots of [1], [13], [14], and [15].....67

49. 70 eV EI mass spectrum of cis-8-oxabicyclo [4.3.0]non-3-ene, [1].....69

50. 70 eV EI mass spectrum of cis-8-oxatricyclo [4.3.3.0]undec-3-ene, [7].....70

51. Deuterium labeled analogues of cis-8-oxabicyclo [4.3.0]non-3-ene, [1].....71

52. Synthesis of cis-7,7,9,9-tetradeutero-8-oxabicyclo[4.3.0]non-3-ene,[42].....71

53. Syntheses of cis-2,2,5,5-tetradeutero-8-oxabicyclo-[4.3.0]non-3-ene, [43] and cis-2,2,5,5,7,7,9,9-ocatadeutero-8-oxabicyclo[4.3.0] non-3-ene, [44].....72

54. 70 eV EI mass spectrum of cis-7,7,9,9-tetradeutero-8-oxabicyclo[4.3.0]non-3-ene, [42].....73

55. 70 eV EI mass spectrum of cis-2,2,5,5-tetradeutero-8-oxabicyclo[4.3.0]non-3-ene, [43].....73

56. 70 eV EI mass spectrum of cis-2,2,5,5,7,7,9,9-octadeutero-8-oxabicyclo[4.3.0]non-3-ene, [44].....74

LIST OF FIGURES - continued

57. Loss of HOCH2 from cis-8-oxabicyclo[4.3.0] non-3-ene, [1].....75

58. Loss of CH3-CH=CH-CH2 from cis-8-oxabicyclo [4.3.0]non-3-ene, [1].....76

59. Loss of CH3-O-CH2 from cis-8-oxabicyclo [4.3.0]non-3-ene, [1].....77

60. Plot of $\ln(c_\infty - c_x)$ vs time (seconds) for the 50% aqueous methanolysis of [19] at 35.84 °C.....84

61. Plot of $\ln(c_\infty - c_x)$ vs time (seconds) for the 50% aqueous methanolysis of [19] at 50.00 °C.....85

62. Plot of $\ln(c_\infty - c_x)$ vs time (seconds) for the 50% aqueous methanolysis of [19] at 62.87 °C.....86

63. Plot of $\ln(c_\infty - c_x)$ vs time (seconds) for the 50% aqueous methanolysis of [31] at 35.78 °C.....87

64. Plot of $\ln(c_\infty - c_x)$ vs time (seconds) for the 50% aqueous methanolysis of [31] at 50.20 °C.....88

65. Plot of $\ln(c_\infty - c_x)$ vs time (seconds) for the 50% aqueous methanolysis of [31] at 63.00 °C.....89

66. Plot of $\ln(c_\infty - c_x)$ vs time (seconds) for the 50% aqueous methanolysis of [24] at 35.82 °C.....90

67. Plot of $\ln(c_\infty - c_x)$ vs time (seconds) for the 50% aqueous methanolysis of [24] at 50.10 °C.....91

68. Plot of $\ln(c_\infty - c_x)$ vs time (seconds) for the 50% aqueous methanolysis of [24] at 63.00 °C.....92

69. Plot of $\ln(c_\infty - c_x)$ vs time (seconds) for the 50% aqueous methanolysis of [32] at 35.70° C.....93

70. Plot of $\ln(c_\infty - c_x)$ vs time (seconds) for the 50% aqueous methanolysis of [32] at 50.15° C.....94

71. Plot of $\ln(c_\infty - c_x)$ vs time (seconds) for the 50% aqueous methanolysis of [32] at 62.90° C.....95

72. Plot of In(k) vs 1/T ($K^{\circ -1}$) for [19].....96

73. Plot of In(k) vs 1/T ($K^{\circ -1}$) for [31].....97

74. Plot of In(k) vs 1/T ($K^{\circ -1}$) for [24].....98

LIST OF FIGURES - continued

75. Plot of In(k) vs 1/T ($K^{\circ -1}$) for [32].....99

76. ORTEP drawing of [19].....112

77. ORTEP drawing of [24].....117

ABSTRACT

The role the oxygen atom plays in influencing the stereochemistry of electrophilic additions to cis-8-oxabicyclo[4.3.0]non-3-ene, [1] and 8-oxatricylo[4.3.3.0]undec-3-ene, [7], was examined. A complete absence of stereoselectivity was observed in [7]. This was consistent with calculations completed on the olefin that suggest: (1) there are two boat conformers existing for the alkene in approximate equilibrium abundances, (2) the conformers have HOMOs of equal energy and as a result should have equal reactivity, and (3) there is no contribution by the oxygen atom in the HOMOs of either conformer which could possibly have directed the addition. The modest stereoselectivity observed in [1] was attributed to simple steric effects.

The role of the oxygen atom in imparting reactivity during solvolysis on the syn- and anti-tosylates derived from [1] and [7] was examined. Identical reactivities and products were observed in the solvolysis of the syn and anti-tosylates of [1]. This was interpreted to mean oxygen does not influence reactivity in these compounds. A slight rate enhancement (1.53) was observed for the anti tosylate of [7] relative to the syn-isomer. A stabilized hydrogen bonded intimate ion pair (IIP) was used to rationalize this increased reactivity.

The role of the oxygen atom to influence the stereochemistry of catalytic hydrogenation in 3-methyl-8-oxabicylo[4.3.3.0]undec-3-ene, [35], was studied and modest stereoselectivity was observed (3 : 1). This is suggestive of an oxygen/catalysts interaction (haptophilicty).

The olefins resulting from the palladium induced bond isomerization of [1] were characterized and examined by the MM2 and MNDO methods. These olefins were found to exhibit increasing thermodynamic stability as measured by heats of formation and hyperstability. This stability was used to rationalize the bond isomerization on the basis of the Polanyi mechanism. A correlation between hyperstability and HOMO π bond order was observed in this system.

The major ions in the EI mass spectrum of [1] were determined from an examination of the mass spectra of a series of deuterium labelled analogues of [1] which were prepared. Fragmentation mechanisms were proposed for the formation of these ions.

CHAPTER 1

INTRODUCTION

Neighboring Group Participation by Oxygen

Oxygen containing heterocycles are ubiquitous to organic chemistry and, therefore, the effects that an oxygen atom imparts on reactivity and structure of the molecule are of great importance to the organic chemist. Classically, this reactivity has been widely studied through the use of absolute and relative kinetics, providing insights into reaction mechanisms and elucidating oxygen's role in the chemical transformation.[1,2,3,4,5] Surprisingly, these studies have often shown conflicting influences imparted by oxygen! In some cases the oxygen atom has been shown to enhance reaction rates; while in other compounds, oxygen has been shown to retard reaction rates. Interpreting oxygen's effect in imparting reactivity on the molecule has also been difficult because oxygen does not easily share its lone pair electrons in the stabilization of positive charges, a consequence of its high electronegativity. As a result, the various effects oxygen imparts on structure and reactivity are not completely understood.

In solvolytic reactions oxygen has been shown to stabilize positive charges with its lone pair electrons through neighboring group participation[5] (NGP). This stabilization typically results in an enhanced rate (anchimeric assistance). Oxygen's influence, however, has been shown to be more subtle than that of nitrogen or sulfur, due to their lower

electronegativities and more diffuse lone pair orbital. This makes nitrogen and sulfur better able to stabilize positive charges.[6,7,8] Gratz and Wilder[9] have compared such heteroatom influences for oxygen and sulfur (Table 1). Note the large 752 rate enhancement of the exo-tricyclic sulfide relative to the carbon analog compared to the subtle 2.53 rate enhancement of the exo-tricyclic ether relative to the carbon analog. The authors have attributed the large rate enhancements to lone pair NGP by the heteroatom, and a stabilized intermediate with delocalized positive charge is proposed (Figure 1). Albeit subtle, oxygen's effect can be considered significant as Schleyer[10] suggests, "the detection of any rate enhancement due to anchimeric assistance, no matter how small, is indicative of strong (not weak!) participation by the neighboring group".

Table 1. Solvolytic rate influences by oxygen and sulfur.

	Z	Relative Rate
	S	0.80
	CH_2	0.70
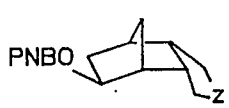	S	752
	O	2.53
	CH_2	1.00

3

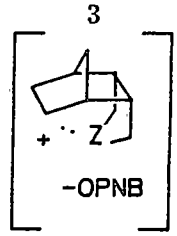

Figure 1. Heteroatom stabilization in a norbornyl system.

Closson et al.[11] also has found anchimeric assistance by the tetrahydrofuranyl group. This rate enhancement was shown to be greater than that for the methoxyl group, which in turn was far greater than the corresponding straight chain alkane (Table 2). Unlike the conformationally rigid norbornyl systems of Wilder, in these systems great conformational flexibility exists. As a result, oxygen is better able to stabilize positive charge through NGP (Figure 2).

Table 2. Relative rates of solvolysis of p-bromobenzenesulfonates in acetic acid at 50 C.

Compound	Relative Rate
$Me-(CH_2)_4-CH_2-OBs$	1.00
$MeO-(CH_2)_4-CH_2-OBs$	657
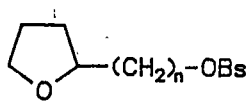	
n = 1	13.1
n = 2	26.3
n = 3	1510
n = 4	12400
n = 5	1380

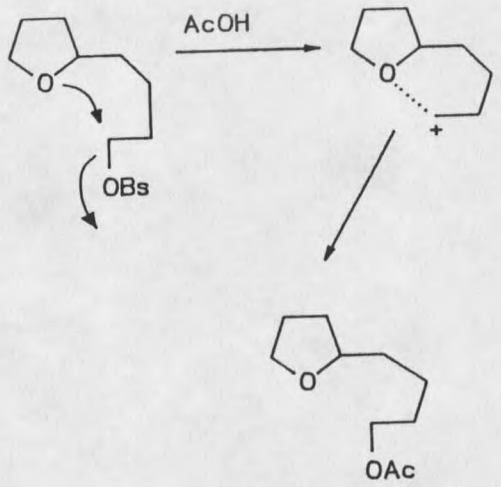

Figure 2. Oxygen intermediate stabilization.

Paquette et al[12] observed a 24 fold rate enhancement in the rate of solvolysis of endo-9-oxabicyclo[4.2.1]-2-yl-p-bromobenzensulfonates compared to its exo-isomer. The endo-isomer was found to produce the oxonium ion upon acetolysis, while the exo-isomer reacted by the carbocation intermediate which rearranges to the oxonium ion (Figure 3).

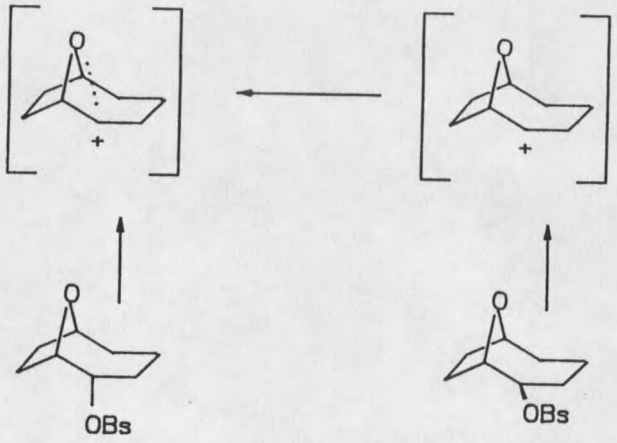

Figure 3. Oxygen participation in endo-9-oxabicyclo[4.2.1]-2-yl-p-bromobenzenesulfonate.

Sunko[13] recently has illustrated oxygen participation in 2-(ethoxybenzyl)-3-methyl-2-cyclohexyl-p-nitrobenzoate. Although he observed a subtle 1.14 rate increase over the corresponding carbon analog, a significantly reduced (1.164) secondary α-deuterium isotope effect was observed, a strong indication of oxygen participation in the ionization of the ester (Figure 4).

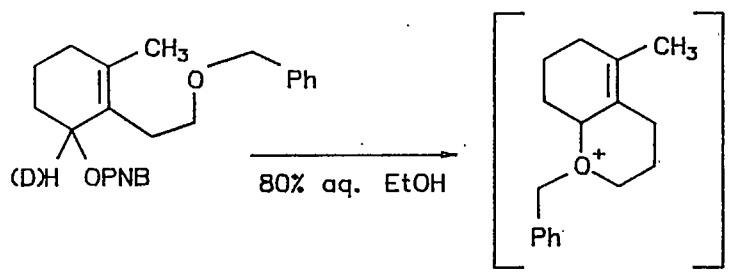

Figure 4. Oxygen participation in 2-ethoxybenzyl-3-cyclohexyl-p-nitrobenzoate.

Conversely, Tarbell and Hazen[14] observed a rate retarding effect by oxygen. They investigated the role oxygen played in the solvolysis of simple oxygen heterocycles (Table 3) and found the rates of solvolysis were an order of magnitude slower than would be expected from an inductive effect by oxygen. This information led them to believe that they were dealing with a transannular dipole effect (Figure 5). The dipole associated with ether oxygen was destabilizing the incipient carbonium ion in the solvolysis, thus retarding the rate.

Table 3. Acetolysis of arenesulfonates.

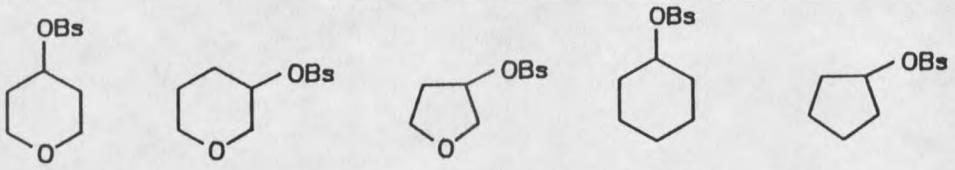



Figure 5. Transannular dipole effect.

Using the method of "increasing electron demand", Gassman[15] examined through bond NGP of the carbon-carbon bond of an epoxide, cyclopropyl group, and a π-system (Table 4). By examining the α-methyl/hydrogen ratio, the changing electronic effects could be isolated from the changing steric effects of the molecule. This method is based on the assumption that if the electron demand of the incipient cabonium ion in the transition state is satisfied by the electron density donated by a substituent on the carbon atom, then a remote function group will not participate in the reaction. The relative ability of a functional group to be involved in NGP was determined by comparing the rate when the electron demand was satisfied by substituents (tertiary carbocations) to the ratio when electron demand was satisfied by a remote functional group (secondary carbocations).

Table 4. Oxygen's inductive effect on carbon-carbon bond participation.

Compound	Relative Ratio (Me/H)
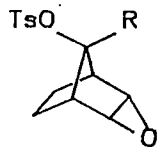	10^8
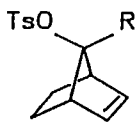	10^{11}
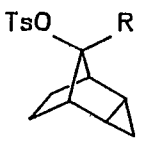	10^{14}
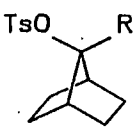	1

Great anchimeric assistance was observed for all functional groups. Note, however, the significantly reduced rate enhancement of the epoxide relative to its cyclopropyl group analog. This is attributed to oxygen's inductive effect on carbon-carbon bond participation.

The Mundy group also maintains an aggressive program directed toward the study of the role oxygen plays in imparting structure and reactivity on the molecule. Otzenberger[16] (1971) initiated this investigation by completing a competitive oxymercuration study. A part of this study is represented in Table 5.

Table 5. Oxymercuration competition results.

Compound		Relative Rate ± 10%
		1.00
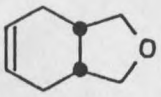	1	0.81
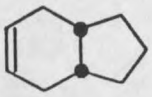	2	0.11
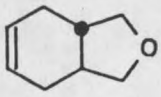	3	0.40
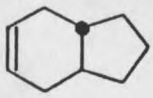	4	0.15

From this study he concluded that any substitution on the ring retards the rate. More interestingly, Otzenberger noted that cis-8-oxabicyclo[4.3.0]non-3-ene, [1], was nearly eight times as reactive as cis-bicyclo[4.3.0]non-3-ene, [2]. A similar, though smaller, rate enhancement was observed for trans-8-oxabicyclo[4.3.0]non-3-ene, [3]. This data seemed to suggest a rate enhancing effect imparted by oxygen.

In considering the preferred conformation of [1], Otzenberger reasoned that the repulsion between the oxygen non-bonding electrons and the π-electrons of the double bond would favor conformation [**1A**] as shown in Figure 6. He used an ^{1}HNMR argument and the work of Cope[17] and Casadevall[18] (who concluded that [2] and cis-bicyclo[4.2.0]oct-3-ene, respectively, exist in pseudo-boat conformations) to support this conclusion.

In this conformation, Otzenberger considered substitution on the ring to be sufficiently remote to result in the π-faces of the double bond to be sterically equivalent.

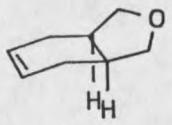

1A

Figure 6. Predicted conformation of cis-8-oxabicyclo[4.3.0]non-3-ene.

Otzenberger also found that oxymercuration of [1] gave predominantly the syn alcohol [5] (Figure 7), in a ratio of 3 to 1 over the anti alcohol [6].

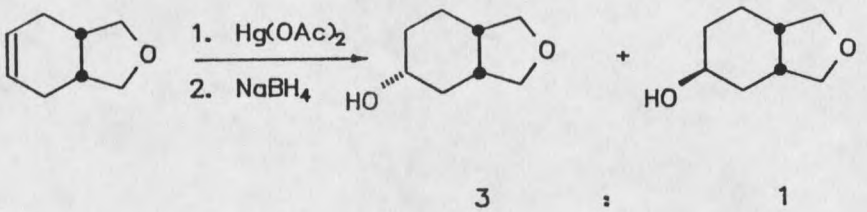

Figure 7. Oxymercuration of cis-8-oxabicyclo[4.3.0]non-3-ene.

To rationalize these findings, and by analogy to the oxygen participation found by Wilder in a analogous norbornyl system (Figure 1), Otzenberger proposed the following mechanism (Figure 8) involving oxygen neighboring group participation. In this mechanism, [1] because of its limited conformational flexibility adopts a conformation in which oxygen donates electron density from its lone pair electrons to stabilize the

mercurinium intermediate. This stabilized intermediate was used to account for the increased reactivity of [1].

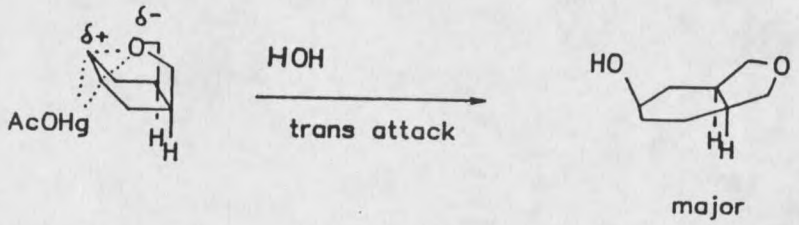

Figure 8. Proposed oxygen participation.

Wilkening[18] (1984), unlike Otzenberger, did not consider the π-faces of [1A] to be sterically equivalent. As illustrated in Figure 9, the π-system of the cyclohexene ring actually appears to be facially dissimilar. One face of the double bond is <u>syn</u> to the oxapropano group while the other face of the double bond experiences only two hydrogen atoms in contradistinction.

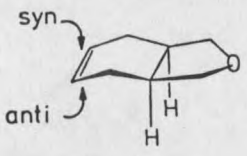

Figure 9. Steric bias in <u>cis</u>-8-oxabicyclo[4.3.0]non-3-ene.

To address this factor of steric nonequivalence and to test Otzenberger's mechanism involving oxygen participation, Wilkening synthesized 8-oxatricyclo[4.3.3.0]undec-3-ene, [7]. In a sense, he considered [7] to be a combination of [1] and [2]. Wilkening also considered the π-

system of [7] to be facially similar, eliminating the steric nonequivalence that he believed existed in [1]. As a result, Wilkening believed any stereoselective additions to [7] could be more accurately attributed to oxygen participation.

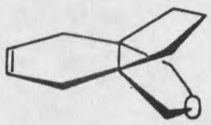

7

When Wilkening subjected [7] to an epoxidation study using mCPBA and to an oxymercuration study catalyzed by trace amounts of nitric acid in methanol, he found no indication of oxygen participation influencing product stereochemistry;[20] the product ratios in both studies were 1 to 1 (Figure 10). As a result, he concluded that simple steric effects, not oxygen participation, were responsible for the observed product distributions in [1] and in [7]. From this study, however, Wilkening was unable to explain the increased reactivity of [1] over [2].

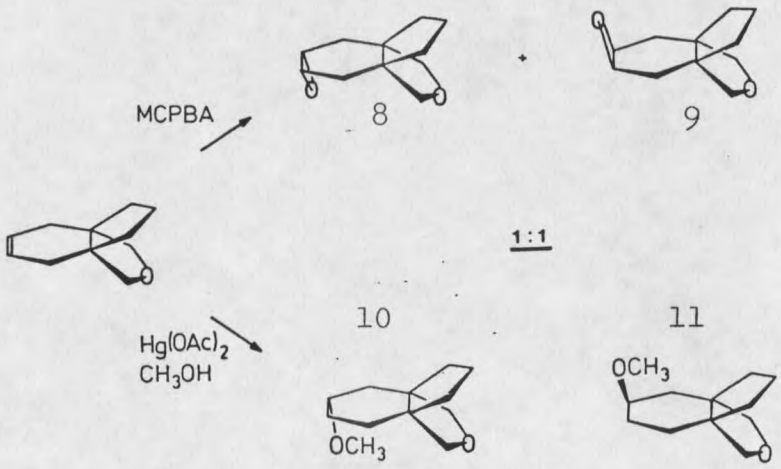

Figure 10. Absence of oxygen participation in 8-oxatricyclo[4.3.3.0]undec-3-ene.

Oxygen Effects on Hydrogenation

The catalytic hydrogenation of olefins has been studied by a number of investigators using a variety of reaction techniques. In these studies reaction solvent, hydrogen pressure, substrate concentration, catalyst metal, the metal to support ratio, the pretreatment of catalyst, and even the sequence in which the olefin and hydrogen are added to the catalyst all have been found to have an effect on the reaction rate.[21,22]

Theodore[23] (1978) investigated the role oxygen imparts on reactivity in an non-ionic situation by comparing the hydrogenation rates of [1], [2], and cyclohexene (Table 6). In the competitive study, carried out by mixing [1] or [2] with cyclohexene in the same reaction vessel, [1] was found to be more reactive than [2] or cyclohexene, again suggestive of an oxygen rate enhancing effect! In the non-competitive study, carried out in separate reaction vessels for the same period of time, [1] was found to be 6 times as reactive as [2], similarly attributed to an oxygen rate enhancing effect.

Table 6. Relative rates of catalytic hydrogenation.

Olefin	Competitive	Non-competitive
cyclohexene	1.00	1.00
1	6.59	0.78
2	4.92	0.13

Theodore also completed a number of competitive and non-competitive heteroatom/catalyst affinity studies (Table 7). These results represent the ratios of complexed to free substrate relative to the ratio of complexed to free cyclohexene. The results of the competitive study represent a greater affinity of [1] to bind to the catalyst over [2] or cyclohexene. The results of the non-competitive study were also used to argue for a positive oxygen/catalyst affinity. Because the ratio of catalyst to substrate was approximately equal to one, Theodore envisioned one molecule of [1] having the ability to complex to more than one catalyst site as shown in Figure 11. This complexation would prohibited subsequent molecules to complex to the catalyst, thus reducing the ratio for [1] in the non-competitive study. Theodore believed this oxygen/catalyst interaction provide an entropic rational to account for the increased reactivity of [1] over [2].

Table 7. Relative substrate/catalyst affinities.

Olefin	Competitive	Noncompetitive
cyclohexene	1.00	1.00
1	3.36	0.75
2	0.88	0.13

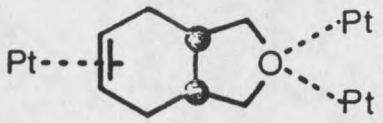

Figure 11. Complexation of cis-8-oxabicyclo[4.3.0]non-3-ene, to platinum.

Glancy[24] (1983) also observed a oxygen/catalyst interaction. He studied the effect of oxygen heterocycles on the catalytic hydrogenation of cyclohexene and found that both tetrahydrofuran (Figure 12) and cis-8-oxabicyclo[4.3.0]nonane, [12], (Figure 13), retarded the rate of reduction of cyclohexene. He rationalized these results by reasoning that the ethereal oxygen in tetrahydrofuran and [12] absorbed on to catalyst sites normally used for hydrogen absorption. This prevented cyclohexene from reaching the catalyst surface thus decreasing its rate of reduction.

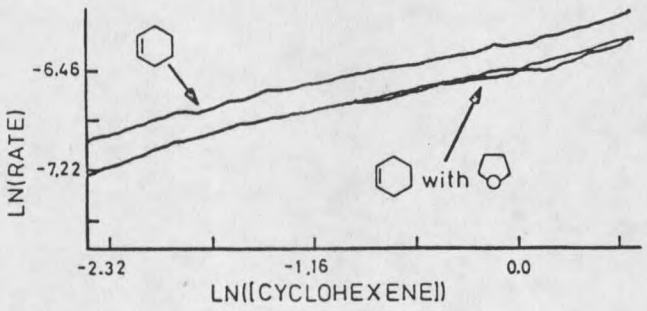

Figure 12. Effect of tetrahydrofuran on the reduction of cyclohexene.

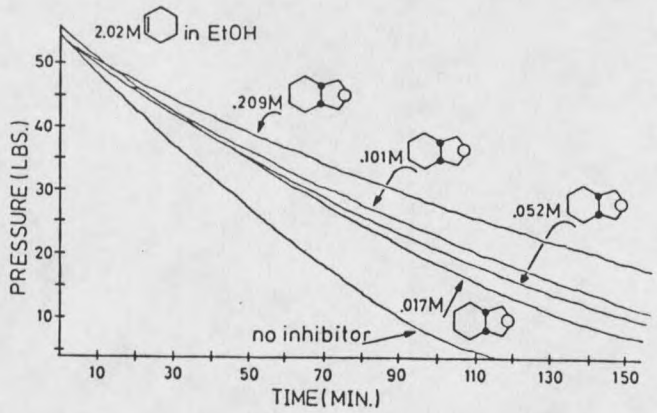

Figure 13. Effect of cis-8-oxabicyclo[4.3.0]nonane on the reduction of cyclohexene.

As a generalization, the stereochemistry of catalytic hydrogenations of olefins results in the cis addition of two hydrogen atoms from the less sterically hindered side of the double bond. However, several accounts of oxygen coordination directing catalytic hydrogenation have recently been reported. This anchoring effect (haptophilicty)[25,26] has been observed by a number of investigators.

Thompson et al[27] observed the directive effect of the methoxy group in the catalytic hydrogenation over Pd/C and Pt/C of 7-methoxy-10a-hydroxymethyl-1,2,3,9,10,10a-hexahydrophenathrene (Figure 14). They found the cis reduction product was highly favored in solvents having high dielectric constants (DMF, EtOH, and THF).

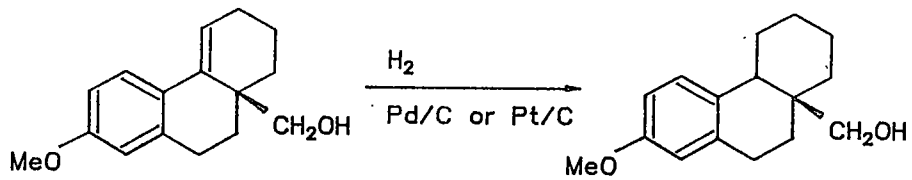

Figure 14. Haptophilicity involving the methoxy group.

Gula and Spencer[28] illustrate a similar anchoring effect for the ester functional group and its corresponding salt. This is illustrated in the stereoselective reduction during catalytic hydrogenation of 10-carbomethoxy-trans-decal-2-one (Figure 15).

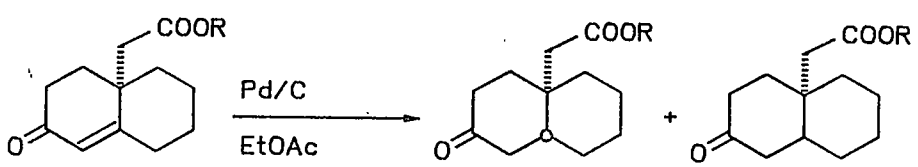

Figure 15. Haptophilicity involving the ester group.

Wilkening[29,30] used this directive ability of the ester group in the reduction of 2-methylene-cis-1,5-dicarboxymethyl[4.3.0]octane (Figure 16). This was used as a key step in his stereospecific synthesis of (dl) modehephene.

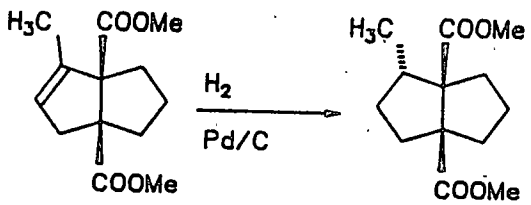

Figure 16. Stereospecific hydrogenation of 2-methylene-cis-1,5-dicarboxymethyl[4.3.0]octane.

Palladium Promoted Bond Isomerization in Cyclic Systems

Palladium has long been known to promote the bond isomerization in cyclic systems, an ability which has been shown to be greater than that of the other noble metal catalysts, ie. iridium, ruthenium, rhodium, osmium, iridium, and platinum.[31,32] Therefore palladium is frequently used when bond isomerization and migration are wanted; platinum when they are to be avoided.[33]

Augustine[34] measured the amount of bond isomerization of methylenecyclohexene, 3-methylcyclohexene, and 4-methylcyclohexene to methylcyclohexene in ethanol over 5% Pd (Figure 17). At 25% completion, he found 100%, 34%, and 37%, respectively, of methylcyclohexene in the olefinic fraction.

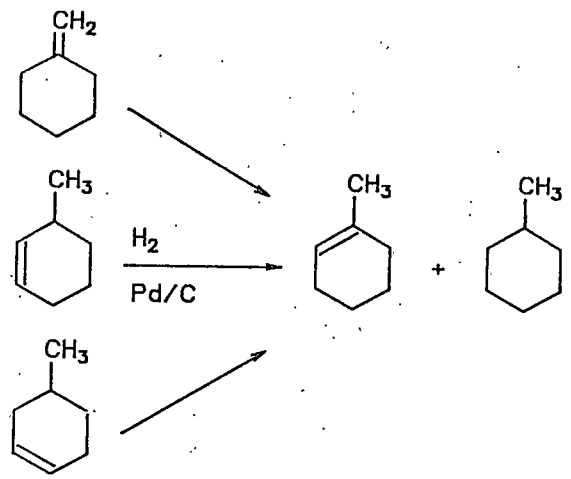

Figure 17. Palladium promoted bond isomerization in the methylcyclohexene system.

Theodore observed bond isomerization with palladium as well. During hydrogenation studies of [1] with Pd/C catalyst, he observed five peaks in the gas chromatogram used to monitor the reaction! Although he was never able to completely characterize all the products resulting from this isomerization, Theodore believed they were the result of the continued isomerization of [1] (Figure 18).

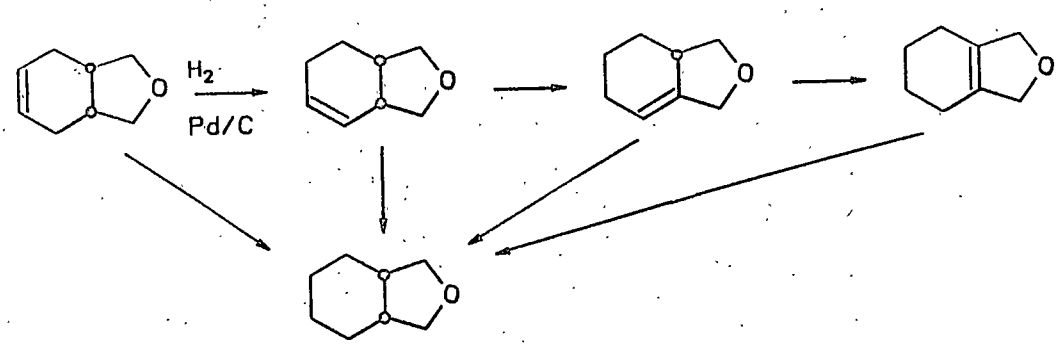

Figure 18. Palladium induced bond isomerization of cis-8-oxabicyclo[4.3.0]non-3-ene.

Scope and Goals of this Investigation

Although a number of observations have been made by the Mundy group suggesting oxygen's role in imparting reactivity and structure on the molecule, many questions remain. Indeed, a group discrepancy exists. Is there oxygen participation in oxymercuration of [1] as Otzenberger reports or are simple steric factors solely responsible in influencing product stereochemistry as Wilkening concludes? Is conformation [1A] actually the preferred conformation of [1]? What then is the preferred conformation of [7]? Is oxygen's affinity for catalyst real as observed by Theodore and Glancy? Can this proposed affinity be detected in new systems? What is the basis of the bond isomerization reported by Theodore? Where else can we search for oxygen's role in imparting reactivity in these systems?

To address the above questions the following investigations were proposed.

(1) Subject [1] and [7] to hydroboration, epoxidation, and oxymercuration/demercuration studies and examine the stereochemistries of the products. Use calculational approaches, MM2 and MNDO, to investigate [1] and [7] to determine their conformational ground state stabilities and observe the HOMO's of each conformation to examine MO energies and the atomic coefficients, especially that of oxygen. By comparing the product studies on [1] and [7], combined with the calculational information, attempt to more clearly distinguish oxygen's role in influencing the stereochemistry of these additions.

(2) Synthesize the syn- and anti-tosylates of [1] and [7]. Monitor the kinetics of the solvolysis of these tosylates, obtaining rate constants and activation parameters, and complete a product analysis of the reaction.

From this data, determine oxygen's role in imparting reactivity to the molecule in solvolysis.

(3) Synthesize and subject to catalytic hydrogenation 3-methyl-tricyclo[4.3.3.0]undec-3-ene. If oxygen is complexing with catalyst (involved in haptophilicity), one would expect a stereoselective reduction. Investigate the reduced products in an attempt to observe this oxygen/catalyst interaction.

(4) Characterize and examine from calculation approaches (the MM2 and MNDO methods) the olefins proposed in the palladium induced bond isomerization of [1] in an attempt to rationalize this process.

(5) As a new system in which to observe oxygen's role in imparting reactivity on the molecule, elucidate the electron impact mass spectroscopy fragmentation mechanism of [1], determining oxygen's role in this process.

CHAPTER 2

RESULTS AND DISCUSSION

Oxygen's Effect in Influencing Stereochemistry

The syntheses of [1] and [7] were carried out following the procedures of Otzenberger[16] and Wilkening[19], respectively, and are illustrated in Figure 19.

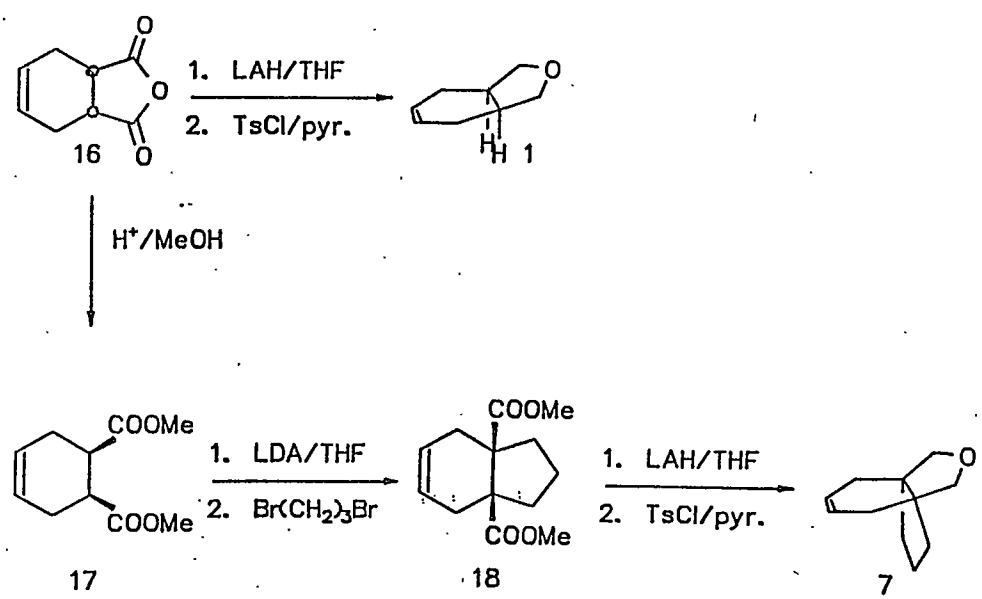

Figure 19. Synthesis of cis-8-oxabicyclo[4.3.0]non-3-ene, [1], and 8-oxatricyclo[4.3.3.0]undec-3-ene, [7].

In an attempt to distinguish simple steric effects from any electronic effects imparted by ethereal oxygen in influencing the stereochemistry of

electrophilic additions to the olefin, a number of studies were conducted on [1] (Table 8) . The results of these studies were then compared to the studies conducted on [7] (Table 9).

Table 8. Product studies on cis-8-oxabicyclo[4.3.0]non-3-ene.

Study	Product Ratios	
	syn-O	anti-O
hydroboration	9	1
epoxidation	4	1
oxymercuration (MeOH)*	1	3
oxymercuration (THF/H20)*	1	3

* The reported stereochemistries are those of the alcohol and methoxy products.

Table 9. Product studies on 8-oxatricyclo[4.3.3.0]undec-3-ene.

Study	Product Ratios	
	syn-O	anti-O
hydroboration	1	1
epoxidation	1	1
oxymercuration (MeOH)*	1	1
oxymercuration (THF/$H_2$0)	-	-

* The reported stereochemistries are those of the methoxy products.

The product ratios were obtained from peak integrations of the GLC traces obtained on the VG MM16 mass spectrometer. The relative stereochemistries of the alcohols derived from [1] and reported in Table 8

were determined from the X-ray crystal structure obtained for the syn-tosylate, [19], derived from [1] (Figure 32). When this tosylate was subjected to saponification (KOH in absolute ethanol) only one alcohol resulted, the corresponding syn-alcohol, [5]. This alcohol reacted with TsCl in pyridine to reform only [19] as determined by ^{1}H NMR spectroscopy, proving that stereochemistry was maintained upon saponification (Figure 20). The other alcohol, having a similar GLC retention time, mass spectral fragmentation pattern, and ^{1}H NMR spectra was obviously the corresponding anti-alcohol, [6].

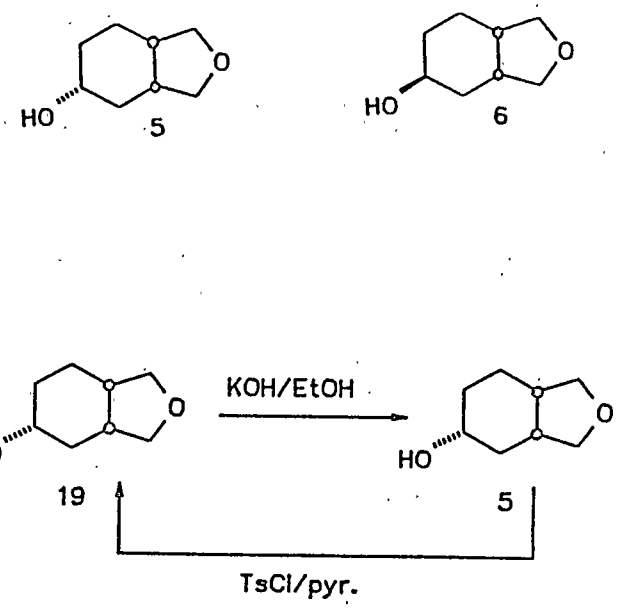

Figure 20. Determination of the stereochemistry of the syn-alcohol of [1].

The epoxide isomers resulting from the epoxidation study of [1], were cleanly collected by preparative GLC (13% DEGS, 10'x1/4"). When the minor epoxide isomer, the first peak to elute, was reduced with LAH in tetrahydrofuran, only the syn-alcohol, [5], was obtained as determined by

its retention time and fragmentation pattern. The second peak, the major epoxide isomer, was similarly reduced yielding only the anti-alcohol, [6], again determined by its retention time and fragmentation pattern. Because stereochemistry is maintained in the reduction of epoxides,[35,36] the minor product was determined to be the syn-epoxide, [20], and the major product the anti-epoxide, [21].

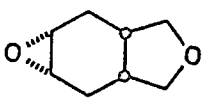

20

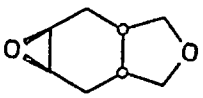

21

A difference nuclear Overhauser effect (NOE)[37] ^{1}H NMR experiment was employed to determine the identities of the methoxy isomers, resulting from the methoxymercuration/demercuration study of [1] and reported in Table 8. Again the isomers were cleanly collected by preparatory GLC (13% DEGS, 10x1/4"). The ^{1}HNMR spectra of the major product, the second to elute, revealed a one proton multiplet at 3.17 δ. When this signal was irradiated a significant positive 7.1 % NOE enhancement was observed at the axial ring juncture proton resonating at 2.18 δ (Figure 21). This enhancement is the result of the close spacial proximity of the two protons. In the other isomer, when the corresponding one proton multiplet at 3.25 δ was irradiated, no NOE enhancement of the ring juncture protons was observed. Therefore, the major product was determined to be the syn-methoxy isomer, [22], and the minor product was determined to be the anti-methoxy isomer, [23].

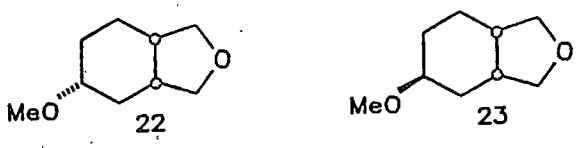

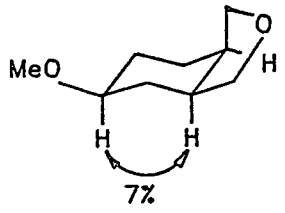

Figure 21. % enhancement of NOE experiment on the syn-methoxy derivative of cis-8-oxabicyclo[4.3.0]non-3-ene.

The absolute stereochemistries of the alcohols and epoxides derived from [**7**] and reported in Table 9 were similarly determined. An X-ray structure for syn-tosylate, [**24**], derived from [**7**] was obtained (Figure 32). When this tosylate was subjected to saponification only one alcohol resulted, the corresponding syn-alcohol, [**25**]. Again, [**25**] reacted with para-toluenesulfonylchloride in pyridine to form only [**24**], as determined by ^{1}H NMR spectroscopy, proving that stereochemistry was maintained upon saponification (Figure 22). The other alcohol, having a similar GLC retention time, mass spectrum, and ^{1}H NMR spectrum, was therefore the anti-isomer, [**26**].

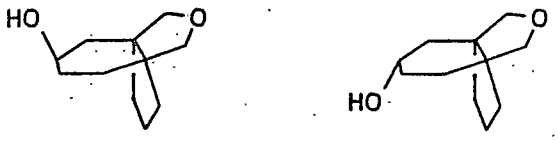

25

26

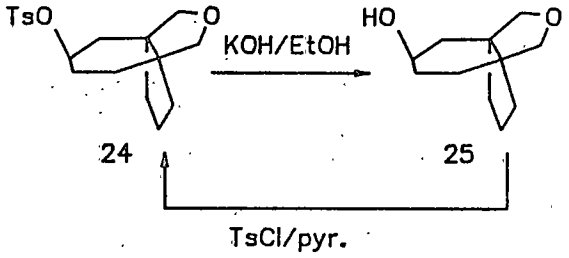

Figure 22. Determination of the stereochemistry of the syn-alcohol of 8-oxatricyclo[4.3.3.0]undec-3ene.

The epoxide isomers, resulting from the epoxidation study of [7], were cleanly collected by preparative GLC (13% DEGS, 10'*1/4"). When the first epoxide isomer to elute was reduced with LAH, pure syn-alcohol, [25], was obtained. When the second epoxide isomer was reduced, only the anti-alcohol, [26], was obtained. The syn-epoxide isomer, [8], and the anti-epoxide isomer, [9], were therefore characterized.



8



9

Wilkening[19] used an ^1H NMR argument to determine the identities of the syn-methoxy isomer, [10], and the anti-methoxy isomer, [11], derived from [7].



10

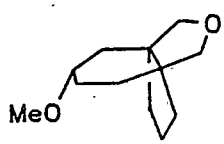

11

The stereochemistries of the products reported in Tables 8 and 9 are all determined upon the initial electrophilic addition. The stereochemistries of the products in the oxymercuration/demercuration studies are thought to be based upon the trans addition of water to the mercurinium ion intermediate.[38] The stereochemistry of this intermediate is determined by the initial electrophilic addition of mercuric acetate to the olefin. In contrast, the stereochemistry of the products from the epoxidation and hydroboration studies are defined directly by the initial electrophilic attack.

The stereochemistry of electrophilic additions to olefins, as Hehre[39] recently reports, will ultimately depend on at least three factors: "(1) the

relative equilibrium abundances of all possible conformations of each olefin (since only they will be present at equilibrium and therefore only these minima can react), (2) the relative reactivities of these conformational minima, and (3) the steroselectivites of the individual conformations." Therefore, to more clearly interpret the results reported in Tables 8 and 9, each of these factors must be individually examined.

The MM2 and MNDO methods were employed to determine the relative equilibrium abundances of olefins [1] and [7] (factor 1). One strength of the MM2 method is its ability to determine conformational minima of a compound by calculating steric energies for all possible conformations of the molecule.[40] MM2 considers a molecule as a collection of atoms held together by harmonic forces which can be described by potential energy functions of structural features such as bond lengths, bond angles, nonbonded interactions and so on. The combination of these potential energy functions constitutes the force field. The steric energy (ES) of the molecule in the force field arises from deviations from "ideal" structural features and can be approximated by a sum of energy contributions

$$ES=E_b+E_{st}+E_{nb}+.....$$

where E_b is the energy arising from bending bond angles from their "ideal" values (ie. all sp^3 bond angles are 109), E_{st} is the energy arising from stretching bond lengths from their "ideal" lengths (ie. all carbon-carbon bond lengths are 1.54 A), and E_{nb} is the energy of nonbonded interactions. The steric energy of the molecule is, therefore, the difference in energy between the actual molecule and a hypothetical molecule where all bond lengths and bond angles have exactly their "ideal" values.[41]

Two global minima were obtained for each olefin by the MM2 method, corresponding to the two anticipated boat conformations and are reported in Tables 10 and 11.

The MNDO method is a semi-empirical molecular orbital calculation developed by Dewar[42] and has, as one of its strengths, the ability to accurately calculate heats of formation (H_f) while requiring only modest computational time. The initial geometries for the MNDO calculation were the optimized geometries obtained by the MM2 method. These geometries were then optimized at the SCF level by minimizing the energy with the Davidon-Fletcher-Powell (DFP) algorithm.[43] These calculated energies are reported in Tables 10 and 11.

Table 10. Ground state conformational energies for cis-8-oxabicyclo[4.3.0]non-3-ene, [1].

Conformation		Energy (Kcal/mole)	
		MM2 (Steric)	MNDO (H_f)
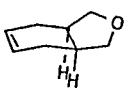	1A	16.76	-42.90
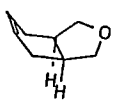	1B	16.73	-42.84

Table 11. Ground state conformational energies for 8-oxatricyclo[4.3.3.0]undec-3-ene, [7].

Conformation		Energy (Kcal/mole)	
		MM2 (Steric)	MNDO (H_f)
	7A	27.39	-48.77
	7B	27.24	-48.81

In addition to suggesting two minima exist for both [1] and [7] (corresponding to the two anticipated boat conformations), these results suggest that the minima for each olefin are energetically equivalent within the errors reported for each calculation.[38,44] As a result, the relative conformational equilibrium abundances, as calculated as $\exp(-\Delta E/RT)$ where ΔE is the conformational energy differences, R is the gas constant and T=298 °K, are approximately equal for each alkene. These conformational equilibrium abundances are illustrated in Figure 23 and Figure 24.

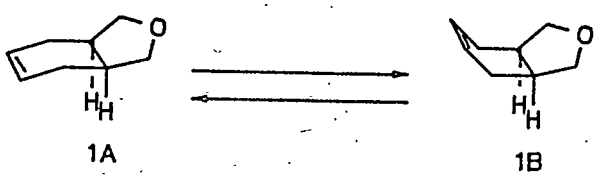

Figure 23. Equilibrium conformations of 8-cis-oxabicyclo[4.3.0]non-3-ene.

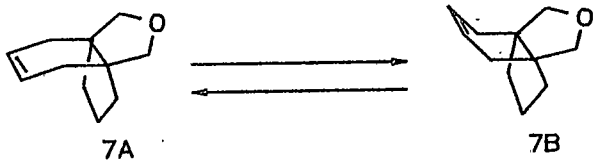

Figure 24. Equilibrium Conformations of 8-oxatricyclo[4.3.3.0]undec-3-ene.

A number of approaches have recently been developed to investigate olefin/substrate reactivities and regio- and stereoselectivities. Hehre et al.[37,45,46] has developed a reactivity model by considering the relative affinities of the diastrophic olefin faces toward a test electrophile (a proton). The test electrophile is mapped onto quantum-mechanical electron density surfaces of the olefin and an electrostatic potential is determined. This energy accounts only for the coulombic interactions between a point charge (the proton) and the substrate, but has proven to be accurate in predicting the regio- and stereochemistry of a number of electrophilic additions to allylic double bonds. This approach is qualitatively similar to attempts to calculate the electrophile/substrate "supermolecule" at select geometries. Houk[47,48] and others have attempted to calculate directly the properties of transition states. This approach has the advantages that no assumptions have to be made, but is presently limited in its applications to very simple system.

Because of its simplicity and elegance, we chose the Frontier Molecular Orbital[49] (FMO) theory to predict the relative reactivities (factor

two) of each conformational isomer existing in equilibrium for [1] and [7]. Within the framework of the FMO model, the reactivity of a olefin towards an electrophile should increase with decreasing energy separation between the olefin HOMO and the LUMO on the electrophile. Since LUMO of the electrophile remains constant for each study, this relative reactivity should parallel the relative HOMO energies, which are reported in Table 12 and Table 13.

Table 12. HOMO conformational energies of cis-8-oxabicyclo[4.3.0]non-3-ene.

Conformation	Energy (eV)
1A	-9.96
1B	-9.94

Table 13. HOMO conformational energies of 8-oxatricyclo[4.3.3.0]undec-3-ene.

Conformation	Energy (eV)
7A	-9.69
7B	-9.69

The above calculations suggest that conformation [**1A**] and [**1B**] have nearly identical reactivities and conformations [**7A**] and [**7B**] have identical reactivities.

The stereochemistry of electrophilic additions to olefins, based on FMO theory, assumes that electrophilic attack will occur where the π-bond

is most heavily concentrated. Such an approach, however, does not distinguish the diastereotopic faces of the olefins, such as [1] and [7], having symmetrical π-bonds. To examine the stereoselectivities of the individual conformations (factor three), we attempted to examine any differences the electrophile "experiences" between the two diastereotopic faces of the π-bond in the ground state by examining the entire HOMO of each conformation. On the bases of hard and soft acid base (HSAB) theories[50], electrophilic attack on olefins is governed by the Coulombic interactions between reactant and substrate at the reactive site (charge control) and the interactions between occupied molecular orbital of the olefin and the unoccupied molecular orbital of the electrophile (orbital control). According to HSAB theory, a soft acid (electrophile) is most likely to interact at the position(s) with the largest coefficient(s), ie. orbital control, while a hard base (nucleophile) will attack the most positive center, ie charge control. Because diborane and $Hg(OAc)_2$ are classified as soft acids (or soft electrophiles) and mCPBA is classified as a hard soft acid (electrophile)[51], orbital control should govern these additions. Therefore, the entire HOMOs of the olefins were examined to see if there were large coefficients, especially on the oxygen atom, that could favorably interact with the electrophiles and thus direct the addition.

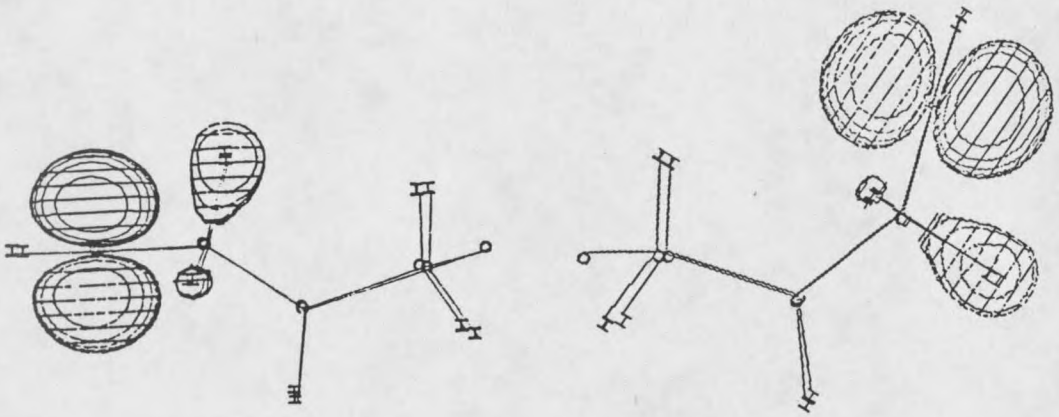

1A 1B

Figure 25. HOMO contour plots of 8-cis-oxabicyclo[4.3.0]non-3-ene.

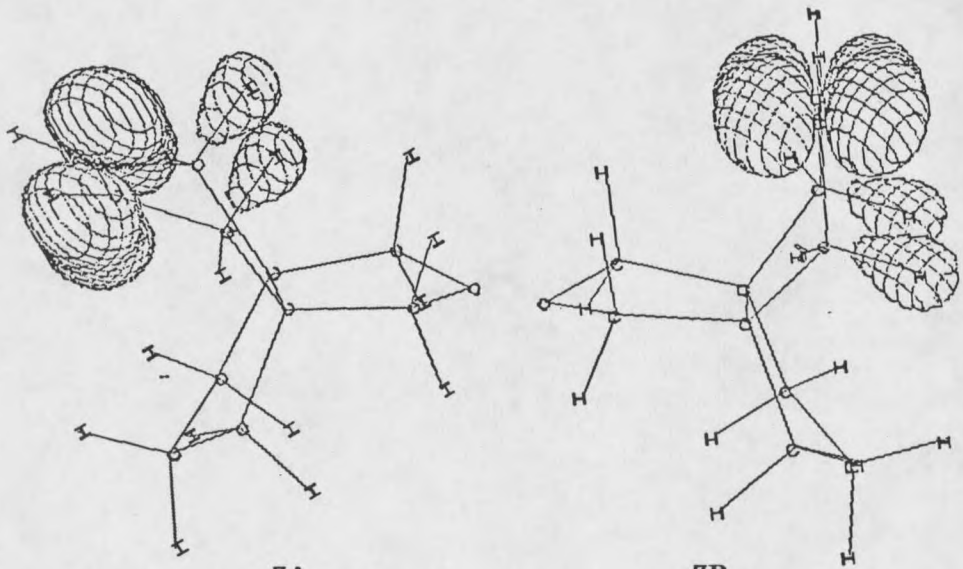

7A 7B

Figure 26. HOMO contour plots of 8-oxatricyclo[4.3.3.0]undec-3-ene.

In examining the contour plots of the HOMOs for [**1A**], [**1B**], [**7A**], and [**7B**], it is obvious that no coefficients exist on oxygen in any conformation. As a result, considering both conformers exist in equilibrium, there appears to be no differences in what the electrophile "experiences" between the two faces of the π-system for [**1**] or [**7**].

From an examination of Table 11, it appears that in [7] two conformational minima exist in equilibrium, [7A] and [7B], in approximate equal abundance. These conformers have HOMO's of equal energy and, therefore should have equal reactivities (Table 13). It also appears that these conformers have no contribution by oxygen (which could possibly have directed electrophilic additions) in their HOMO's (Figure 26). Since the π-faces of [7] have identical steric environments (considering both conformations exist in equilibrium for the molecule), from these combined data, there is no reason to predict any stereoselective additions to [7]. Not surprisingly, a complete absence of stereoselectivity is observed (Table 9).

In [1], again, it appears that two conformational minima exist in equilibrium, [1A] and [1B], in approximate equal abundances (Table 10). FMO theory predicts these conformers to have nearly equal reactivities (Table 12) and again, there appears to be no contribution by oxygen (to possibly direct electrophilic additions) in the HOMO of either conformation.

There are, however, obvious steric differences between the π-faces of [1]. In [1B], the face anti to oxygen is much less hindered and the initial electrophilic attack anti to oxygen would appear to be favored. In [1A], the π-faces are also dissimilar. Electrophilic attack on the face syn to oxygen "experiences" two pseudo-axial protons α to the double bond and an oxapropano ring at the ß positions, while attack on the face anti to oxygen "experiences" two pseudo-equatorial protons α to the double bond and two ring juncture protons ß to the double bond in contradistinction. As a result, the face anti to oxygen in [1A], again, appears to be the less sterically hindered face and initial electrophilic attack anti to oxygen

appears to be favored. Not surprisingly, Table 8 illustrates some stereoselectivity in which initial electrophilic attack anti appears to be favored.

At first glance the results reported in Table 8 appear inconsistent. In the hydroboration and epoxidation studies completed on [1], the major products are anti to oxygen, while in the oxymercuration/demercuration studies the major products are syn to oxygen. These results can be clarified by recalling that in oxymercuration/demercuration, product stereochemistry is trans to that of the initial electrophilic attack. After formation of a mercurinium ion intermediate, trans-addition of either the MeOH of H_2O nucleophiles results. This positions the methoxy or alcohol groups opposite to that of the initially electrophilic attack. In contrast, in the hydroboration and in the epoxidation studies, the reported stereochemistries are determined by the initial attack of the electrophile.

Although Hoffman[52] as early as 1872 states that "steric effects are used like patriotism by a scoundrel as a last resort for those who have difficulty in interpreting reactivities",.... in light of this investigation, **it appears that there is no oxygen participation influencing the stereochemistry of electrophilic additions to [1] or [7]. The observed stereoselectivity in [1] appears to be the result of simple steric effects.** These findings are consistent with those reported by Wilkening (Figure 10) and seem to refute the proposed oxygen stabilized intermediate suggested by Otzenberger in the oxymercurataion of [1] (Figure 8).

Oxygen's Effect in Influencing Reactivity

The series of compounds in Figure 27 were designed to attempt to elucidate the oxygen atom's role in influencing reactivity in solvolysis. In this series the anti-compounds, [**A**] and [**C**], could undergo a conformational flip that places the leaving group in a pseudo-equatorial position (Figure 28). This would be expected to result in oxygen being in rather close spacial proximity to the carbon atom bearing the leaving group. Similarly, a conformational flip of the syn-compounds, [**B**] and [**D**], would place the leaving group in pseudo-equatorial positions (Figure 29). In the case of [**B**], this would result in the carbon bearing the leaving group being in close spacial proximity to the two ring juncture protons. While in the case of [**D**], the carbon bearing the leaving group would be in close spacial proximity to a methylene group. Note the similarity of compounds [**A**] and [**C**], in this boat conformation, to the corresponding norbornyl analog in which Wilder observed subtle NGP by oxygen (Table 1). One could therefore imagine NGP existing in compounds [**A**] and [**C**] but having no possibility of existing in [**B**] and [**D**]. If NGP is occurring, an increase in rate would be predicted for the syn-compounds relative to their corresponding anti-analogues.

The tricylic tosylates, [**C**] and [**D**], are unique in that the steric environments for the two compounds are identical. In [**C**], the tosylate group is syn to the propano group while in [**D**] the tosylate group is syn to the oxapropano group. Therefore, the backside attack by solvent, on the carbon bearing the tosylate, should experience the same steric environment. Any observed rate enhancement of [**D**] over [**C**] might then be attributed solely to oxygen participation. If a rate enhancement of the

anti-tosylates is observed, this would lend support to Otzenberger's proposed oxygen NGP in the oxymercuration of [1] (Figure 8).

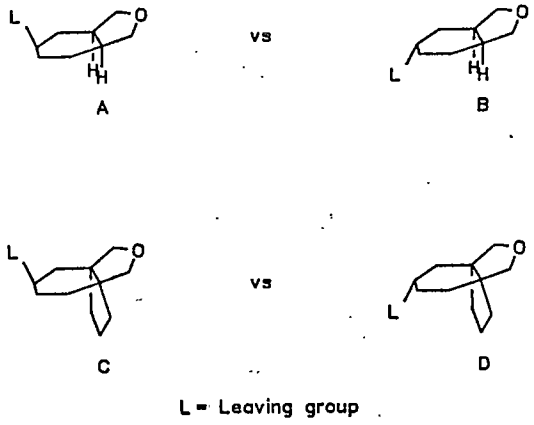

Figure 27. Does the oxygen atom influence reactivity in the solvolysis of these tosylates?



Figure 28. Boat conformations of anti-isomers, [A] and [C].



Figure 29. Boat conformations of syn-isomers, [B] and [D].

We initially chose para-nitrobenzoate as our leaving group. To form the bicyclic compounds, [1] was subject to hydroboration yielding the corresponding alcohol mixture which was subsequently converted to the

bicyclic para-nitrobenzoate mixture. After scores of solvent systems were examined by TLC, a mixture of methylene chloride, ethyl acetate, and hexanes in the relative ratio 20 : 1: 1:, respectively, afforded a clean separation of syn- and anti- bicyclic para-nitrobenzoates, [27] and [28], respectively. Flash chromatography was then employed to isolate the products.

The syntheses and isolation of the tricylic para-nitrobenzoates, were identical to that of the bicyclic para-nitrobenzoates, except the initial alkene in the syntheses was [7]. This procedure yielded the isomerically pure syn- and anti-tricyclic para-nitrobenzoates, [29] and [30], respectively.

Unfortunately, these para-nitrobenzoates proved to be surprisingly stable. They would not undergo solvolysis in 80% aqueous acetone, even when the reaction was attempted in sealed tubes at temperatures as high as 250 °C over a period of 48 hours.

The 80% aqueous acetone solvent system was, initially, the system of choice. We intended to complete product studies on each compound and we assumed the corresponding alcohols, which had been previously characterized, would be the major products along with the alkenes resulting from an elimination process. Therefore, in this solvent system, we believed the product analysis would be quite simply accomplished.

In order to increase the reactivity of this series, we completed two new syntheses derivatizing the alcohols with tosylate, a better organic leaving group. Unfortunately, the solvent system which afforded flash separation in the case of the para-nitrobenzoates, yielded no separation with these tosylates. Again, many additional solvent systems were

investigated by TLC but none were found which produced a separation.

We therefore proposed the following synthetic schemes to obtain the isomerically pure tosylates. In the syntheses of the syn-tosylate, [19], and anti-tosylate, [31], derived from cis-8-oxabicyclo[4.3.0]non-3-ene, [1] was subjected to hydroboration to yield the corresponding alcohol mixture which was subsequently converted to the para-nitrobenzoate derivatives. Flash chromatography was then employed to cleanly separate this mixture into [27] and [28]. Saponification of the isomerically pure syn- and anti- para-nitrobenzoates afforded the respective syn- and anti- alcohols which maintained their isomeric purity. The alcohols were then easily converted to [19] and [31]. Figure 30 outlines these syntheses.

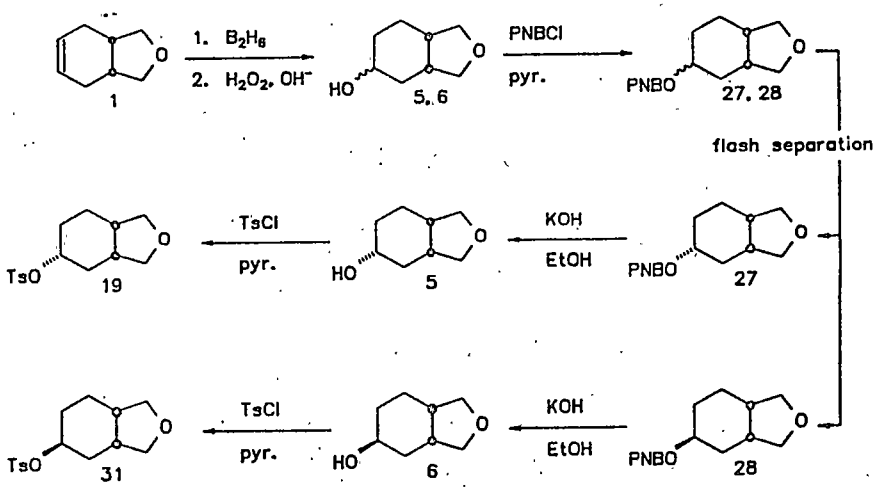

Figure 30. Syntheses of syn- and anti-tosylates derived from [1].

The syntheses of syn-3-tosyl-8-oxatricyclo[4.3.3.0]undecane, [**24**], and anti-3-tosyl-8-oxatricyclo[4.3.3.0]undecane, [**32**], were identical to that of the bicyclic series except the initial alkene in the synthesis was [**7**], as is shown in Figure 31.

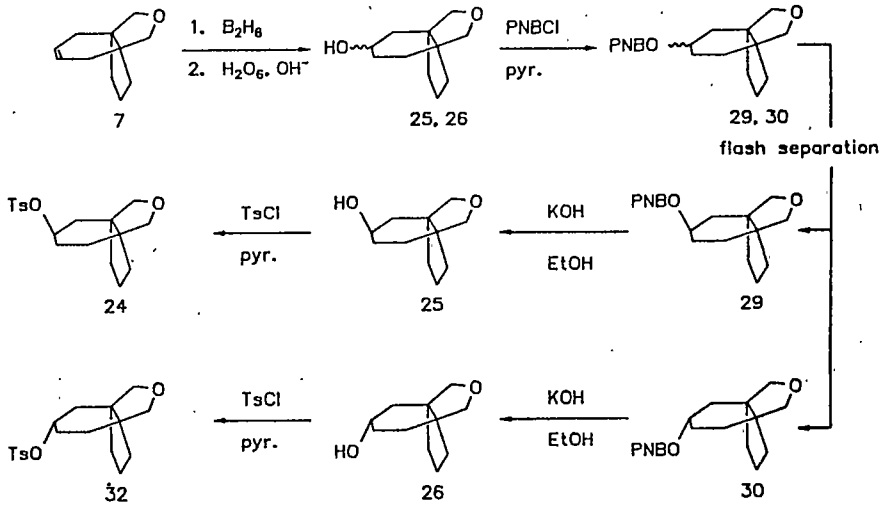

Figure 31. Syntheses of syn- and anti-tosylates derived from [**7**].

Tosylates [**19**] and [**24**] were white solids, which after a number of crystallization attempts yielded crystals in hexane and dichloromethane (50 : 1, respectively) from which x-ray structures were obtained. This x-ray data confirmed the relative stereochemistries reported for the tosylates (and the corresponding alcohols from which they were derived) in the syntheses. Their ORTEP drawings are illustrated in Figure 32. Note the similarity of the conformations for each tosylate. Unfortunately, tosylates [**31**] and [**32**] were oils which would not, even after considerable effort, crystalize.

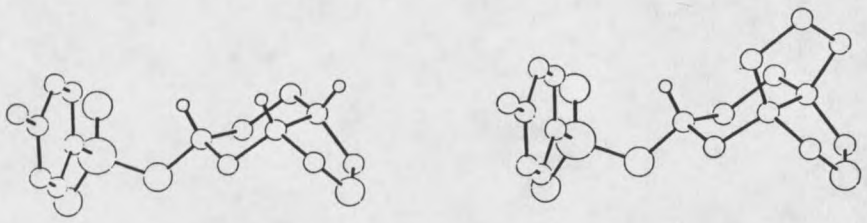

Figure 32. ORTEP drawings of the x-ray structures of [**19**] and [**24**].

An attempt at solvolyizing the tosylates in 80% aqueous acetone was accomplished, but only after refluxing the reaction period for a period of several days. Obtaining kinetic data over several half-lives of such a slow process was difficult, so other solvent systems were investigated.

We discovered that in 50% aqueous methanol, a solvent system with a higher dielectric constant and a higher ionizing power parameter, Y, and nucleophilicity parameter, N, the reactions proceed within hours.[53] This solvent system was then used to complete all the solvolysis experiments. It was assumed that the substitution products would be the previously characterized alcohol and methoxy compounds, greatly simplifying the product studies.

The kinetic studies were completed conductrimetrically. A conductance cell and thermistor were interfaced[54] to a computer allowing for the simultaneous acquisition of conductance, temperature, and time measurements. A standard solution of 50% aqueous methanol was prepared. The standard solution (25 ml) was added to the pretreated conductance cell which was then placed in the constant temperature bath. The temperature

was allowed to equilibrate, then approximately 2 mg of the tosylate were added to the cell and upon temperature equilibration, data acquisition began. (The initial tosylate concentrations were only 10^{-3}-10^{-4} M!) Data were collected approximately every second over 3 to 5 half-lives of the reaction and an infinity point was obtained after approximately 15 half-lives. Least squares treatment of $\ln(c_\infty - c_x)$ vs time (seconds) yielded first order rate constants (k) for each tosylate, at three temperatures differing by approximately 14°C. The Arrhenius equation was used to obtain energies of activation (E_a) and the activation complex theory was employed to obtain the enthalpy ($^{\ddagger}\Delta H$) and entropy ($^{\ddagger}\Delta S$) of activation. The results of these studies are reported in Tables 14-16.

Table 14. Kinetic results of the 50% aqueous methanolysis of [19] and [31].

Compound	Temp. (°C) ± .03	k x 10^4 (s^{-1})	R	E_a (Kcal/mole)
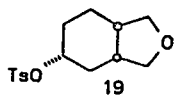 19	35.84	0.607	1.0000	
	50.00	3.47	1.0000	26.2 ± 0.3
	62.87	14.3	1.0000	
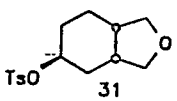 31	35.78	0.607	0.9999	
	50.20	3.32	0.9996	25.8 ± 0.3
	63.00	13.9	1.0000	

Table 15. Kinetic results of the 50% aqueous methanolysis of [**24**] and [**32**].

Compound	Temp. (°C) ± .03	k x 10^4 (s^{-1})	R	E_a (Kcal/mole)
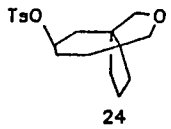 24	35.82	1.91	0.9999	
	50.10	9.35	0.9998	22.7 ± 0.3
	63.00	37.9	1.0000	
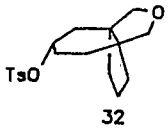 32	35.70	2.90	0.9999	
	50.15	14.7	0.9999	21.9 ± 0.4
	62.90	52.7	0.9997	

Table 16. Activation parameters of the 50% aqueous methanolysis of [**19**], [**31**], [**24**] and [**32**].

	$\Delta H^{\ddagger}$ (Kcal/mole)	$\Delta S^{\ddagger}$ (eu)
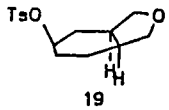 19	23.49 ± .27	-1.87 ± .81
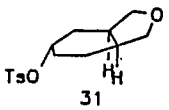 31	23.09 ± .31	-3.18 ± .92
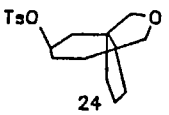 24	22.10 ± .30	-4.11 ± .98
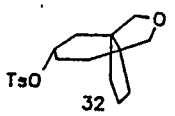 32	21.37 ± .41	-5.56 ± 1.22

Products studies were completed by combining the three runs for each tosylate, distilling off most of the methanol, and then extracting the resulting residue repeatedly with dichloromethane. Product studies were completed by comparing retention times and mass spectral fragmentation patterns of the observed products to those of the authentic samples that were synthesized and characterized previously. Product ratios were obtained from peak integrations completed on GLC capillary column equipped with a flame ionization detector. Only peaks with relative areas greater than 1% of the product mixture were reported. The results of these studies are summarized in Figures 33-36.

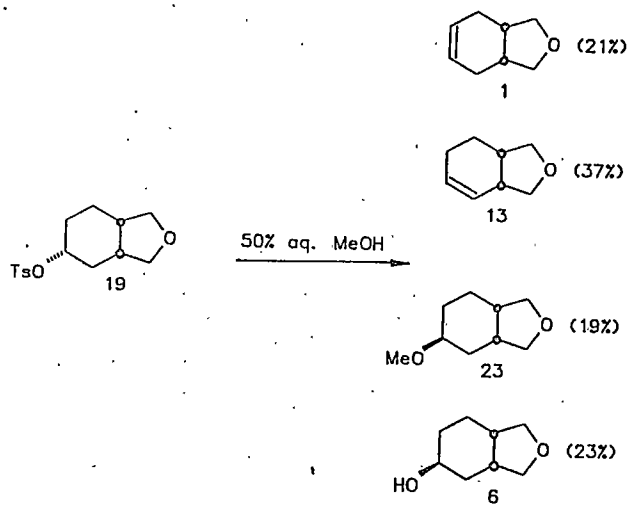

Figure 33. Product studies of 50% aqueous methanolysis of [19].

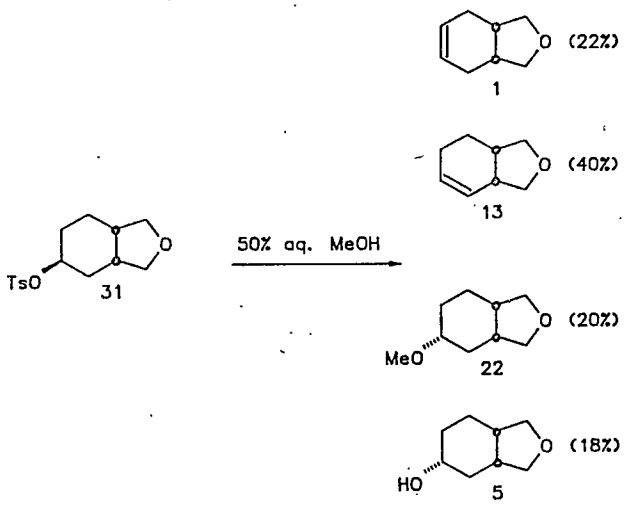

Figure 34. Product studies of 50% aqueous methanolysis of [**31**].

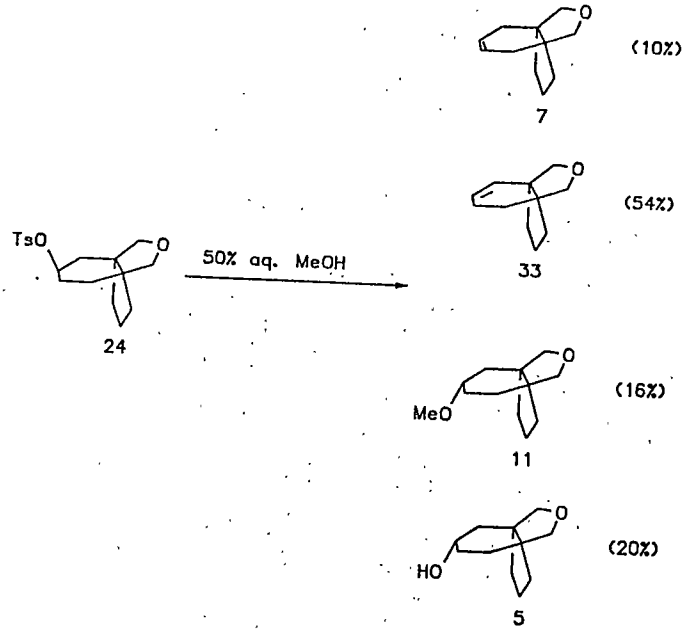

Figure 35. Product Studies of 50% aqueous methanolysis of [**24**].

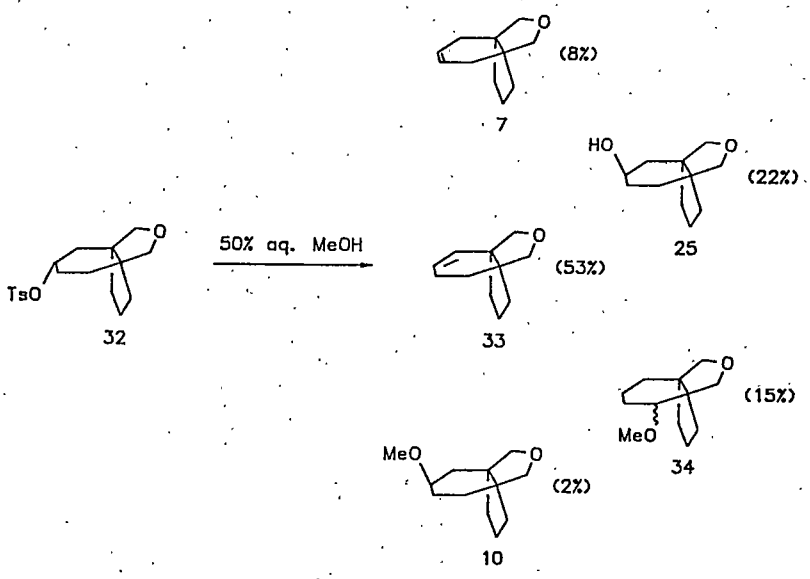

Figure 36. Product studies of 50% aqueous methanolysis of [**32**].

From an examination of the rate constants obtained from the bicyclic tosylates, there appears to be no rate enhancement of [**31**] over [**19**]. The relative rate of [**31**]/[**19**] is 1.00 at 35.8°C and the energies of activation for the two tosylates are equal within a standard deviation.

The ground state energies of the syn- and anti-bicyclic tosylates are also believed to be identical. These tosylates were modelled as their corresponding alcohol and methoxy derivatives, in chair conformations. In each case no significant energy differences were observed between the syn- and anti-isomers (Table 17).

Table 17. Modelled bicyclic tosylate energies.

Compound	MM2 (Steric Energy)	MNDO (H_f)
5	10.25	-106.54
6	10.26	-106.53
22	11.47	-111.76
23	11.31	-111.62

The product analyses for both compounds appear to be directly related as well. In each case there is a mixture of alkenes, [1] and [13], in the approximate relative ratio of 40 : 20 and the methoxy and alcohol compounds, resulting with complete inversion of configuration, in the approximate relative ratio of 20 : 20. No direct substitution with complete retention of configuration is observed for either tosylate. This suggests no free carbocation is formed in these reactions; the reactions appear to exhibit no classic S_N1 character.

The product studies for the bicyclic series are consistent with a number of solvolysis studies completed on substituted cyclohexyl tosylates.[55,56,57] In these processes an intimate ion pair (IIP)[58] is believed to be formed in the rate determining step, followed by subsequent partitioning into various reaction pathways. These processes have been found to result, primarily, in products formed by substitution (with complete inversion of configuration, characteristic of the classic S_N2 mechanism), and elimination. In addition, a significant portion of substitution products have been found to result from a 1,2 hydride shift, products not observed in the bicyclic series.

From an examination of the kinetic data, the modelled ground state energies of the bicyclic tosylates, and the product analyses, the reaction profiles for the solvolysis of [**19**] and [**31**] appear to be very similar, if not identical. We are, therefore, left with the conclusion that there is no apparent effect by oxygen in the solvolysis of [**31**].

To rationalize these data on the bicyclic tosylates, we also envision a carbocation intermediate formed in the rate determining step in the reaction. This carbocation is depicted in Figure 37 as an IIP showing explicitly only one nearest solvent molecule. Note that the observed negative entropies of activation are consistent with this proposed intermediate (Table 16). In this depiction the cyclohexyl ring is drawn in the chair conformation, although its exact conformation is not known. After formation of the IIP there is partitioning into the various reaction pathways. Elimination of para-toluenesulfonic acid results in a mixture of olefins, while substitution by solvent results in the completely inverted methoxy and alcohol products.

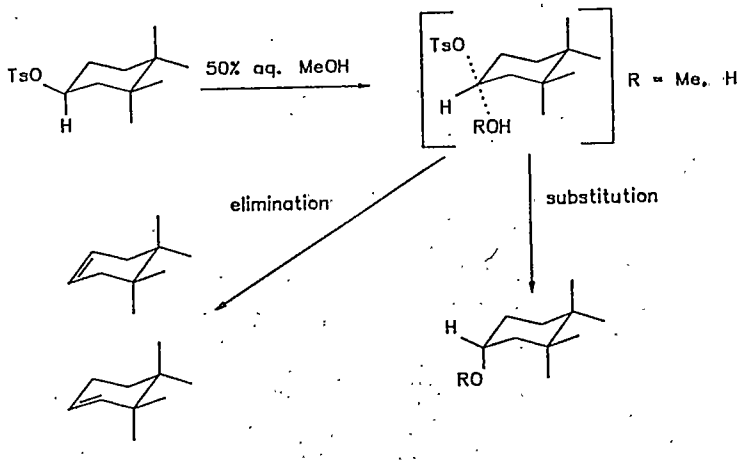

Figure 37. Reaction scheme for the solvolysis of [**19**], [**24**], and [**31**].

An examination of the stabilities of olefins [1] and [13], by MM2 and MNDO calculations, indicates that [13] is the thermodynamically more stable alkene by 2-3 kcal/mole (Table 18). The Hammond postulate can then be used to rationalize the relative abundance of [13] over [1] in the elimination process. The transition state for the formation of [13] should be more similar in energy and structure to the IIP than in the case of [1].

Table 18. Calculated olefinic energies (Kcal/mole).

Olefin	MM2 (Steric Energy)	MNDO (H_f)
1	10.14	-42.90
13	7.02	-44.47
7	16.77	-48.77
33	14.73	-49.63

In the tricyclic series, the relative rate of [32]/[24] is 1.53 at 35.8°C. This is reflected as a difference in the energies of activation of approximately 800 calories. Although this is a subtle rate enhancement, it is strong evidence for some form of involvement by the oxygen atom. There is also a marked difference in the product analysis of the two tricyclic tosylates.

The products formed from [24] are similar to those formed from the bicyclic tosylates. In [24], there is a mixture of alkenes [7] and [33] in the relative ratio of 10 : 50, respectively, and a mixture of the completely inverted methoxy and alcohol products in a relative ratio of 20 : 20. Once again, no retention of configuration is observed. This suggests no free carbocations (characteristic of the classic S_N1 mechanism) are generated in

the process.

Because the product composition of [**24**] is similar to that of the bicyclic tosylates, we envision a reaction sequence like that proposed for [**19**] and [**31**] (Figure 37). After formation of an intermediate ion pair in the rate determining step, elimination of para-toluene sulfonic acid results to from the olefinic mixture while substitution produces the completely inverted methoxy and alcohol products. Again MM2 and MNDO calculations reveal a thermodynamic stability of [**33**] over [**7**] (Table 18) and the Hammond postulate can be used to rationalize the relative olefinic abundances.

The products resulting from [**32**] contain the mixture of alkenes in a relative ratio of approximately 10 : 50 and the completely inverted alcohol in approximately 20%, products which are directly analogous to the results obtained from [**24**]. However, the completely inverted methoxy compound is present in only 2% and a new methoxy compound, [**34**], (at the C_2 position) apparently resulting from a 1,2 hydride shift followed by substitution exists in 15%.

Because the product study for [**32**] contained the rearranged methoxy compound, [**34**], a product not observed in the solvolysis of the other tosylates, the reproducibility of this study was questioned. As a result, a second product analysis was completed by placing [**32**] in 50% aqueous methanol at 50° C. and stirring the solution overnight. The product analysis of this run was identical to that of the original. In addition, there was a question as to whether the products obtained from [**32**] were the result of the actual kinetic process or the result of a thermodynamic rearrangement occurring subsequent to the kinetic products. To address this

question, the reaction was repeated a third time under the identical reaction conditions in which aliquots were removed after 30%, 50%, and 75% completion of the reaction. In each case, the product ratios were identical to that of the original. These results strongly suggest that the products of the solvolysis of **[32]** are due to a kinetic process.

By definition neighboring group participation (NGP) is the stabilization resulting from a substituent bonding to a reaction center of an intermediate or transition state. This stabilization typical results in a rate enhancement, ie. anchimeric assistance. Because there is bonding between the substituent and the reaction center in NGP, subsequent additions to this center are directed by this bonding and **retention** of configuration is favored.

In the product study of **[32]**, no substitution products with retention of configuration are observed (Figure 35). As a result, it appears that there is **no NGP by oxygen existing in [32]**; oxygen is not bonding to the reaction center in the transition state or the intermediate. If NGP does not exist, what then causes the observed relative rate increase (anchimeric assistance) of **[32]** over **[24]**?

We do not believe the rate enhancement is due to differences in the ground state energies of the tricyclic tosylates. Again, these tosylates were modelled as their corresponding alcohol and methoxy derivatives in chair conformations and examined by the MM2 and MNDO methods. In each case, no significant energy differences were observed between the syn- and anti-isomers (Table 19).

Table 19. Modelled tricyclic tosylate stabilities, (Kcal/mole).

Compound	MM2 (Steric Energy)	MNDO (H_f)
25	20.73	-120.32
26	20.59	-120.38
10	21.78	-115.06
11	21.72	-115.07

An explanation, however, to account for this rate increase is a modification of the reaction scheme used to describe the solvolysis of [**19**], [**24**], and [**31**]. In the solvolysis of [**32**], we again envision a carbocation formed in the rate determining step, depicted as an IIP showing explicitly the nearest solvent molecule (Figure 38). In the case of [**32**], however, the carbocation is stabilized, albeit slightly, by the hydrogen bonding that can exist between ethereal oxygen and the hydroxy hydrogen of the solvent. This stabilized IIP is consistent with the observed negative entropy of activation obtained for [**32**] (Table 16). And this stabilization cannot exist in [**31**] and therefore seems to account for the observed rate enhancement in [**32**]. Again after formation of the IIP, partitioning into the various reaction pathways occurs. Elimination of para-toluenesulfonic acid will once again result in a mixture of olefins and substitution by solvent affords the inverted alcohol and methoxy compounds. A 1-2 hydride shift followed by substitution accounts for the methoxy compound at C_2. Because the driving force to migration in solvolysis is the formation of a more stable carbocation,[59] carbocation stabilities were determined by the MNDO method. These calculations illustrate a thermodynamic driving force promoting this

rearrangement. The carbocation at C_2 is favored by approximately 5 kcal/mole over the carbocation at C_3.

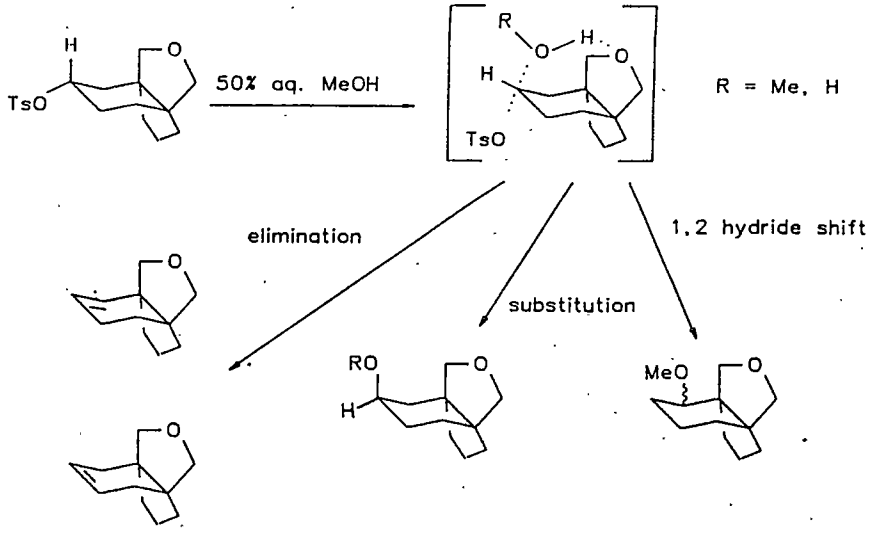

Figure 38. Proposed reaction scheme for the solvolysis of [**32**].

Table 20. Calculated carbocation stabilities (Kcal/mole).

Carbocation	MNDO (H_f)
	140.32
	135.58
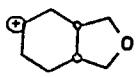	143.38
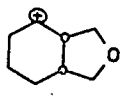	141.28

Many important questions were answered from this investigation. Most notably, no NGP was observed in the bicylic or tricylic tosylates. These data seem to refute the intermediate involving NGP by the oxygen atom proposed by Otzenberger in the oxymercuration of [1] (Figure 8).

This investigation has generated a number of intriguing questions as well. For example, if such a stabilization exists in [32] why does it not exist in the closely related [31]? An examination of the crystal structures of syn-tosylates, [19] and [24], indicates nearly identical structures. Both compounds in the crystal lattice are in the chair conformation with the tosylate group equatorial. Both tosylates also have identical O_3-O_1 interatomic distances, 4.20 ± 1 A° for [24] and 4.18 ± 1 A° for [19]. One could assume that the crystal structures for the anti-tosylates, [31] and for [32] would be as closely related. Why then is there not a rate enhancement in [31]?

Perhaps the absence of stabilization in [31] is due to the decreased rigidity in this compound relative to the more constrained tricyclic compound, [32]. The bicyclic compound experiences more conformational freedom and therefore the IIP is of higher entropy. This is consistent with the entropies of activation obtained for the bicyclic tosylates (Table 16). This increased disorder may be responsible for the absence of the hydrogen bonding stabilization.

Another question arising from this study is, why is there a 1,2 hydride existing only in [32]? An examination of carbocation stabilities indicates only a 2 Kcal/mole driving force favoring the 1,2 hydride shift in the bicyclic compounds compared to a 5 Kcal/mole driving force in the tricyclic system (Table 20). This decreased thermodynamic driving force

could possibly explain the absence of the 1,2 hydride shift in the bicyclic compounds, but what about the absence of the 1,2 shift in [24]?

Yet another questions is, why is there only a rearranged methoxy product and not the corresponding alcohol product in [32]? Could the stabilized IIP formed from methanol and [32] promote the rearrangement? A transition state calculation on the IIP, could possibly provide some insight to this question. This questions remain to be answered.

A Search for an Oxygen Catalyst Interaction

Theodore and Glancy both observed what they believed to be an oxygen/catalyst interaction. In an attempt to detect this proposed interaction in a new system, 3-methyl-8-oxatricyclo[4.3.3.0]dodec-3-ene, [35], was synthesized and subjected to catalytic hydrogenation.



35

The π-faces in [35], like the π-faces in [7], are by design sterically equivalent. One face is syn to the propano group while the other face experiences an oxapropano group in contra-distinction. Because of this steric equivalence, [35] is a sensitive system in which to attempt to detect an oxygen/catalyst interaction. If such an interaction exists, one could expect a stereoselective reduction.

Figure 39 illustrates the proposed oxygen/catalyst interaction and the resulting stereochemistry of the reduced product. This interaction would be reflected as an observed isomeric abundance of the anti-product.

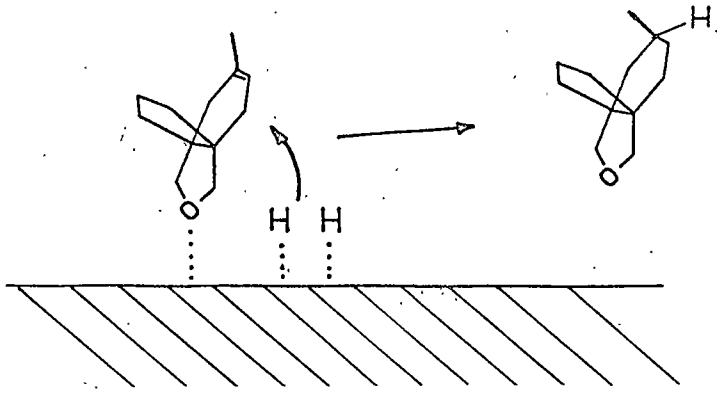

Figure 39. Proposed oxygen/catalyst interaction.

In the synthesis of [**35**], 1.1 equivalents of 1,3 dibromopropane were added to the lithium dienolate of cis-1,6-dicarbomethoxy-3-methylcyclohex-3-ene, [**36**]. The diester, [**37**], was obtained in high yield. Reduction of the diester with LAH afforded the diol, which was subsequently ring-closed to the desired propellane, [**35**]. Figure 40 outlines the synthesis.

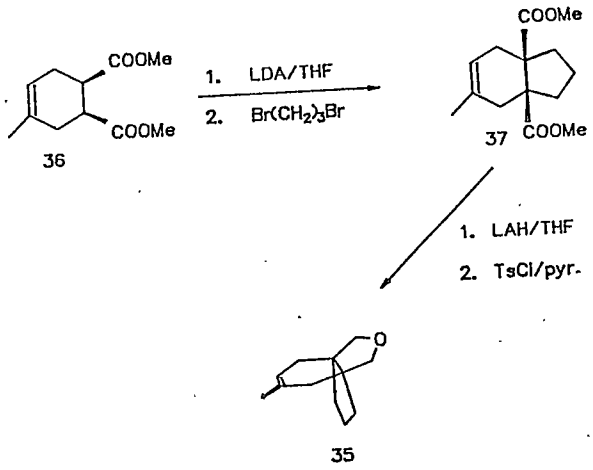

Figure 40. Synthesis of 3-methyl-8-oxatricylo[4.3.3.0]dodec-3-ene, [**35**].

When [**35**] was exposed to 10% Pt on carbon catalyst at 50 psi for 12 hours, a stereoselective addition was observed! The reduced products were formed in the relative ratio of 3 : 1. The reaction was completed three times, each yielding the identical product ratio.

Unfortunately, the reduced products were separable only by capillary GC/MS analysis, leaving the stereochemistry of the major isomer unknown. In order to determine the stereochemistry of these isomers, a separation scheme will have to be developed and most probably a two dimensional NMR experiment employed. These are techniques which are unavailable to this researcher at the present time.

As a primary investigation however, these results lend strong support to the proposed oxygen/catalyst interaction of Theodore and Glancy. A stereoselective addition is the anticipated result of such an interaction. It is therefore believed that the major isomer will be proven, at a later date, to be the anti-product.

An Examination of the Palladium Induced Bond Isomerization of cis-8-oxabicyclo[4.3.0]non-3-ene

Palladium has long been known to promote bond isomerization during catalytic hydrogenation of cyclic olefins. We have observed such an isomerization during reduction of cis-8-oxabicyclo[4.3.0]non-3-ene, [1]. When [1] was exposed to 10% Pd on carbon, at one atmosphere of hydrogen gas, rapid bond isomerization was observed. Figure 41 illustrates the compound(s) existing in the initial reaction mixture (a), the composition at three minutes (b), and upon complete reduction at fifteen minutes (c). Aliquots were removed from the reaction vessel at the various times and analyzed by GC/MS.

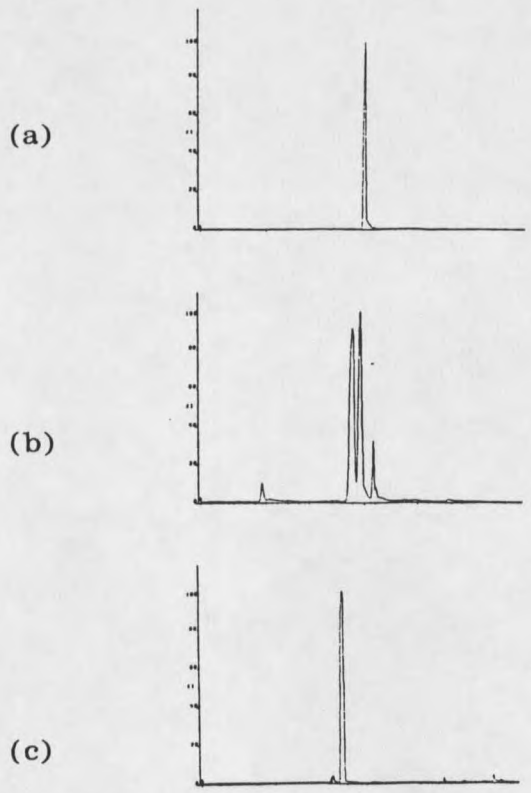

Figure 41. GC traces of the palladium induced bond isomerization of cis-8-oxabicyclo[4.3.0]non-3-ene.

Figure 42 illustrates a reaction sequence which describes the observed bond migrations and olefinic reductions. In this sequence, [1] isomerizes to [13]. This, in turn, rearranges to [14] which subsequently isomerizes to [15]. In addition, olefins [1], [13], and [14], are reduced to [12]. In the reduction of [14], hydrogen addition cis to the ring juncture proton also results in [12], while addition anti to the ring-juncture proton results in trans-8-oxabicyclo[4.3.0]nonane, [16].

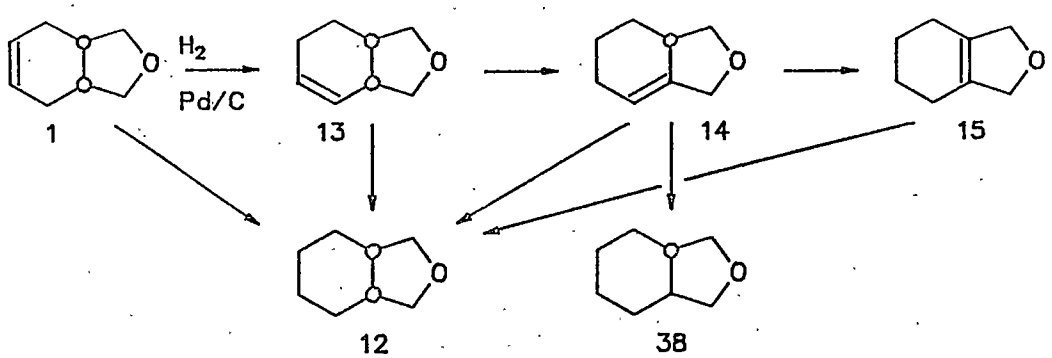

Figure 42. Bond migrations and olefinic reductions of cis-8-oxabicyclo[4.3.0]non-3-ene.

The identities [1], [12], [13], [15], and [16] were unambiguously characterized by comparisons of their retention times and mass spectral fragmentation patterns to those authentic samples. Compounds [1] and [13] were prepared by heating the mixture of [19] and [31] to 250° C, promoting elimination of para-toluenesulfonic acid. Olefins [1] and [13] were produced in the ratio of 1:4, respectively (Figure 43). Olefin, [13], was then cleanly collected by preparatory GLC (10% DEGS, 10"x¼') and characterized, in part, based upon an ^{1}HNMR spectra containing two distinct one-proton olefinic multiplets at 5.63 ppm and 5.81 ppm. This is consistent with the non-symmetrical disposition of the alkene.

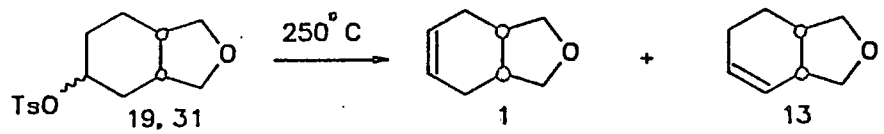

Figure 43. Preparation of cis-8-oxabicyclo[4.3.0]non-2-ene.

In the synthesis of [**15**], phthalic anhydride was reduced with LAH in THF to the corresponding diol which was subsequently ring-closed with TsCl in pyridine to phthalan. The Birch reduction of phthalan cleanly yielded -1,6- -3,4-8-oxabicyclo[4.3.0]nondiene, [**26**]. When [**26**] was hydrogenated, with 10% Pt/C catalyst for 5 minutes at one atmosphere of hydrogen, only two products resulted, 8-cis-oxabicyclo[4.3.0]nonane [**12**] and △-1,6-8-oxabicyclo[4.3.0]nonene [**15**], in a 5 to 1 ratio, respectively (Figure 44). Note that [1] was not formed in the reduction. Olefin, [**15**] was again collected by preparative GLC, (13% DEGS 10"x 1/4'), and characterized by ^{1}HNMR. Here, there was an expected absence of vinyl protons in the spectrum.

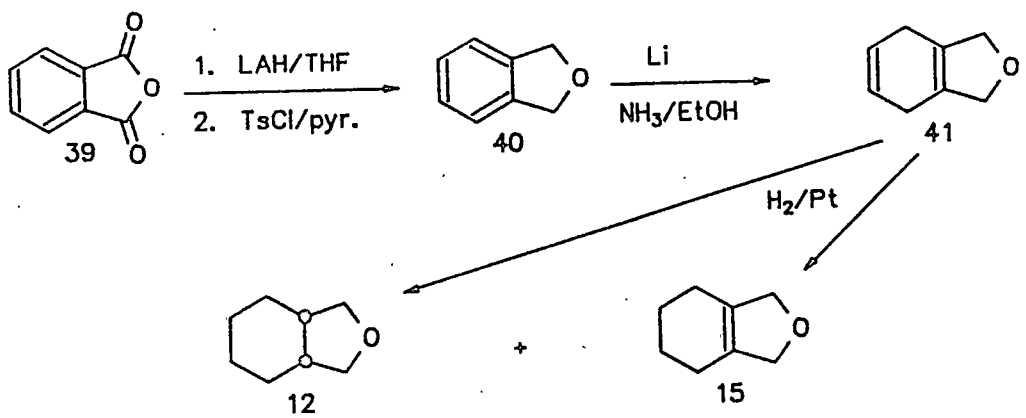

Figure 44. Synthesis of △-1,6-8-oxabicyclo[4.3.0]nonene.

Theodore had previously synthesized [**16**]. This compound was isolated from the reaction mixture and characterized by comparing its ^{1}HNMR to that of the authentic sample. The only data obtained on cis-8-oxabicyclo[4.3.0]non-1-ene, [**14**], was its mass spectrum, which had a fragmentation pattern and retention time consistent with that of the compound.

The identities of the peaks in the reaction mixture at three minutes and upon complete reduction were therefore determined and are illustrated in Figure 45.

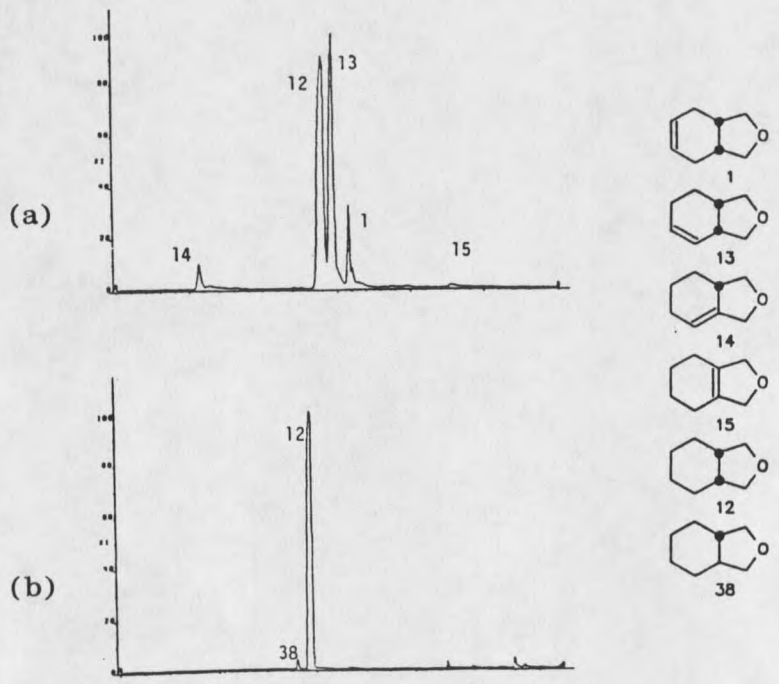

Figure 45. Reaction composition of the hydrogenation (Pd/C) of cis-bicylco[4.3.0]non-3-ene at 3 minutes (a) and 15 minutes (b).

The mechanisms of olefin hydrogenations are complex and many details are still unknown, however, a mechanism proposed long ago by Horiuti and Polanyi[60] (Figure 46) still provides an accurate way of accounting for all aspects of olefin hydrogenation of interest to the organic chemist.

In step (1), hydrogen is disassociately absorbed on two catalyst sites (indicated by asterisk). These sites need not be on different atoms. The olefin is then diabsorbed onto two adjacent sites as shown in step (2). In step (3), a hydrogen atom adds to one carbon leaving a monoabsorbed species and subsequent addition of a second hydrogen atom forms the reduced alkane which is deabsorbed from the catalyst (step 5). Olefin migration will occur if the monabsorbed species returns to a diabsorded species different than the original as shown in step (4), followed by deabsorbtion (step (2) in reverse). All steps except the last are thought to be reversible.

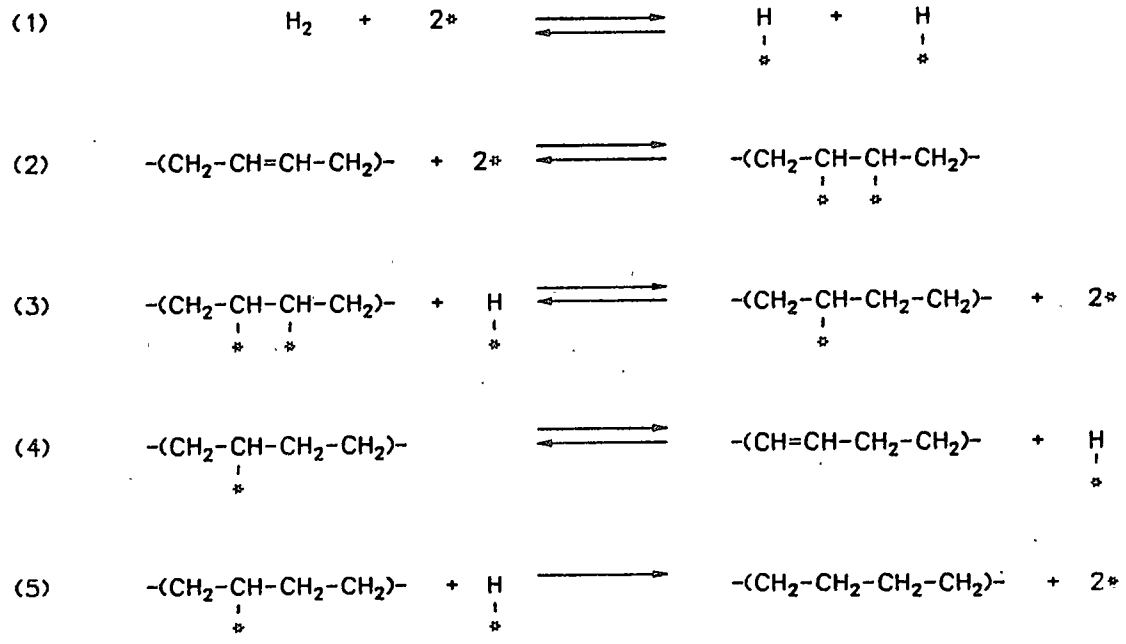

Figure 46. Polanyi's hydrogenation mechanism.

Because olefin migration during catalytic hydrogenation is considered to be an equilibrium process, calculational approaches were employed to investigate the thermodynamic stabilities of olefins [**1**], [**13**], [**14**], and [**15**]. Table 21 lists the MM2 generated steric energies (ES) and olefinic strain energies (OS). The OS is the energy difference between the olefin and the parent hydrocarbon both in their most stable conformations. All reasonable conformations for each compound were examined, and the most stable conformations are reported. These energies are believed to be those of the global minima however there is no rigorous way to demonstrate this belief.

Table 21. MM2 Calculated Energies (Kcal/mole)

Olefin	ES	OS
1	10.14	1.99
13	7.02	-1.13
14	6.94	-1.21
15	5.04	-3.11
Parent Hydrocarbon		
12	8.15	—

Recently Schleyer[61,62], et. al., has defined a class of "hyperstable olefins", medium sized polycyclic ring systems with bridgehead double bonds that have negative OS energies. These olefins have low heats of hydrogenation. Some, having OS energies less than approximately -13 Kcal/mole, are completely resistant to hydrogenation.[63,64,65] This reduced thermodynamic driving force, "hyperstability", has been used to explain the

difficulties in hydrogenating these compounds. In addition, the steric hindrance inhibiting the approach of substituted olefins to the catalyst surface has also been used to account for the difficulties in hydrogenating these olefins.[66,67] Representative examples of these olefins, resisting hydrogenation and exhibiting large hyperstabilities, have recently been reported by Schleyer and others[68], and some representative compounds are illustrated in Figure 47.

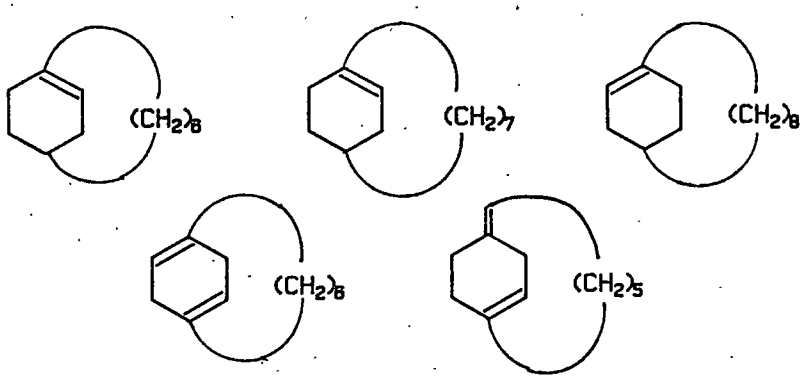

Figure 47. Hyperstable olefins.

Note that olefins [13], [14], and [15] have negative OS energies (Table 21) and therefore also exhibit increasing "hyperstability", a thermodynamic driving force promoting bond isomerization.

Further examination of these olefins by the MNDO method, again, reveals a large thermodynamic driving force promoting bond isomerization (Table 22). The geometries of these olefins were optimized at the SCF level by minimizing the heats of formations with the Davidon-Fletcher-Powel (DFP) algorithm. The initial geometries used in these calculations were those of the global minima as determined by MM2 calculations.

Table 22. MNDO calculated heats of formation (Kcal/mole)

Olefin	H_f
1	-42.90
13	-44.47
14	-47.36
15	-50.43

To further study the olefins involved in this isomerization, HOMO π-bond orders were calculated (Table 23) and HOMO contour plots were examined (Figure 48) by the MNDO method. From an examination of the HOMO π-bond orders of these compounds, it is clear that as the double migrates, the electron densities on the carbons constituting the double bonds are decreasing. **There is a 20% decrease in the HOMO π-bond orders between olefins [1] and [15]!** The molecular orbital are exhibiting increasing electron delocalization, ie. hyperconjugation.

Table 23. HOMO P_z atomic orbital coefficients of olefinic carbonsand HOMO π bond orders.

Olefin	Cp_{zi}	Cp_{zj}	HOMO πBO
1	.65062	.65060	.8466
13	.64978	.64484	.8380
14	-.61811	-.62237	.7694
15	-.58179	-.58200	.6772

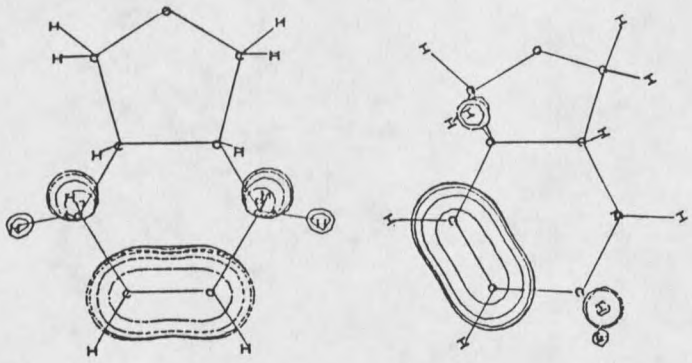

1 **13**

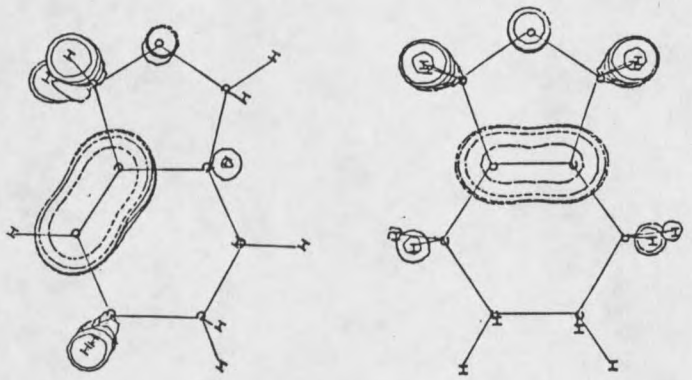

14 **15**

Figure 48. HOMO contour plots of olefins [1], [13], [14], and [15].

From the calculational approaches used to investigate this simple system, there clearly seems to be a strong thermodynamic driving force favoring bond isomerization. This thermodynamic driving force has been calculated by two independent methods, MM2 and MNDO.

In addition, and perhaps more importantly, in this system there also appears to be a strong correlation between increasing "hyperstablility" and decreasing HOMO π-bond order density; as the hyperstability increases the HOMO π-bond order decreases. This leads us to question, does significant electron delocalization, as measured by HOMO π-bond orders, also exit in some of the polycyclic rings systems exhibiting great hyperstability? Schleyer recently has stated, " Empirical force field calculations are the only computational methods which allow total optimization of all conformational isomers of large molecules while consuming modest amounts of computer time".[60] Therefore, these large, conformationally flexible, hyperstable olefins have not as yet been examined by MO calculations and this question remains unanswered.

If delocalization exists in the HOMOs of these olefins, perhaps this hyperconjugation is responsible, in addition to their hyperstabilities (thermodynamic stabilities) and steric hindrances, for the difficulties in the hydrogenating these compounds. As experimental support for this conjecture, recall that the relative stability of **[15]** over **[1]** seemed to be observed in the hydrogenation of **[26]** which yield only the more thermodynamically stable (and hyperstable), **[15]**. This hyperstable olefin was not observed to isomerize and has a HOMO exhibiting significant electron delocalization. Perhaps this delocalization is, in part, a molecular orbital bases for the concept of hyperstability.

An Examination of the Mass Spectrum of cis-8-oxabicyclo[4.3.0]non-3-ene

Mass spectroscopy was widely accessed to aid in the characterization of the various compounds appearing in this thesis. Because compounds [1] and [7] were the "parent" compounds of these investigations (compounds from which all others were derived), their mass spectra were routinely acquired and examined. The mass spectra of [1] and [7] are shown below in Figures 49 and 50.

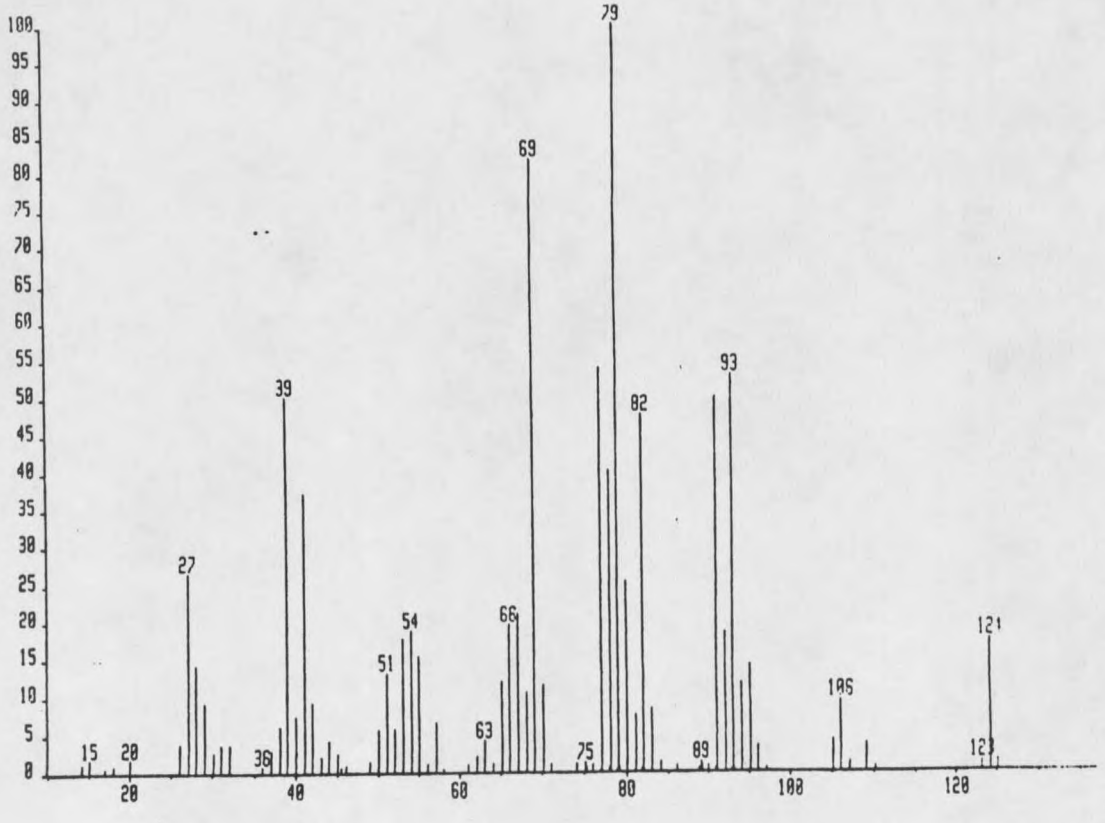

Figure 49. 70 eV EI mass spectrum of cis-8-oxabicycol[4.3.0]non-3-ene, [1].

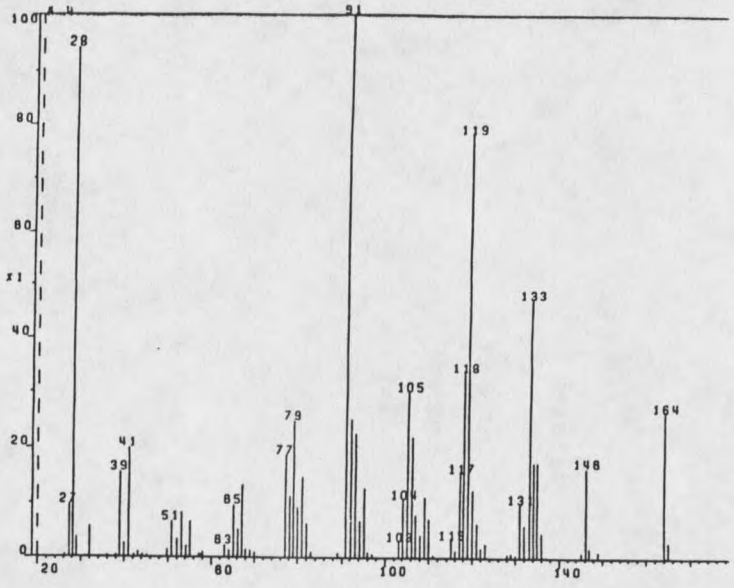

Figure 50. 70 eV EI mass spectrum of 8-oxatricyclo[4.3.3.0]undec-3-ene, [**7**].

Note that in the spectrum of each compound, a loss of water is observed. It is obvious as to where the oxygen originates in this loss; there is only one oxygen in each compound. But where do the hydrogens originate?

Assuming a similar mechanism accounts for the loss of water in each compound, one could rule out the ring-juncture protons. These protons do not exist in [**7**]. Then, by the process of elimination, there are only three remaining proton positions in [**1**]. Equivalent protons exist at C_2-C_5, at C_7-C_9, and at the vinyl positions.

To address the question as to where the protons originate in the loss of water, a series of deuterium labelled analogues of [**1**] were prepared. In this series, the C_2-C_5 positions were deuterium labeled to form [**42**], the C_7-C_9 positions were deuterium labelled to form [**43**], and both these

positions were labelled to form [**44**]. These compounds are illustrated below (Figure 51). From an examination of the mass spectra of these compounds, it was hoped that the major ions in the spectrum of [1] (m/z = 93, 79, and 69) could be identified in addition to the question as to the loss of water.

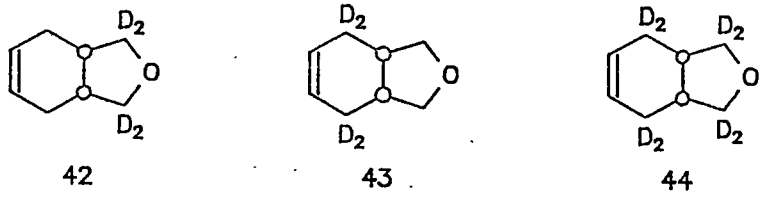

Figure 51. Deuterium labeled analogues of cis-8-oxabicyclo[4.3.0]non-3-ene, [1].

In the synthesis of [**42**], cis-tetrahydrophthalic anhydride, [**16**], was reduced with LAD in THF. The resulting deuterium labelled diol was then ring-closed with TsCl in pyridine (Figure 52).

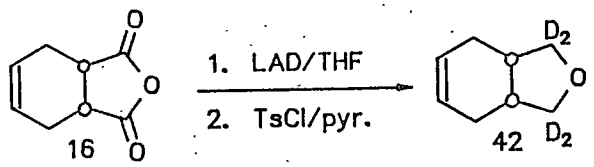

Figure 52. Synthesis of cis-7,7,9,9-tetradeutero-8-oxabicyclo[4.3.0]non-3-ene, [**42**].

In the syntheses of [**43**] and [**44**], butadiene sulfone was dissolved in deuterium oxide to which was added a catalytic amount of metal sodium. After stirring this solution for 48 hrs at room temperature, ^{1}HNMR indicated that deuterium exchange had occurred in high yield (>95%). The deuterium labelled butadiene sulfone, [**46**], was then refluxed with maleic anhydride in xylene to yield the Diels-Alder product, [**47**]. Reduction of [**47**] with LAH in THF followed by ring-closure with TsCl in pyridine results in [**43**]. Similarly, reduction of [**47**] with LAD in THF followed by ring-closure with TsCl in pyridine results in [**44**]. Figure 53 outlines these syntheses.

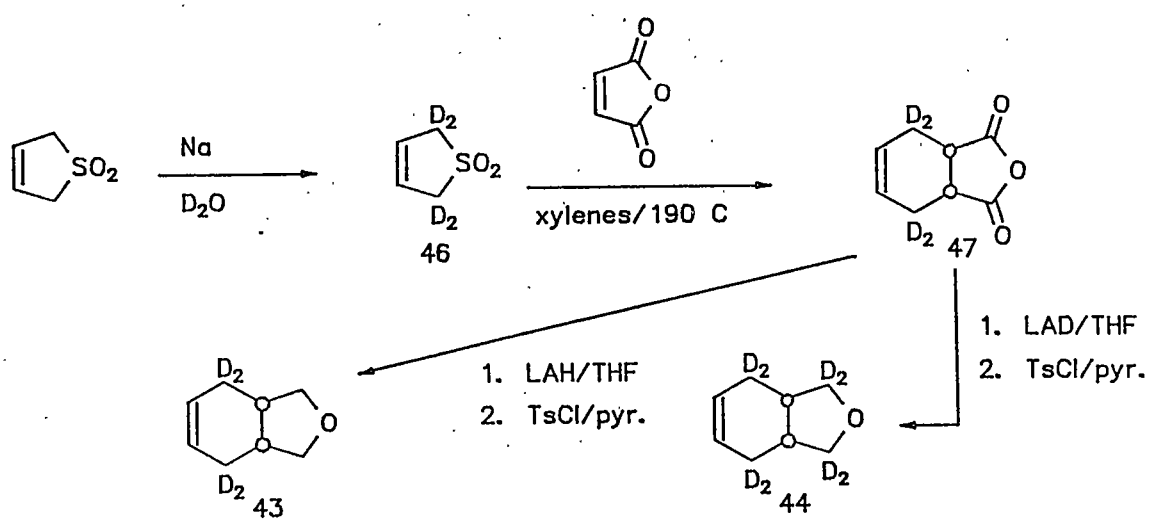

Figure 53. Syntheses of cis-2,2,5,5-tetradeutero-8-oxabicyclo-[4.3.0]non-3-ene, [**43**] and cis-2,2,5,5,7,7,9,9-octadeutero-8-oxabicylo[4.3.0]non-3-ene, [**44**].

The electron impact (EI) mass spectra of these compounds are illustrated below in Figures 54-56.

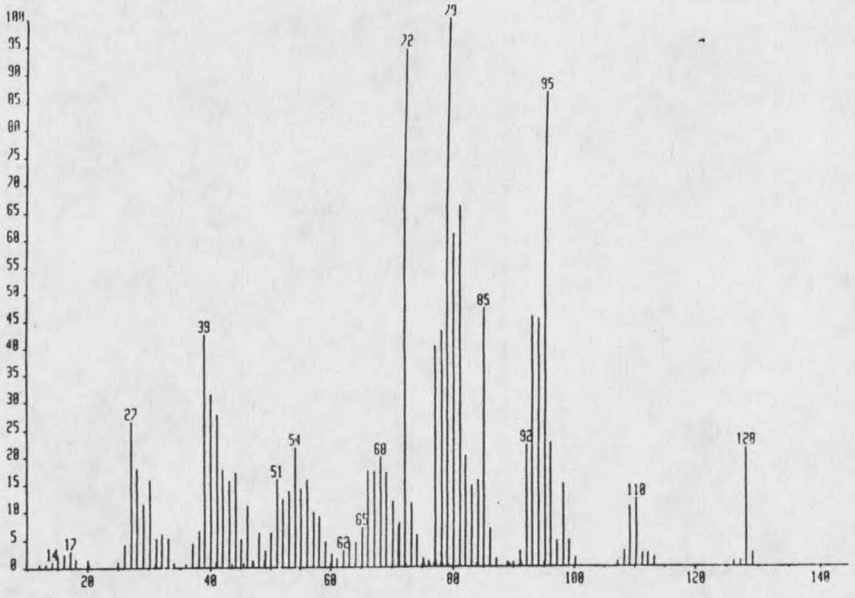

Figure 54. 70 eV EI mass spectrum of cis-7,7,9,9-tetradeutero-8-oxabicyclo[4.3.0]non-3-ene, [**42**].

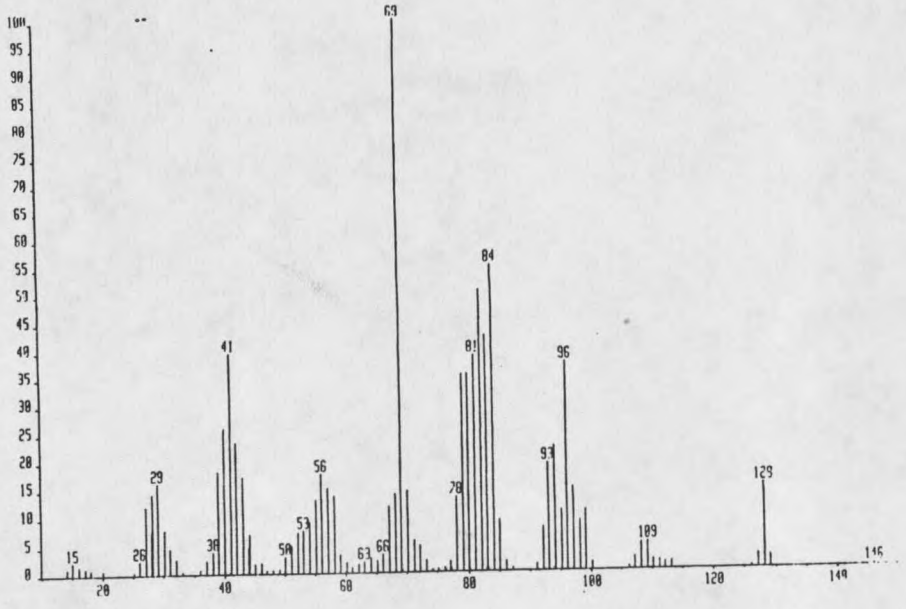

Figure 55. 70 eV EI Mass Spectrum of cis-2,2,5,5-tetradeutero-8-oxabicyclo[4.3.0]non-3-ene, [**43**].

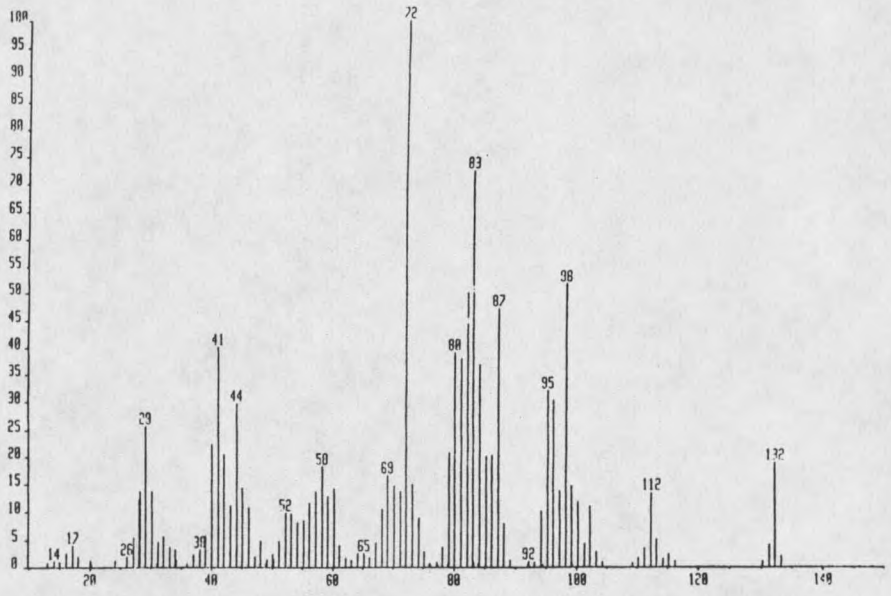

Figure 56. 70 eV EI Mass Spectrum of cis-2,2,5,5,7,7,9,9-octadeutero-8-oxabicylo[4.3.0]non-3-ene, [**44**].

From an examination of these spectra, it appears that there is a loss of 18, (H_2O), in [**1**] and a loss of 20 (D_2O) in [**44**]. While in [**42**], there appears to be the loss of 18 (H_2O) and 19 (HDO) and in [**43**] there appears to the loss of 19 (HDO) and 20 (D_2O).

These data suggest that the loss of water results from at least two different processes. In the loss of 18 from [**42**], the two protons appear to originate from the C_2-C_5 position. While in the loss of 19 from [**42**], a proton appears to originate from the C_2-C_5 position and a deuterium atom appears to originate from the C_7-C_9 position. Similarly, in the loss of 20 from [**43**] two deuterium atoms appear to originate from the C_2-C_5 position. While in the loss of 19 from [**43**], a deuterium atom appears to originate from the C_2-C_5 position and a proton appears to originate from the C_7-C_9 position.

Note the second loss in [1], [42], [43], and [44]. In [1] this loss results in a ion m/z = 93, in [42] m/z = 95, in [43] m/z = 96, and in [44] m/z = 98. This is a loss of 31 for [1], 33 for [42], 32 for [43], and 34 for [44]. These data suggest the losses of ($HOCH_2$), ($HOCD_2$), ($DOCH_2$), and ($DOCD_2$), respectively, for [1], [42], [43], and [44]. The following mechanism, illustrated on [1], appears to account for all of the observed losses (Figure 57).

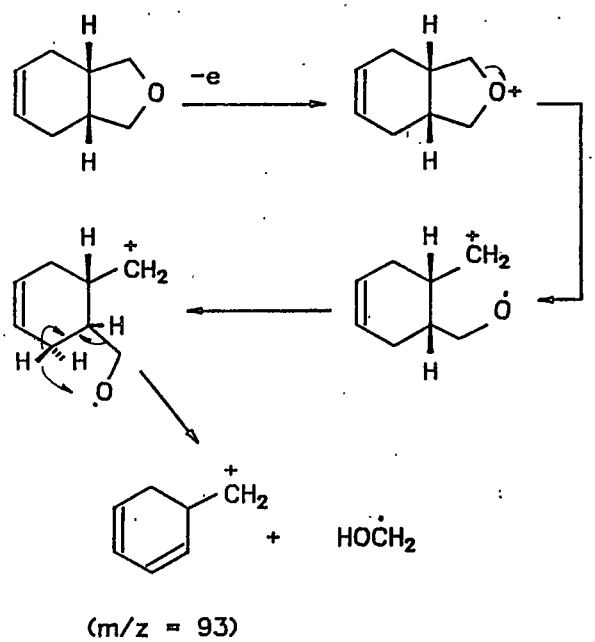

Figure 57. Loss of $HOCH_2$ from cis-8-oxabicyclo[4.3.0]non-3-ene, [1].

Note the major ion, m/z = 69, in [1] and [42] This ion seems to correspond to the major ion, m/z = 72 in [43] and [44]. These ions are the result of a loss of 55, 56, 59, and 60, respectively, for [1], [42], [43], and [44]. These data suggest the loss of (CH_3-CH=CH-CH_2) for [1], (CH2D-CH=CH-CH_2) for [42], (CD_2H-CH=CH-CD_2) for [43], and CD_3CH=CH-CD_2) for [44]. The following mechanism, again illustrated on [1], seems to account for all of these losses.

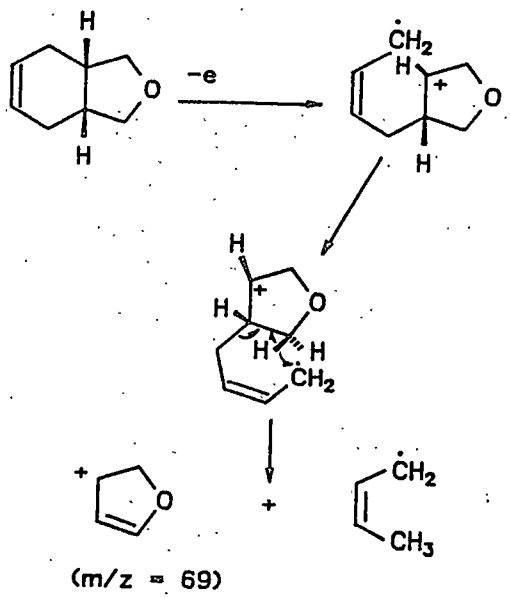

Figure 58. Loss of CH_3-CH=CH-CH2- from cis-8-oxabicyclo[4.3.0]non-3-ene, [1].

Note the loss of the major ion m/z = 79 in [1] and in [**43**]. Note also the major ion m/z = 82 in [**43**] and in [**44**]. These ions are the result of a loss of 45 in [1], 49 in [**42**], 46 in [**43**] and 50 in [**44**]. These data suggest the loss of (CH_3-O-CH_2), (CHD_2-O-CD_2), (CH_2D-O-CH2), and (CD_3-O-CD_2), respectively, for [1], [**42**], [**43**], and [**44**]. A mechanism accounting for all these observed losses is illustrated for [1] in Figure 59.

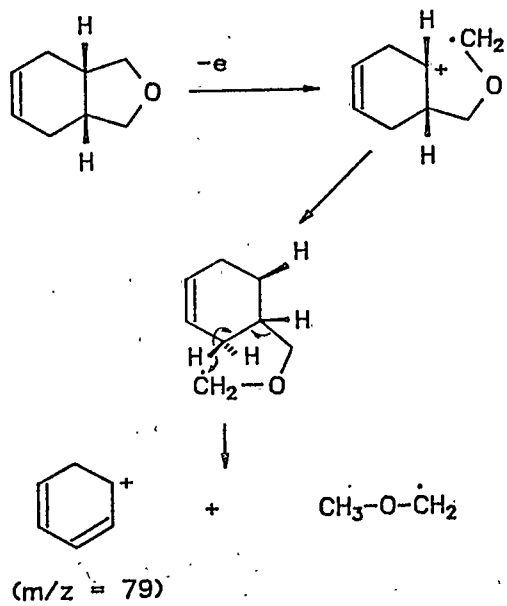

Figure 59. Loss of CH_3-O-CH_2 from cis-8-oxabicyclo[4.3.0]non-3-ene, [1].

From this study, the oxygen atom's role in a number of fragmentation processes have been studied. The major ions in the (EI) mass spectrum of [1] have been determined and mechanisms, illustrating the oxygen atom's role in the fragmentation processes, have been proposed.

CHAPTER 3

CONCLUSIONS

Summary of the Research

We have carried out a comprehensive program combining experimental and calculational methods to examine the role the oxygen atom plays in imparting structure and reactivity on a series of oxygen containing heterocycles. These studies have clearly and elegantly addressed a number of fundamental questions which are summarized below.

An absence of stereoselectivity was observed in a number of electrophilic additions conducted on [7]. This was interpreted to mean the oxygen atom does not influence stereoselectivity in this system. These results are consistent with calculation studies conducted on [7] which suggest: (1) The π-faces of the double bond are sterically equivalent (because the two anticipated boat conformations of [7] are energetically equivalent and therefore both conformations exist in approximate equal equilibrium abundance). (2) These conformations have HOMOs of equal energy and therefore should have identical reactivities. (3) There is no contribution by the oxygen atom in the HOMOs of these conformations which could have possibly directed the initial electrophilic addition (based upon hard and soft acid base theories).

The modest stereoselectivity observed in a number of electrophilic additions conducted on [1] were attributed to the steric nonequivalence of the π-faces of the double bond. The initial electrophilic attack appears to

occur on the less sterically hindered face anti to the oxygen atom.

Identical reactivities and products (a mixture of alkenes and the completely inverted alcohol and methoxy compounds) were observed in the solvolysis of the syn- and anti-tosylates of [1]. This was interpreted to mean the oxygen atom is not involved in influencing the reactivity of these compounds. A reaction scheme, involving the formation of an intimate ion pair (IIP) in the rate determining step of the reaction followed by partitioning into various reaction pathways of elimination and substitution, was proposed to describe these processes.

A subtle rate enhancement (1.53) was observed for the anti-tosylate derived from [7] relative to the syn-isomer. In addition to a mixture of alkenes and completely inverted alcohol and methoxy compounds (found in the syn-isomer), a methoxy compound, apparently resulting from a 1,2 hydride shift, was observed in the product study of the anti-isomer. A reaction scheme, involving a hydrogen bonded stabilized IIP formed in the rate determining step of the reaction followed by partitioning into reaction pathways of elimination, substitution, and a 1,2 hydride shift, was proposed to rationalize the rate enhancement. While, a reaction scheme identical to that proposed in the bicyclic tosylates was used to describe the syn-tosylate of [7].

Modest stereoselectivity (3 : 1) was observed in the catalytic hydrogenation of [35]. Although the absolute stereochemistries of the products were not determined, as a preliminary investigation, this data seems to suggest an oxygen/catalyst interaction directing the hydrogenation. This interaction was previously suggested by Otzenberger and Wilkening.

The olefins resulting from double bond isomerization during the catalytic hydrogenation of [1] were characterized. An examination of their thermodynamic stabilities, by the MM2 and MNDO methods, revealed a thermodynamic driving force promoting the bond isomerization. A correlation between the hyperstability (a measure of thermodynamic stability as determined by MM2 calculations) of these compounds and their HOMO π-bond orders was observed. As hyperstability increased, the HOMO π-bond orders decreased (the HOMOs experienced more electron delocalization). This electron delocalization was used, along with the increased thermodynamic stability and steric hindrance to rationalize the difficulty in hydrogenating hyperstable olefins.

The major ions in the EI mass spectra of [1] were determined by an examination of a series of deuterium labelled analogues of [1], which were synthesized.

Suggested Future Work

An obvious extension of this work would be to prepare the nitrogen and sulfur analogues of [1] and [7] and determine the role of the nitrogen and sulfur atoms in influencing the stereochemistry of electrophilic additions to these alkenes. In addition, an examination of the solvolysis of the tosylates derived from these compounds would also illuminate the nitrogen and sulfur atoms role in imparting reactivity on the molecule in these rather conformationally rigid systems. Because the lone pair electron orbitals of these heteroatoms are more polarizable than oxygen, one would expect greater influences in imparting both stereochemistry and reactivity on the molecule than was observed in this work.

It would also be interesting to examine the role the oxygen atom plays in influencing structure and reactivity in a more conformationally flexible system. A system in which to address this question is 8,12-bioxatricylo[4.3.5.0]tetradec-3-ene and the tosylates derived from this alkene. Here, because far greater conformational flexibility exists (as compared to [7]), the oxygen atom has the possibility of getting much closer to the reactive site. One might therefore predict a greater influence imparted by the oxygen atom.

To further examine the role the oxygen atom imparts on influencing stereochemistry in catalytic hydrogenations, one should synthesis and subject to catalytic hydrogenation 7,11-dioxa-3-methyltricylo[4.3.3.0]undec-3-ene. Here, one would predict increased reactivity towards hydrogenation relative to [**35**]. If this is indeed the case, additional support for the oxygen/catalyst interaction, providing an entropic rational to account for the increased reactivity of oxygen containing heterocyles would be gained.

An obvious extension to the work correlating hyperstability and π-bond order would be to examine by the MNDO method a number of Schleyer's hyperstable olefins to determine if large electron delocalization exists in the HOMOs of these olefins. This would address the question regarding the universality of the correlation involving hyperstability and HOMO π-bond order.

CHAPTER 4

EXPERIMENTAL

General Procedure for Solvolysis

A glass conductivity cell was treated with para-toluenesulfonic acid (the acid generated upon solvolysis) for 24 hours. The acid solution was then removed from the cell and the cell oven-dried. Then 25 ml of the standard 50% aqueous methanol solution were added to the cell which was then placed in a constant temperature bath and allowed to equilibrate. Upon temperature equilibration, approximately 2 mg of the substrate was added to the cell. The substrate was allowed to dissolve and the temperature equilibrate (2-4 minutes). Upon equilibration, the solvolysis reactions were followed for 3-5 half-lives and, after 15 half lives, an infinity conductance value (c_∞) was measured. The infinity value was checked to insure that it was not changing. If the infinity was changing the kinetic run was repeated. The conductance and temperature measurements were recorded with a Laboratory Interface. This digital to analog converter interfaced the conductivity cell and thermistor to a PC, allowing for simultaneous acquisition of conductance, temperature, and time measurements. Rate constants were calculated by a least-squares treatment of $\ln(c_\infty - c_x)$ vs time (seconds). Correlation coefficients greater than 0.9995 were obtained. Activation parameters were calculated by least squares treatment of ln(k) vs 1/T (K°). Correlation coefficients greater than 0.9998 were obtained. All kinetic experiments were completed using the same

conductance cell.

The products of solvolysis for each tosylate were combined and most of the methanol was removed by gentle column distillation. Then, the residue was extracted several times with dichloromethane, and this solution was dried over $MgSO_4$. Product analyses and peak integrations were obtained by GLC equipped with a DB5.53m-ID capillary column and FID.

Plots of $\ln(c_\infty - c_x)$ vs time (seconds) for the 50% aqueous methanolysis for each tosylate at three different temperatures are illustrated in Figures 60-71. Plots of ln(k) vs $1/T$ (K^{o-1}) for each tosylate are illustrated in Figures 72-75.

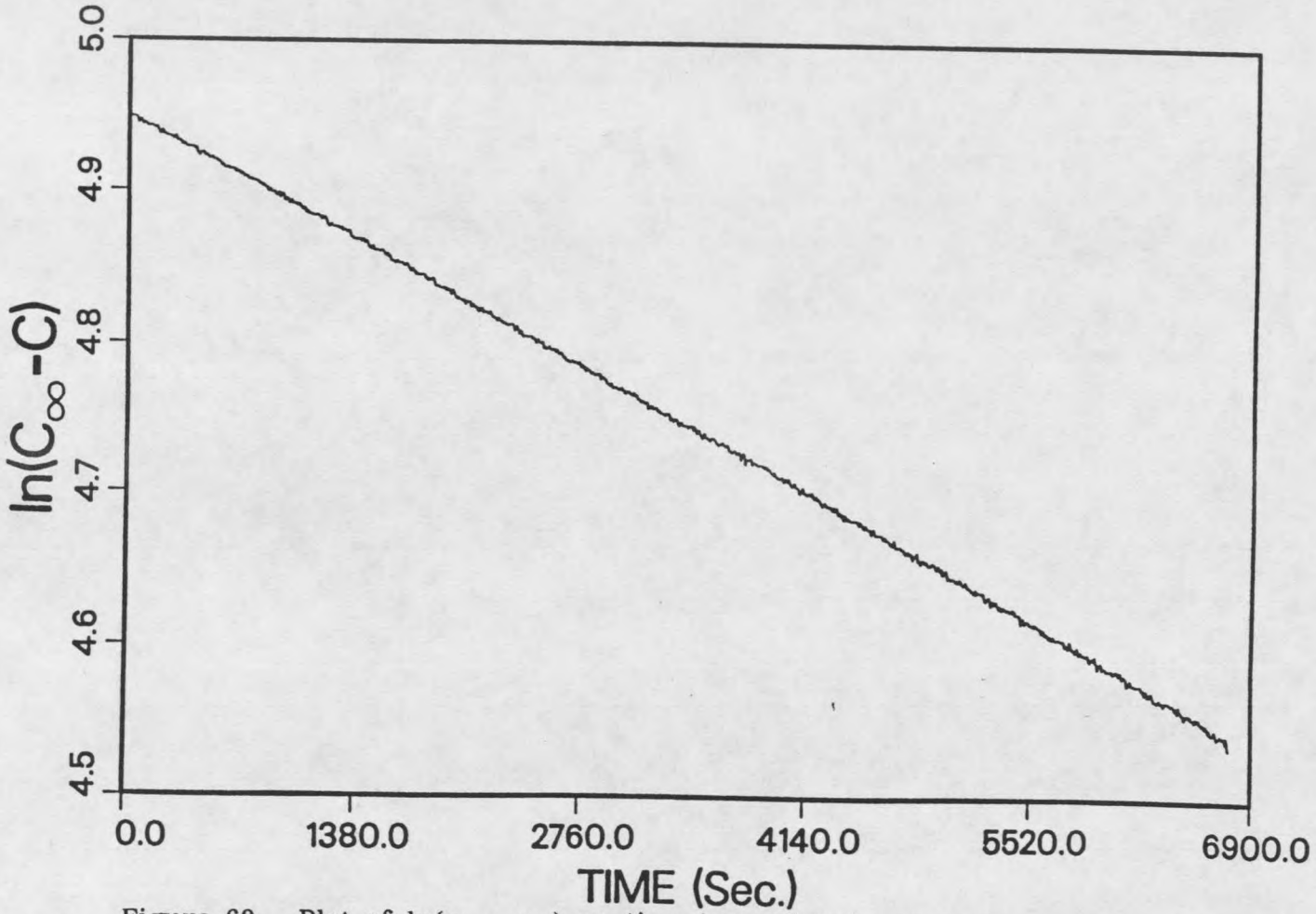

Figure 60. Plot of $\ln(c_{\infty} - c_{x})$ vs time (seconds) for the 50% aqueous methanolysis of [**19**] at 35.84° C. [y = 0.60714 * 10^{-4}x + 4.9517; R = 1.0000].

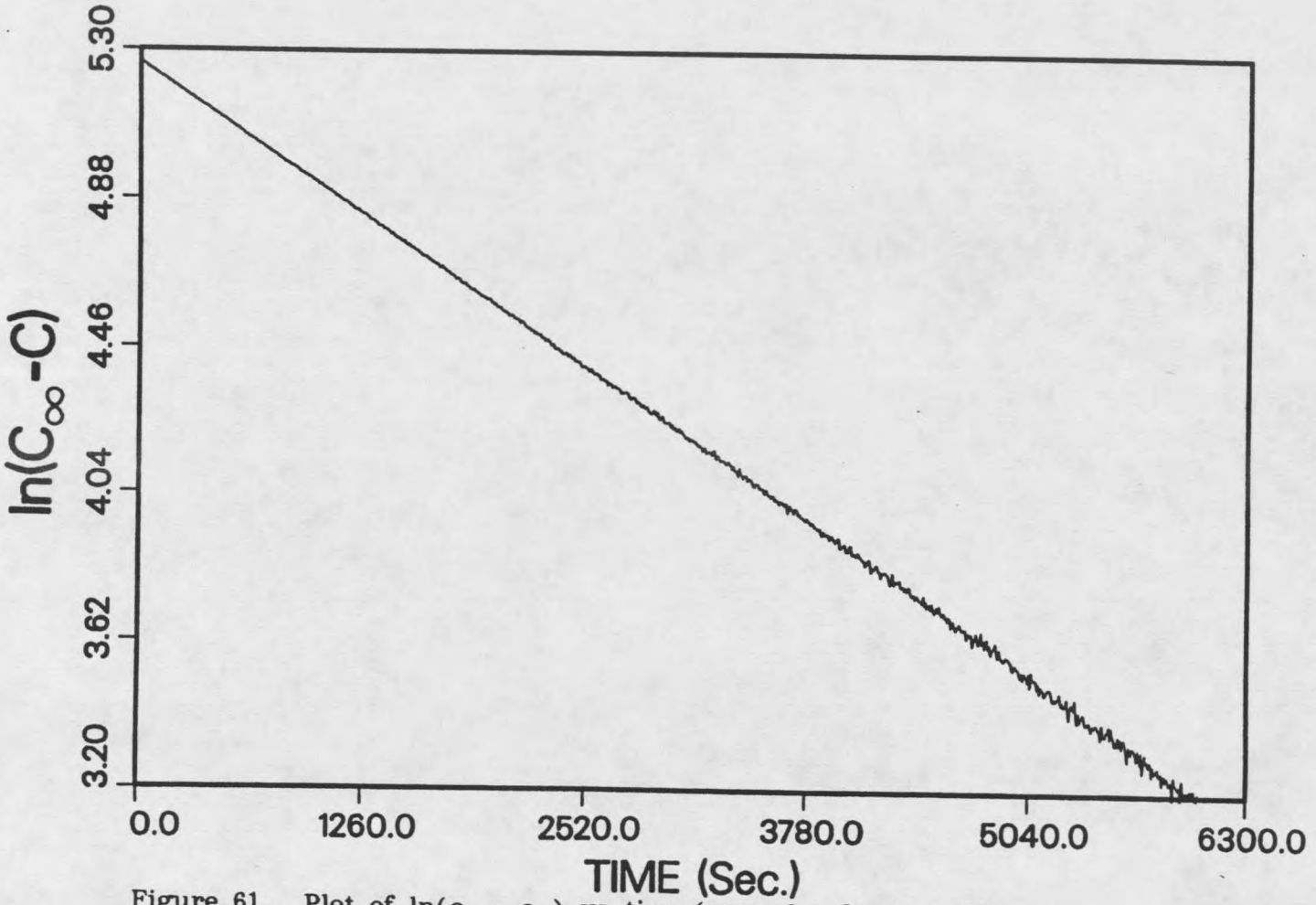

Figure 61. Plot of $\ln(c_{\infty} - c_x)$ vs time (seconds) for the 50% aqueous methanolysis of [**19**] at 50.00° C. [y = 3.47144 * 10^{-4}x + 5.2682; R = 1.0000].

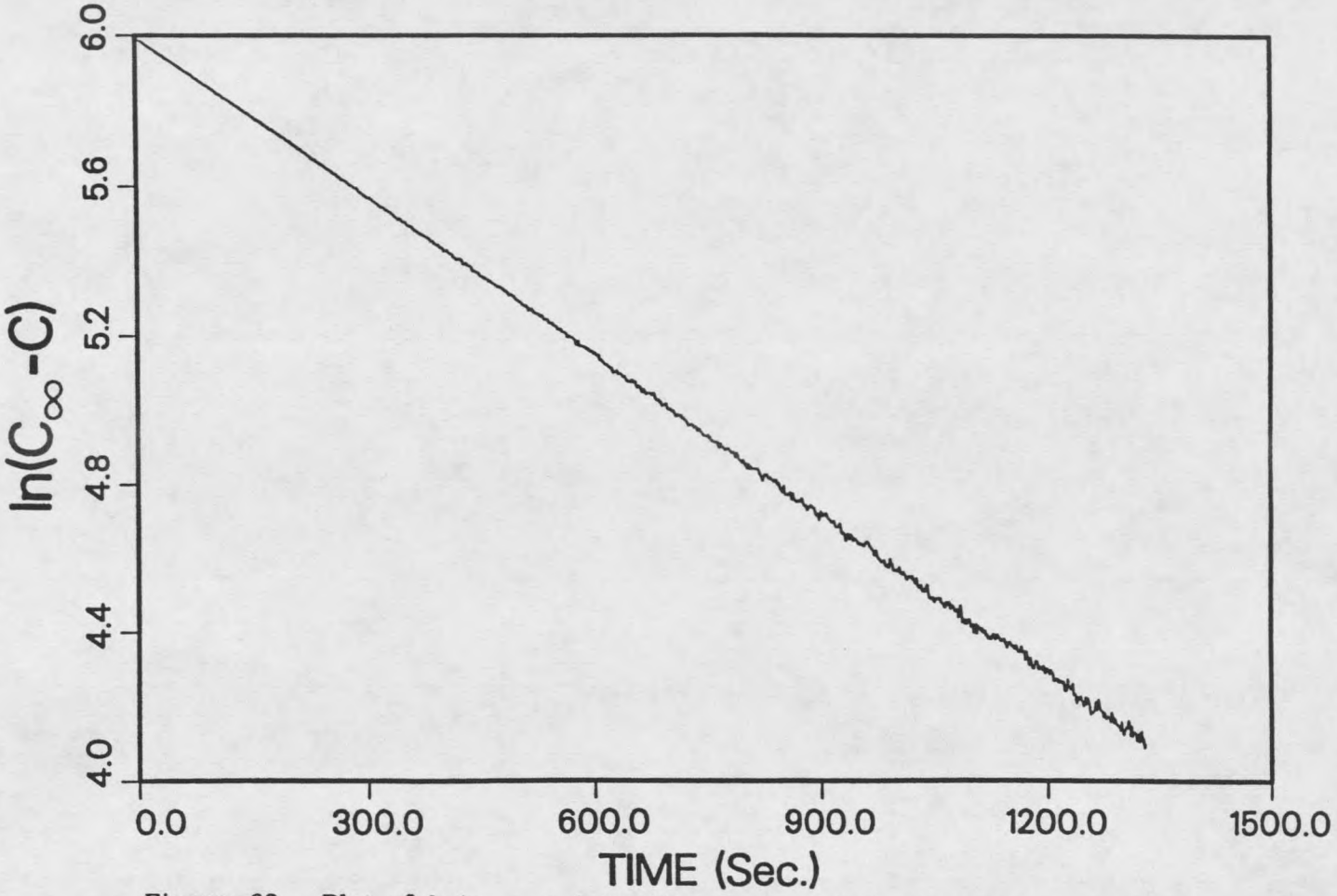

Figure 62. Plot of $\ln(c_\infty - c_x)$ vs time (seconds) for the 50% aqueous methanolysis of [**19**] at 62.87° C. [y = 14.314 * 10^{-4}x + 5.9913; R = 1.0000].

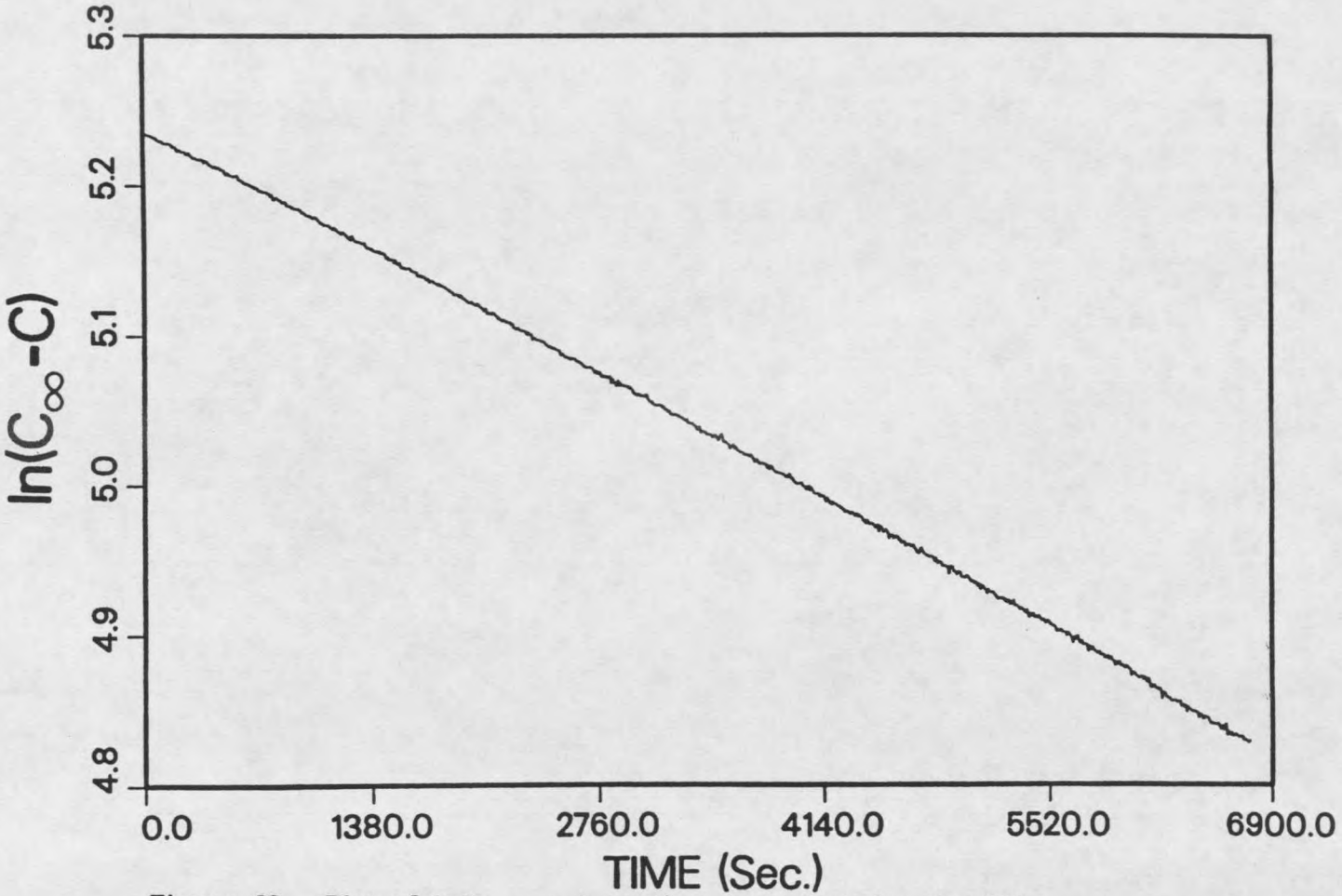

Figure 63. Plot of $\ln(c_{\infty} - c_x)$ vs time (seconds) for the 50% aqueous methanolysis of [**31**] at 35.78° C. [y = 0.60730 * 10^{-4}x + 5.2310; R = 0.9999].

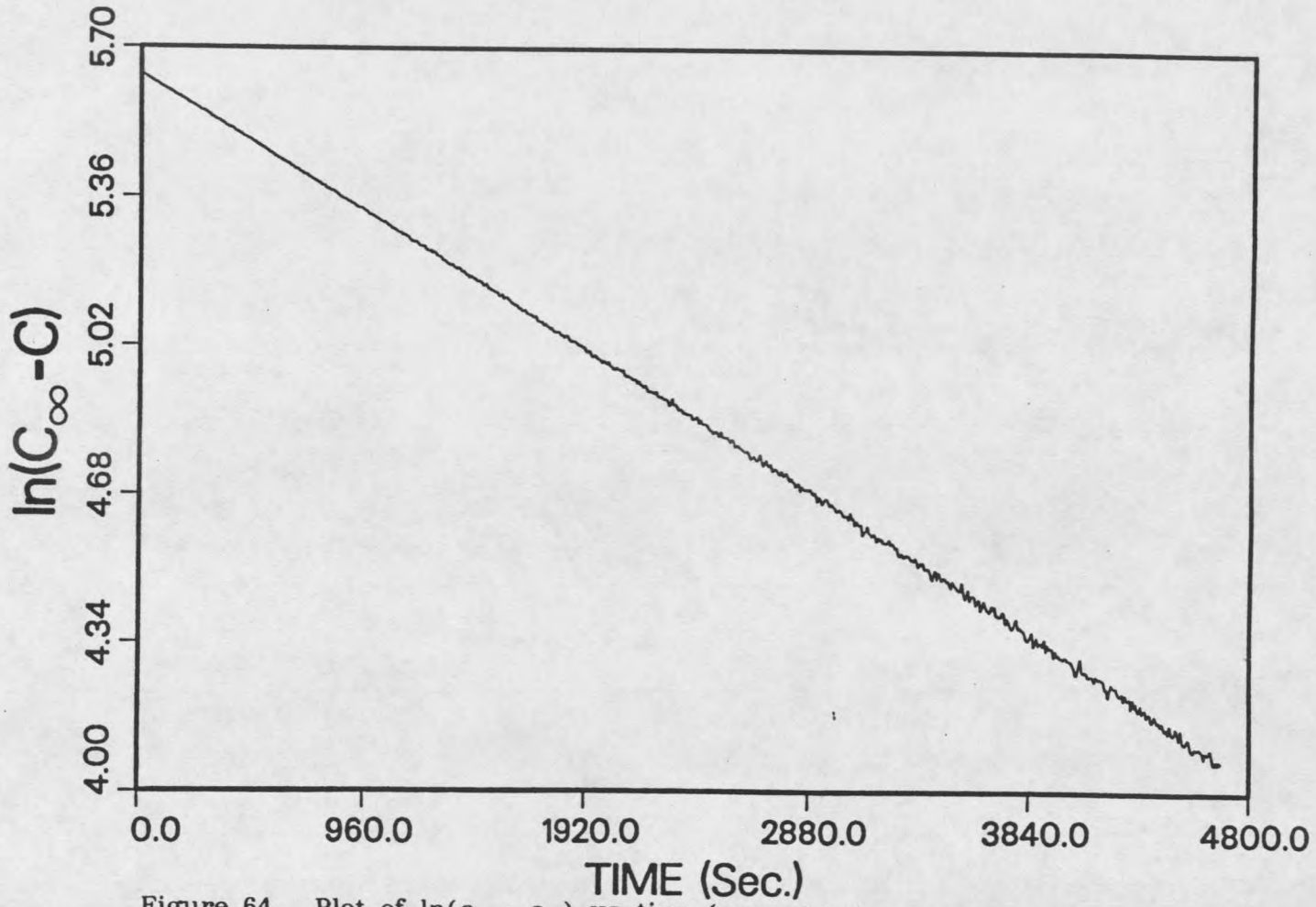

Figure 64. Plot of $\ln(c_{\infty} - c_x)$ vs time (seconds) for the 50% aqueous methanolysis of [**31**] at 50.20° C. [$y = 3.3231 * 10^{-4}x + 5.6252$; $R = 0.9996$].

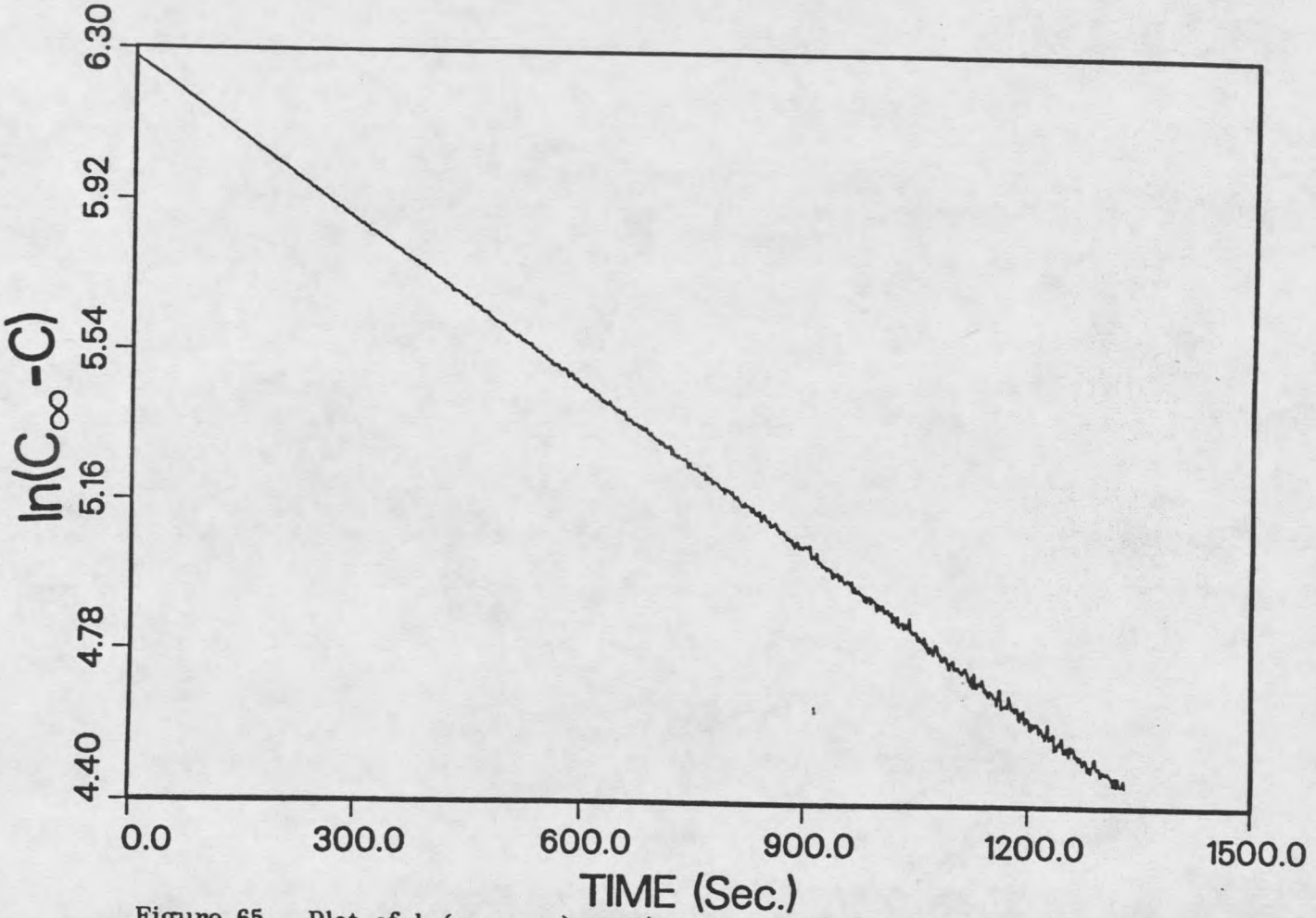

Figure 65. Plot of $\ln(c_{\infty} - c_x)$ vs time (seconds) for the 50% aqueous methanolysis of [31] at 63.00° C. [y = 13.912 * 10^{-4}x + 6.2719; R = 1.0000].

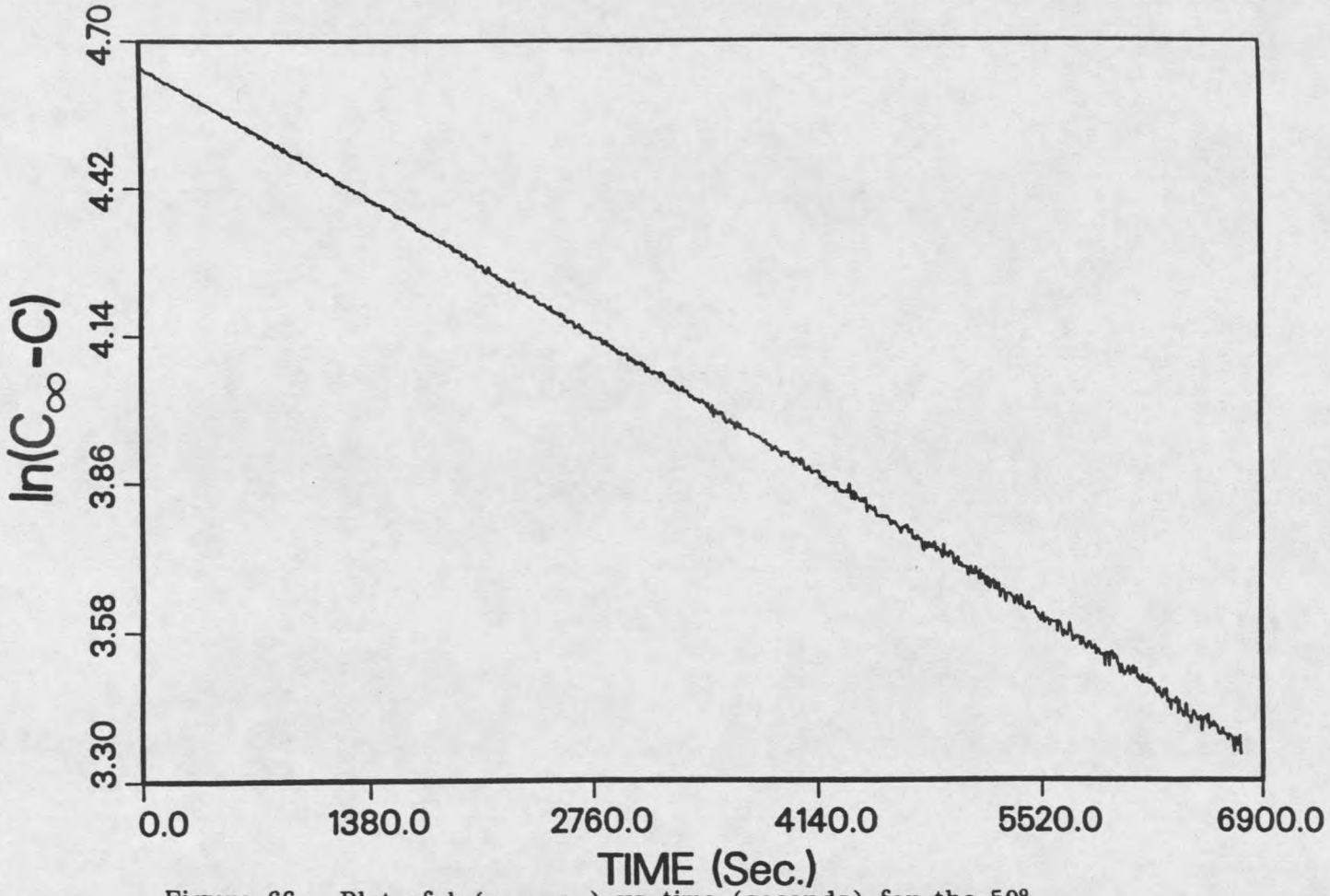

Figure 66. Plot of $\ln(c_{\infty} - c_x)$ vs time (seconds) for the 50% aqueous methanolysis of [**24**] at 35.82° C. [y = 1.9123 * 10^{-4}x + 4.6321; R = 0.9999].

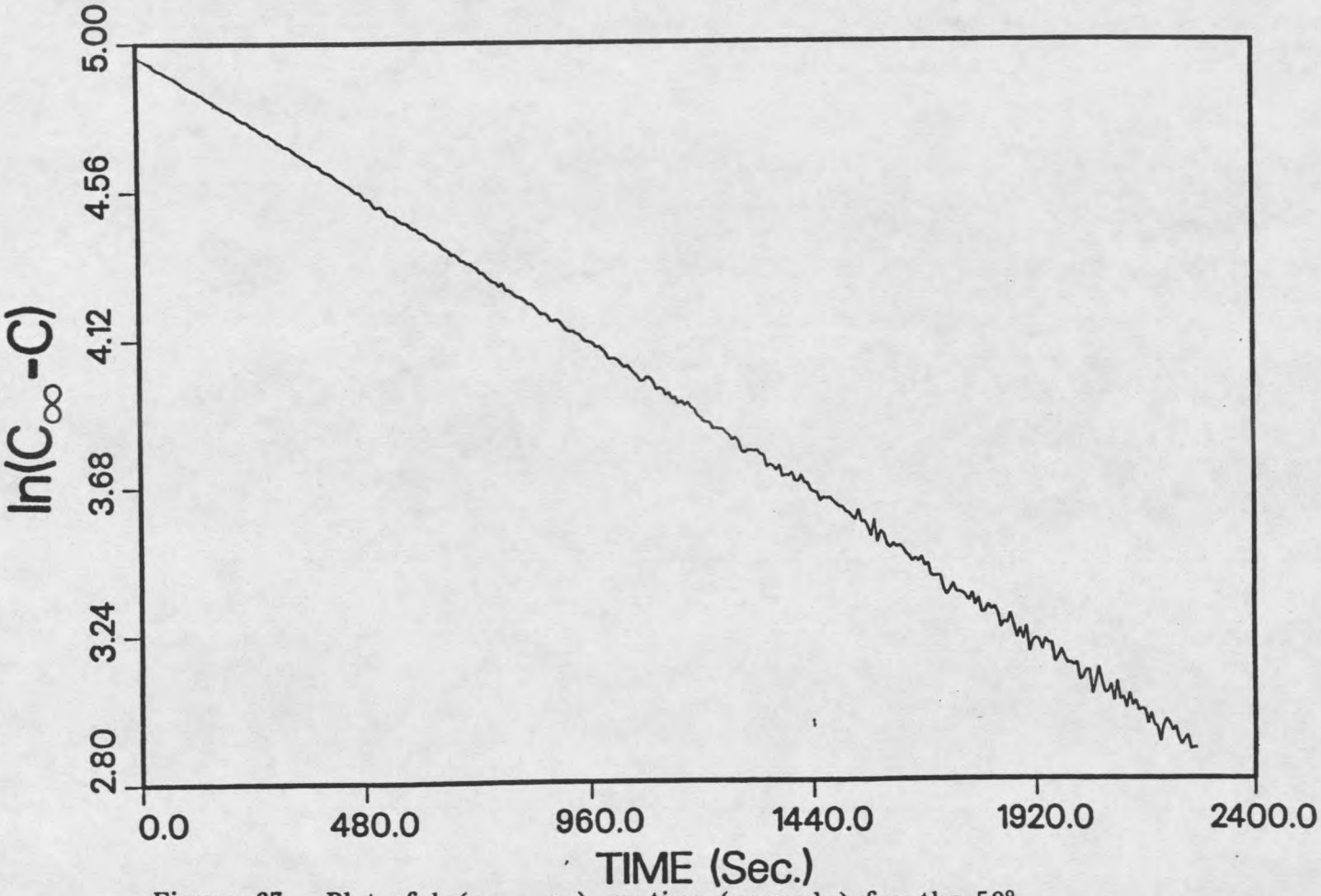

Figure 67. Plot of $\ln(c_{\infty} - c_x)$ vs time (seconds) for the 50% aqueous methanolysis of [**24**] at 50.10° C. [y = 9.3501 * 10^{-4}x + 4.9987; R = 0.9998].

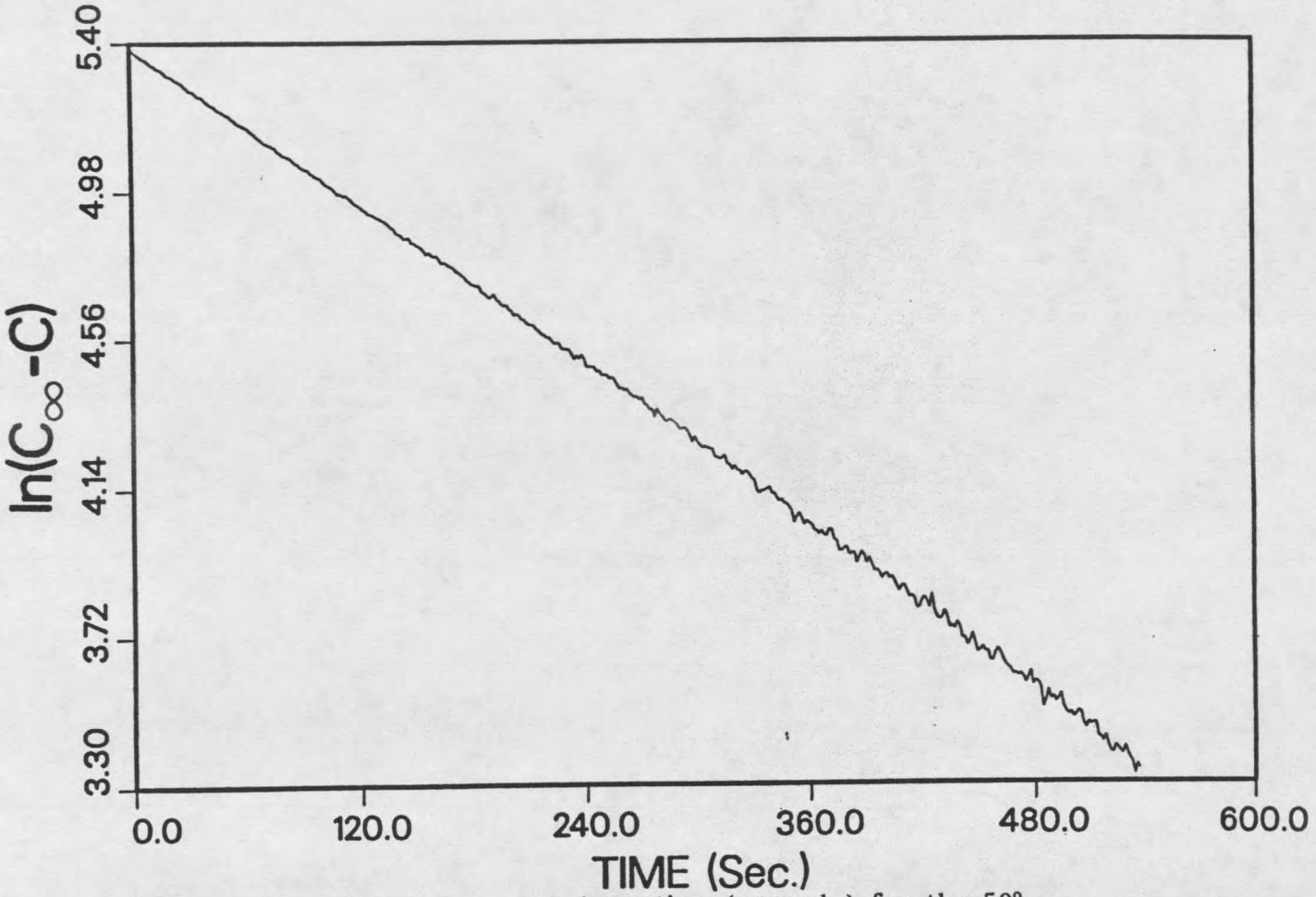

Figure 68. Plot of $\ln(c_\infty - c_x)$ vs time (seconds) for the 50% aqueous methanolysis of [24] at 63.00° C. [y = 37.923 * 10^{-4}x + 45.3860; R = 1.0000].

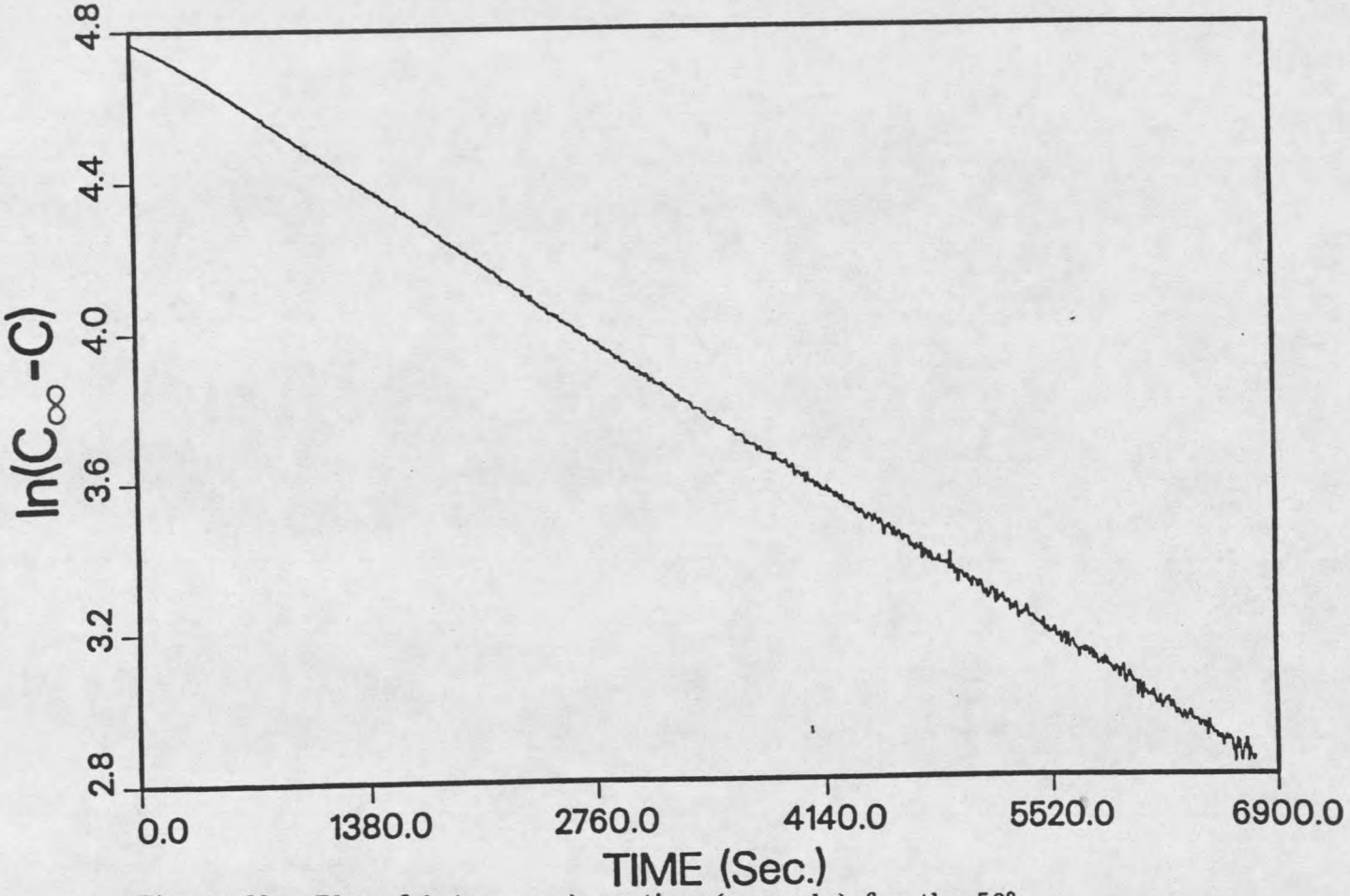

Figure 69. Plot of $\ln(c_{\infty} - c_x)$ vs time (seconds) for the 50% aqueous methanolysis of [**32**] at 35.70° C. [$y = 1.4270 * 10^{-4}x + 4.9175$; $R = 0.9999$].

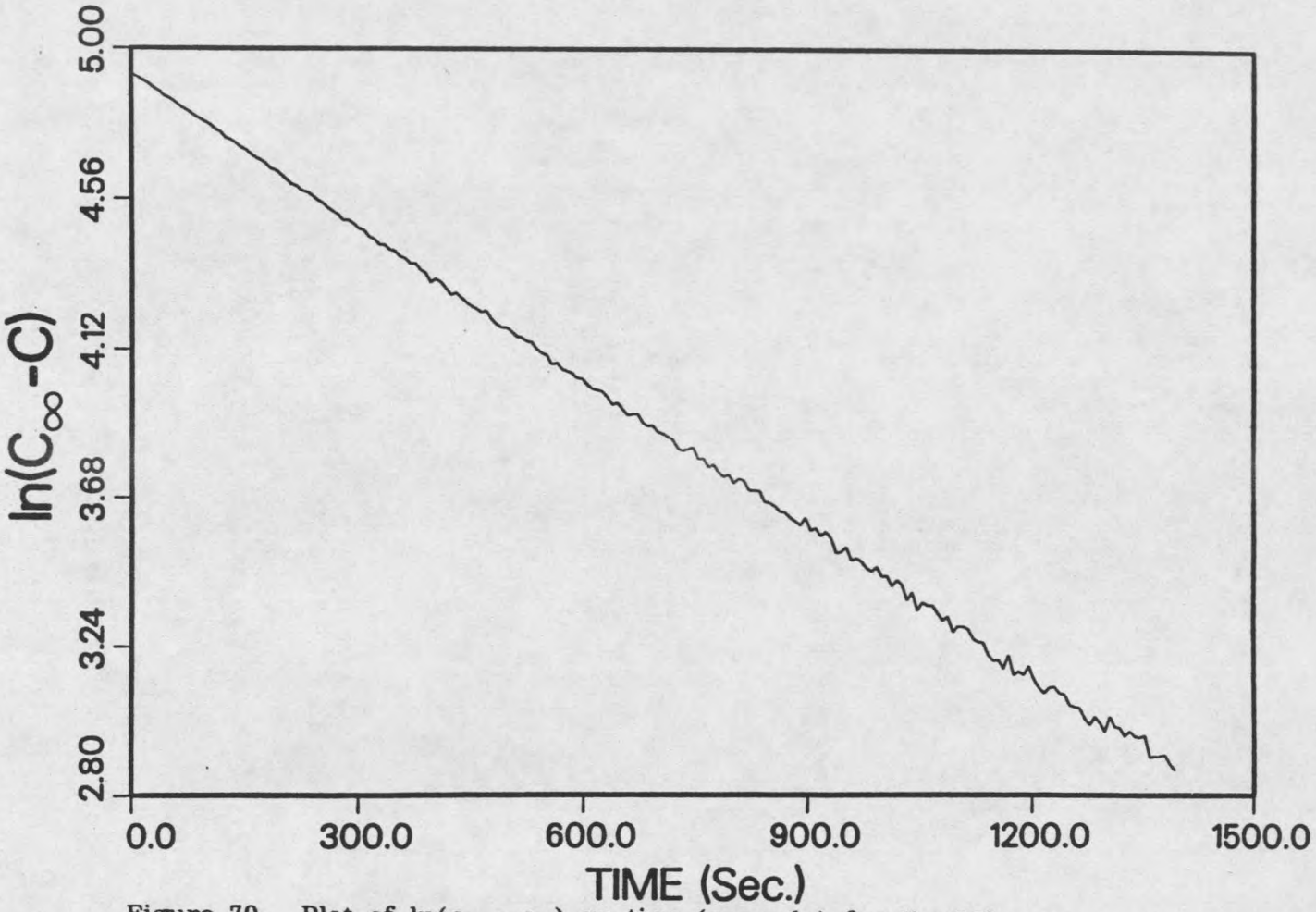

Figure 70. Plot of $\ln(c_\infty - c_x)$ vs time (seconds) for the 50% aqueous methanolysis of [**32**] at 50.15° C. [$y = 2.9031 * 10^{-4}x + 4.7612$; $R = 0.9999$].

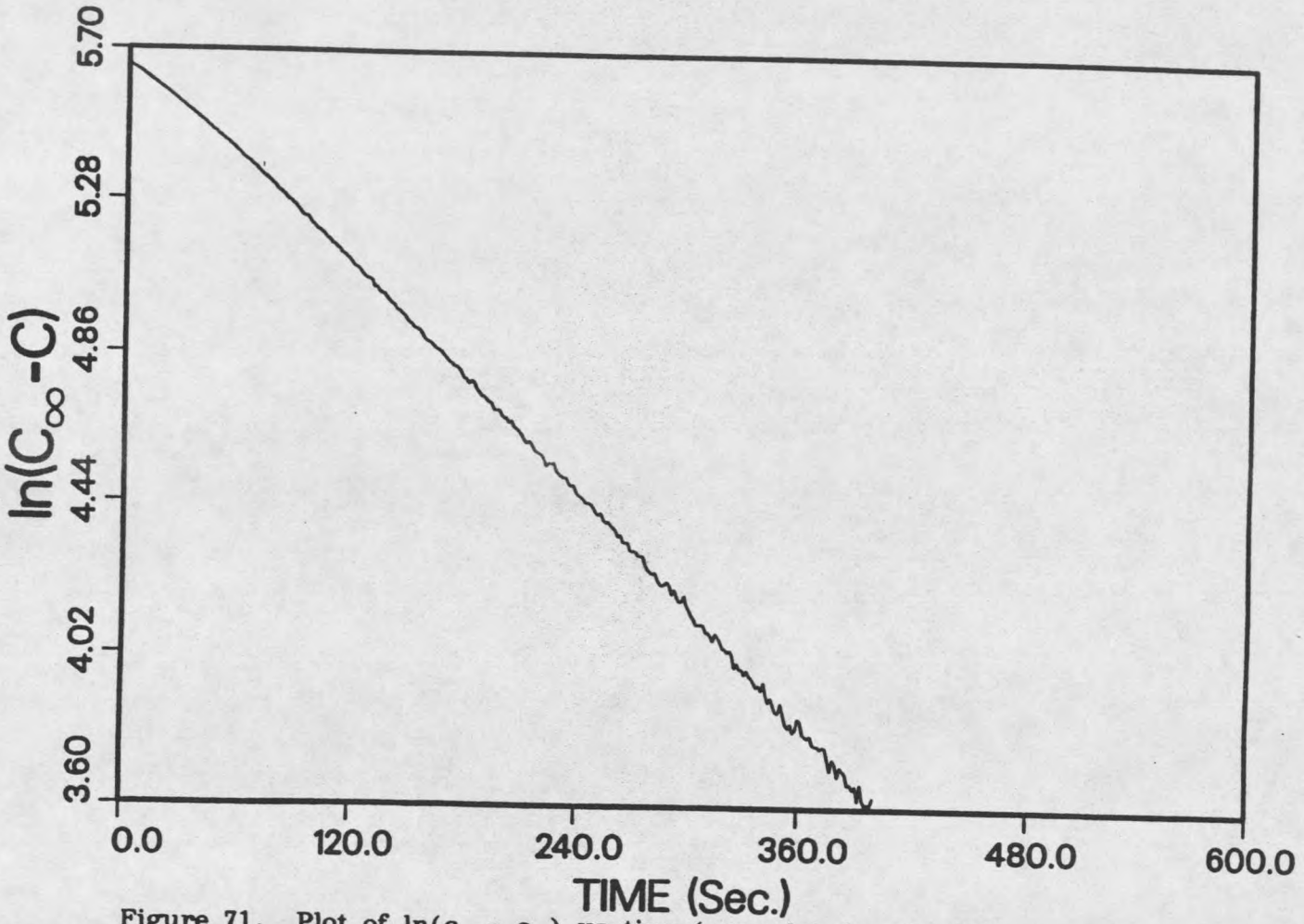

Figure 71. Plot of $\ln(c_{\infty} - c_x)$ vs time (seconds) for the 50% aqueous methanolysis of [**32**] at 62.90° C. [$y = 52.731 * 10^{-4}x + 5.6532$; $R = 0.9997$].

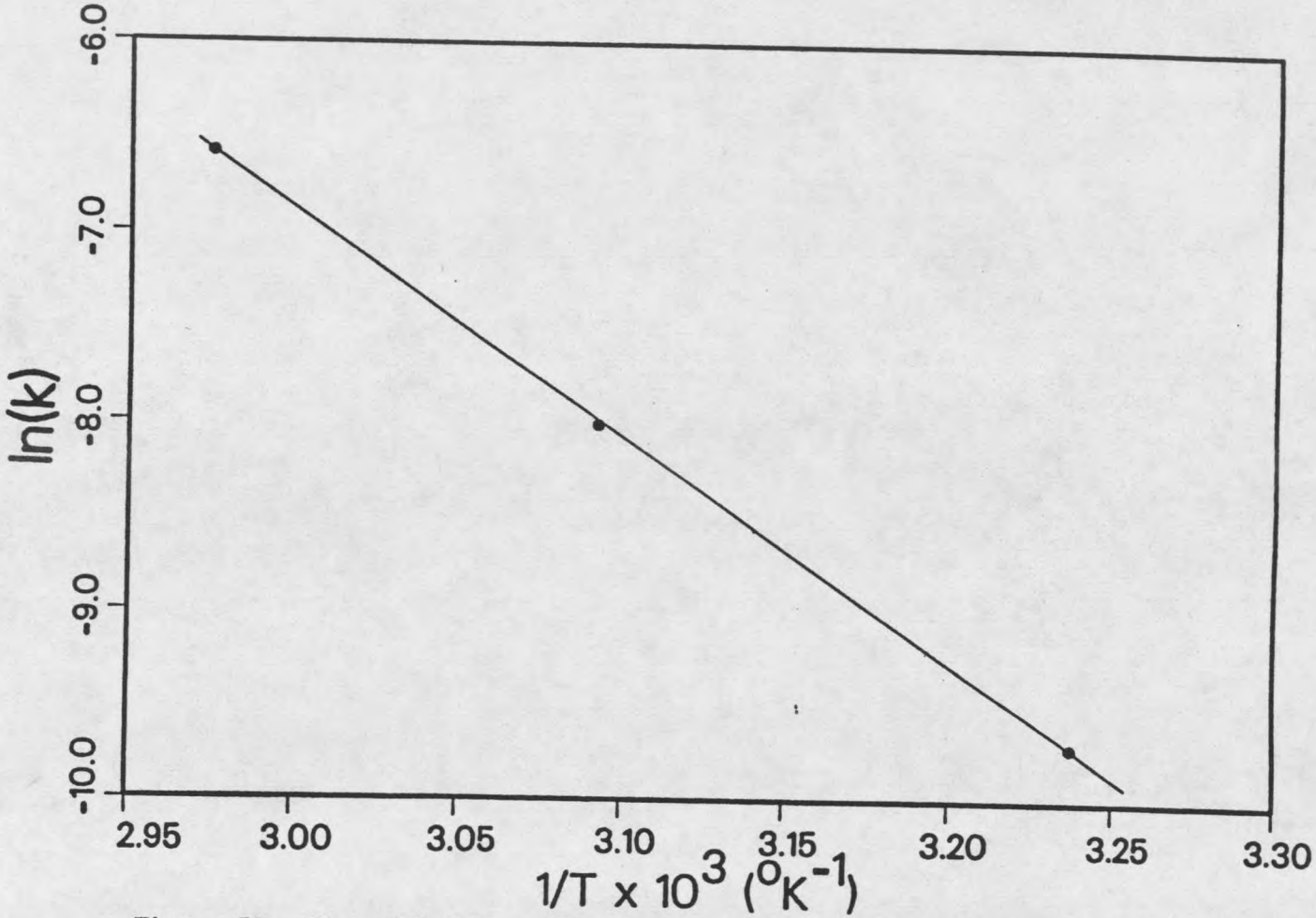

Figure 72. Plot of ln(k) vs 1/T (K^{-1}) for [19]. [y = 12141.6x + 29.591; R = 1.0000].

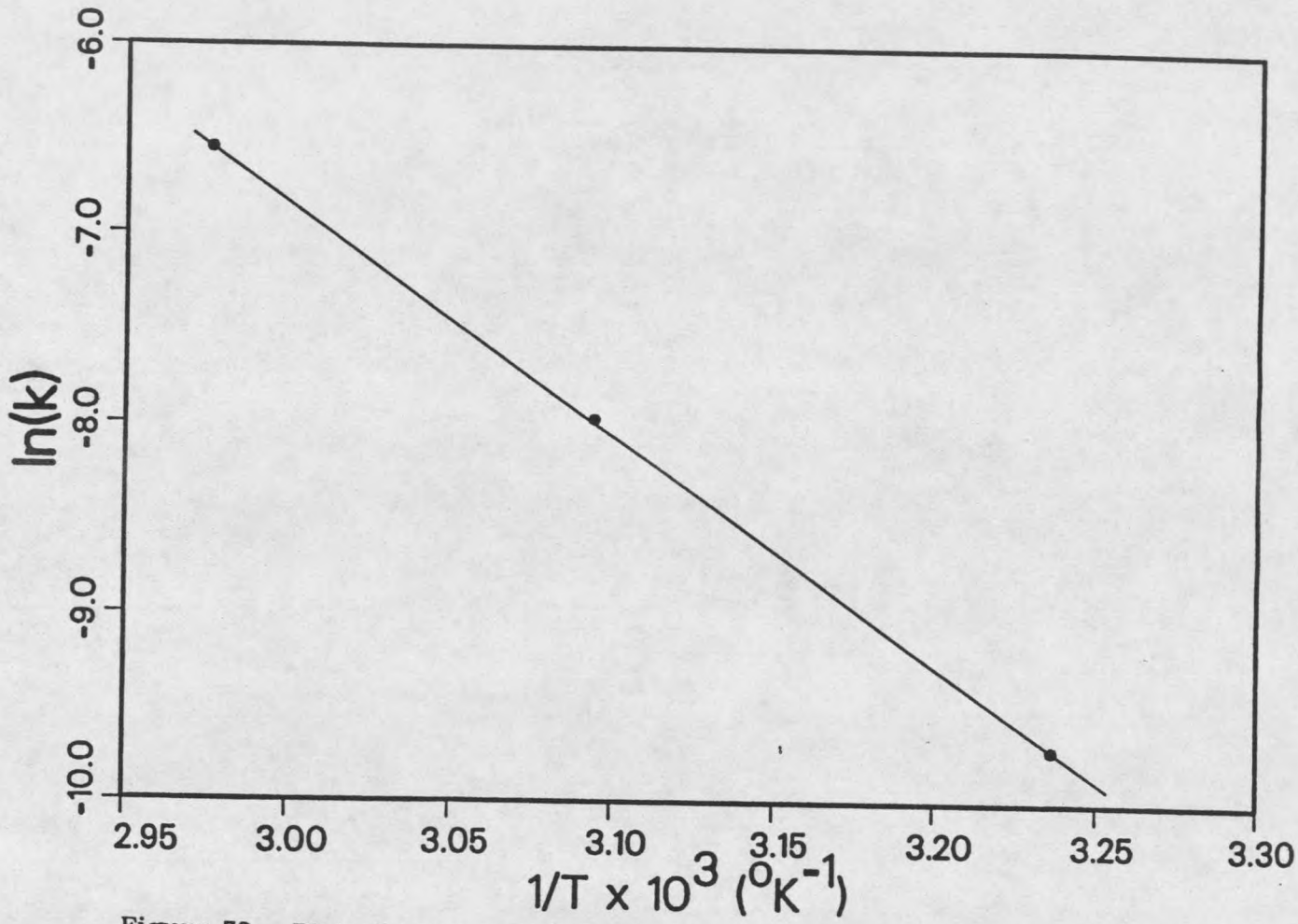

Figure 73. Plot of ln(k) vs 1/T (K^{-1}) for [31]. [y = 11941.0x + 28.935; R = 1.0000].

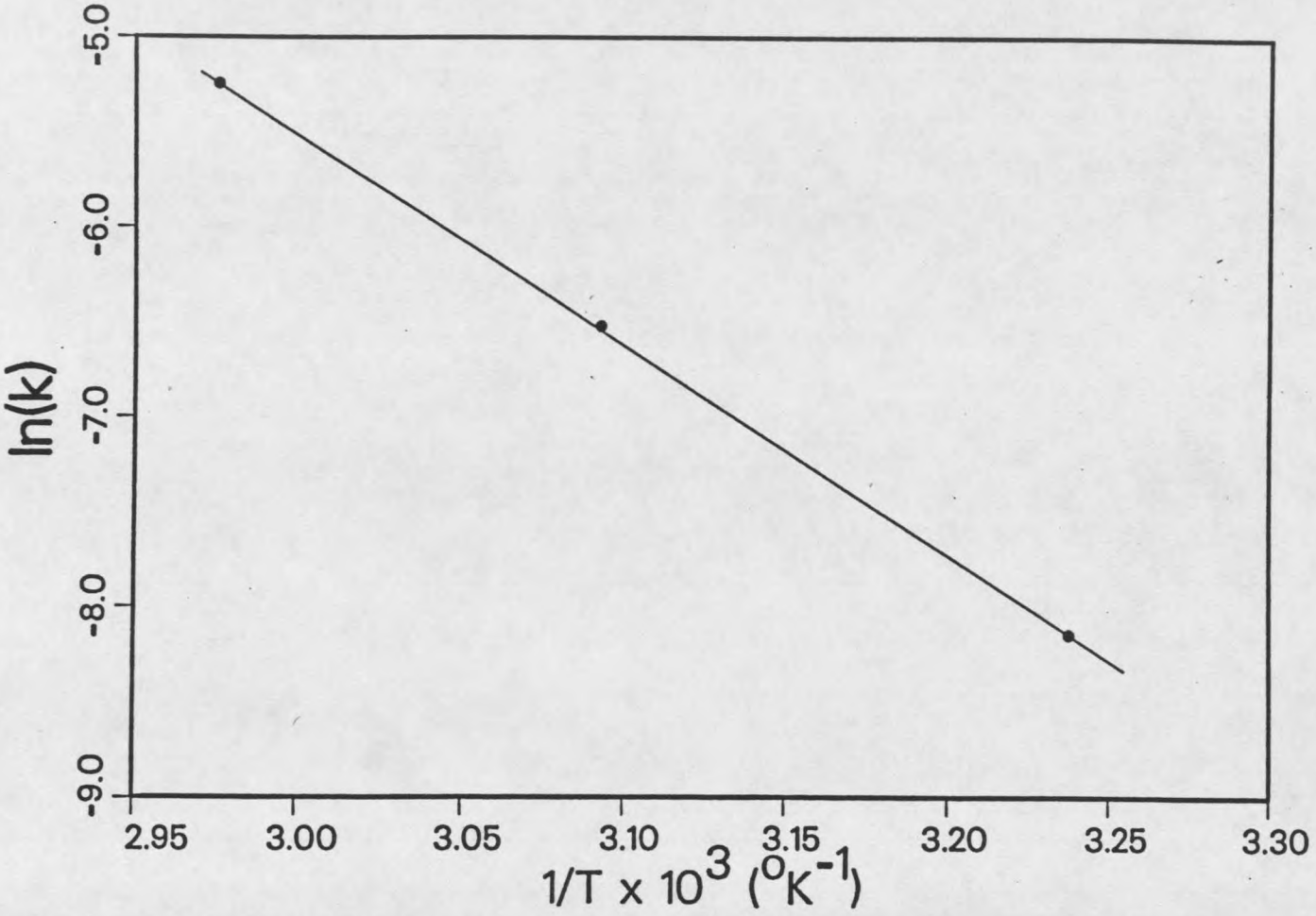

Figure 74. Plot of ln(k) vs 1/T (K^{-1}) for **[24]**. [y = 11446.82x + 28.470; R = 1.0000].

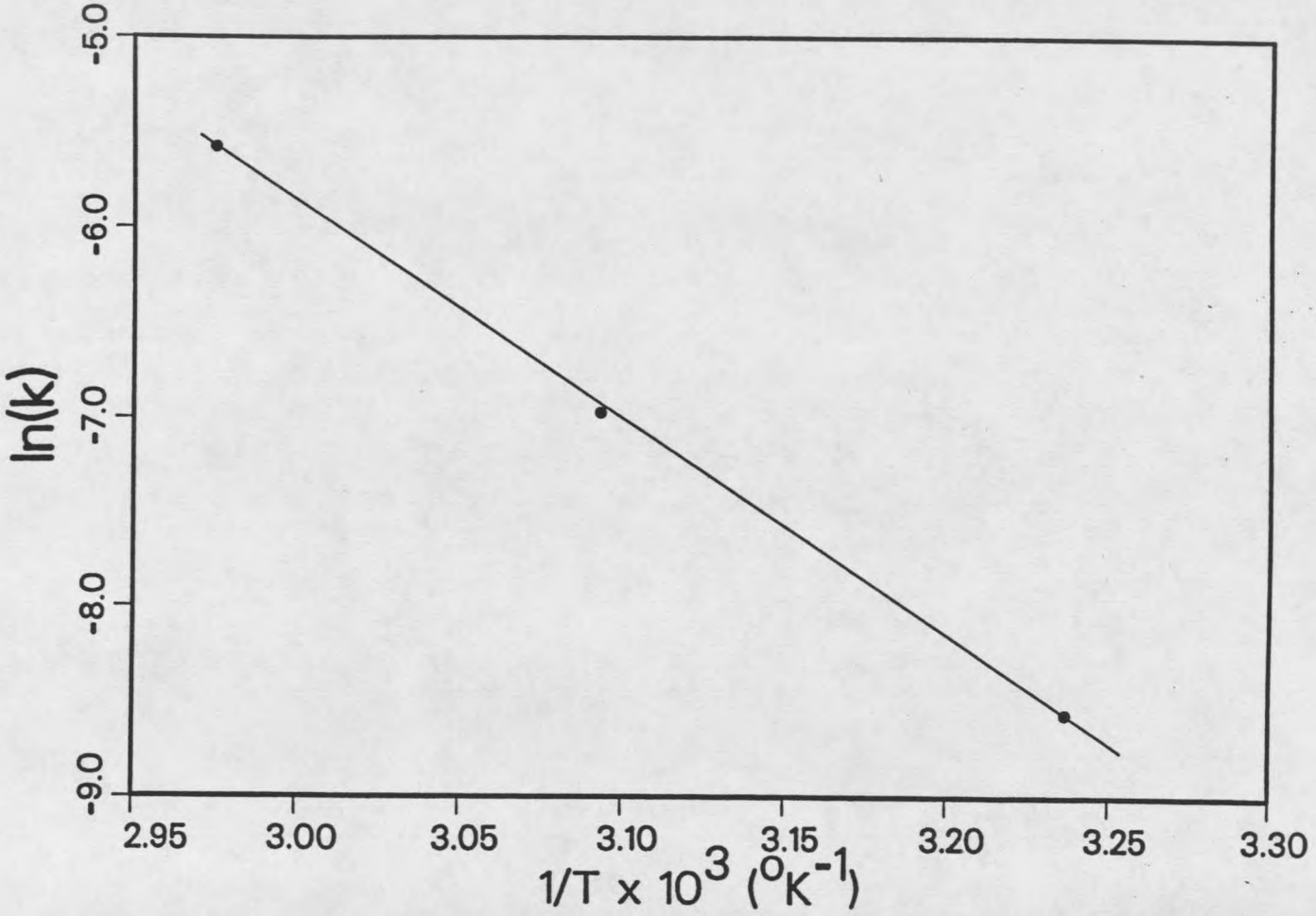

Figure 75. Plot of ln(k) vs 1/T (K^{-1}) for [**32**]. [y = 11077.5x + 27.733; R = 0.9999].

Reported boiling and melting points are uncorrected. Carbon and proton NMR spectra were recorded on a 250 MHz spectrophotometer equipped with an ASPECT 2000 data processing system. Spectra were obtained using deuterochloroform as solvent and chemical shifts were reported in ppm relative to TMS. Electron impact (EI) analyses were conducted on a VG MM16 mass spectrometer interfaced with a Varian Model 3700 gas chromatograph equipped with a 30mDB-1 capillary column. Accurate mass and chemical ionization (CI) mass spectral measurements were completed on a VG 7070E mass spectrometer. X-ray crystallographic data were obtained with a Nicolet R3mE diffractometer and processed by direct methods using Solve or Rant. IR data were obtained using a Nicolet DX FT-IR spectrometer. Semi-empirical molecular orbital calculations were completed by the MNDO method and force field calculations by the MM2 method. These calculations were preformed using the TRIBL program residing on a VAX-8550 computer. Anhydrous THF, diethyl ether, and hexane were obtained by distillation from benzophenone ketyl. Diisopropyl amine and pyridine were distilled from calcium hydride and dichloromethane was distilled from P_2O_5. Flash separations were completed using a 500 ml flash column packed with 40 μm diameter silica gel and equipped with a UV absorbance monitor. A solvent system of dichloromethane : hexane : ethyl acetate in the relative ratio 20 : 1 : 1 was used in all separations. Baseline resolutions were obtained only when the column was spotted with less than 200 mg of product.

Preparation of (cis)-8-oxabicyclo[4.3.0]non-3-ene, [1].

A solution of cis-1,2,3,6-tetrahydrophthalic anhydride (40.0 g, 0.264 moles) in 150 ml of dry THF was added to a stirring solution of LAH (11.0 g, 0.240 moles) in 100 ml of dry THF. After addition was completed the gray mixture was stirred for 12 hrs. at room temperature. The reaction was then cooled to 0°C and hydrolyzed by dropwise addition of 100 ml of wet ether. The resulting white salts were suction filtered off and the solvent removed by rotary evaporation to yield 22.4 g of the clear diol (60% yield).

The diol was then taken up in 200 ml of dry pyridine and stirred, under argon at a gentle reflux, while a solution of TsCl (33.4 g, 0.125 moles) in pyridine was added dropwise. After the addition was completed, the mixture was stirred at reflux for an additional 12 hrs. The resulting darkened solution was then poured over a concentrated sulfuric acid on crushed ice. The resulting acidic solution was extracted three times with dichloromethane. The extracts were combined and washed with saturated sodium bicarbonate solution followed by an aqueous wash. After drying over $Mg(SO_4)_2$ and the removal of solvent by rotary evaporation, the resulting clear liquid was distilled to yield 16.0 g (0.129 moles) of a clear liquid (80 % yield).

$BP_{2.3}$ = 45-48°C literature BP_{18} = 90-93°C

IR: 3024, 2968, 2925, 2843, 1088, 1055, 468, 462 cm^{-1}

^{1}HNMR: 1.90 (2H), 2.15 (methylene envelope, 4H), 3.51 (q, 2H), 3.85 (q, 2H), 5.65 (t, 2H).

^{13}C NMR: 23.80 (2C), 34.97 (2C), 72.80 (2C), 125.58 (2C).

MS (EI): M+ = 124, 106, 93, 79 (base), 69, 54, 39, 27.

MS (CI): MH+ = 125 (base), 107

analysis - HRMS calculated for $C_8H_{12}O$ = 124.18424; found = 124.08879.

Preparation of (cis)-1,6-dicarbomethoxybicyclo[4.3.0]-non-3-ene, [**18**].

A solution of 250 ml of dry THF, 203 ml of 2.6 M n-BuLi (0.528 moles) and 75.0 ml of diisopropylamine (0.528 moles) was stirred under argon at -78°C for 15 minutes. Then 41.7 g (0.211 moles) of cis-3,4-dicarbomethoxycyclohexene was added dropwise, creating a bright red solution. After addition was completed, the solution was allowed to stir for 15 minutes. The solution was then warmed to -10°C and 25.0 ml (0.230 moles) of 1,3-dibromopropane were added dropwise, slightly lightening the bright red solution. The solution was allowed to warm to room temperature and stirred for 2.5 hrs. The solution was then neutralized with a dilute HCl solution. The resulting phases were separated and the aqueous layer extracted three times with dicloromethane. The combined extracts were dried and the solvent removed by rotary evaporation. The resulting light yellow liquid was distilled to yield 25.6 g (0.108 moles) of a clear viscous liquid (52% yield).

$BP_{1.5}$ = 104-111°C

IR: 2900, 1730, 1690, 1140, 1320, 1280, 1205, 1176, 735 cm^{-1}.

^1H NMR: 5.64 (t, 2H), 2.65 (m, 4H), 2.50 (ddd, 2H), 2.21 (m, 2H), 2.19 (ddd, 2H).

MS (EI): 207 (-OMe), 206, 178, 163, 152, 119 (base), 105, 91.

Preparation of 8-oxatricyclo[4.3.3.0]undec-3-ene, [**7**].

A solution of 16.0 g of [**18**] (0.067 moles) in 40 ml of dry THF was added dropwise at 0°C to a stirring solution of 3.60 g of LAH (0.095 moles) in 350 ml of dry THF. The reaction was stirred overnight and then

hydrolyzed with wet ether. The white lithium salts were filtered off and the solvent removed by rotary evaporation to yield 9.14 g (0.053 moles) of the diol, a white solid.

The diol was dissolved in 200 ml of dry pyridine and brought to reflux under argon. Then 11.7 g of TsCl (0.062 moles) in 50 ml of pyridine were added dropwise to the stirring solution. The reaction was stirred at reflux overnight. The darkened solution was then poured over concentrated H_2SO_4 on ice to acidify. Extraction with dicloromethane yield a clear liquid, with a camphor-like fragrance, which was distilled resulting in 7.38 g (0.045 moles) of the desired product (88% yield).

$BP_{1.0}$ = 50-53°C

^1H NMR: 5.86 (t, 2H), 3.57 (s, 4H), 2.03 (s, 4H), 1.60 (methylene envelope, 6H),

^{13}C NMR: 128.5 (d), 81.4 (t), 55.1 (s), 40.0 (t), 32.5 (t), 24.1 (t).

MS (EI): M+ = 164, 146, 133, 119, 105, 91 (base), 79, 77.

MS (CI): MH+ = 165 (base), 147, 135, 119, 109

Analysis - HRMS: calculated for $C_{11}H_{16}O$ = 164.1197, found = 164.1190

Hydroboration of (cis)-8-oxabicyclo[4.3.0]non-3-ene, [1].

The alkene, [1], (6.30 g, 0.044 moles) in 40 ml of dry THF was added to 1.68 g (0.044 moles) of $NaBH_4$. A nitrogen atmosphere was created and the solution was cooled to 0°C. Then 10.9 ml (0.088 moles) of $BF_3O(C_2H_5)$ were added dropwise to the stirring solution. After 1 hr., the reaction was quenched with a small amount of water followed by the slow addition of 25 ml of 3N NaOH and 25 ml of 30% H_2O_2. After the addition was complete, the solution was stirred for 30 minutes. The solution was then extracted with dichloromethane; the extracts were dried and the solvent removed by

rotary evaporation to afford the clear liquid which was distilled to yield 4.81 g (0.034 moles) of the alcohol mixture. GLC analysis showed that the syn- and anti- alcohols were present in a 9 : 1 ratio, respectively (75% yield).

$BP_{.5}$ = 90-92°C (mixture)

syn-Bicyclic alcohol, [5].

IR: 3320, 2930, 2880, 1450, 1127, 1072, 1025, 987, 888 cm^{-1}.

^1H NMR : 1.45-1.20 (methylene envelope, 2H), 1.58-1.90 (m, 5H), 2.10-2.35 (m, 2H), 3.52-3.68 (m 3H), 3.74-3.84 (m, 2H).

MS (EI): 124 ($-H_2O$), 109, 95, 82, 79, 69 (base), 55, 43, 41.

MS (CI): MH+ = 143, 125, 109

analysis - HRMS calculated for $C_8H_{12}O_2$ = 142.1996; Found = 142.0979.

anti-Bicyclic alcohol, [6].

IR: 3320, 2930, 2880, 1450, 1150, 1127, 970 cm^{-1}.

^1H NMR: 1.58-1.15 (methylene envelope 4H), 1.85-1.65 (m, 3H), 2.15-2.05 (m, 1H), 2.50-2.35 (M, 1H), 3.58-3.45 (m, 2H), 3.83-3.68 (m, 3H).

MS (EI): 124 ($-H_2O$), 114, 109, 95, 83, 79 (base), 68, 55, 43, 41.

MS (CI): MH+ = 143, 125, 107.

analysis - HRMS calculated for $C_8H_{12}O_2$ = 142.1996; Found = 142.0949.

Epoxidation of (cis)-8-oxabicyclo[4.3.0]non-3-ene, [1].

The alkene, [1], (500 mg, 4.00 moles) was dissolved in 15 ml of chloroform to which was added 760 mg (4.40 moles) of mCPBA. The solution was stirred under argon at room temperature overnight. Then 10 ml of 10% NaS_2O_3 was added along with 10 ml of water and 20 ml of dichloromethane. The organic layer was collected and washed with saturated $NaHCO_3$ and water, dried over $MgSO_4$, and the solvent removed

by rotary evaporation to yield 500 mg of a clear liquid (80% yield). GLC (13% DEGS, 10'x1/4", 120°C) showed the syn- and anti-epoxides of [1] in the ratio 1 : 4, respectively.

To determine the relative stereochemistry of the two isomers, the major epoxide was cleanly collected by GLC. This epoxide was then combined with 10 ml of dry THF to which was added a "pinch" of LAH. The solution was allowed to stir under argon overnight. A small amount of wet ether was added to quench the reaction, the salts were filtered off and the solvents removed by rotary evaporation to yield a clear liquid. The GC/MS and ^{1}H NMR of this compound were identical to that of the anti-alcohol, thus determining the relative stereochemistry of the major epoxide to be the anti-isomer. In a similar fashion the minor epoxide was reduced yielding only the syn-alcohol.

syn-bicylic epoxide, [20].

^{1}H NMR: 2.27-1.82 (methylene envelope, 6H), 3.18 (s, 2H), 3.61-3.55 (ddd, 2H), 3.92-3.81 (ddd, 2H).

MS (EI): M+ = 140, 122, 92, 79 (base), 69, 53, 41.

anti-bicylic epoxide, [21].

^{1}H NMR: 1.89-1.81 (dd, 2H), 2.15-2.05 (m, 2H), 3.12 (s, 2H), 3.25-3.20 (ddd, 2H) 3.94-3.88 (ddd, 2H).

MS (EI) M+ = 140, 110, 96, 81, 69 (base), 53, 41.

Oxymercuration/demercuration of cis-8-oxabicyclo[4.3.0]non-3-ene, [1].

The alkene (7.00 g, 0.056 moles) was dissolved in 40 ml of a 50:50-THF:H_2O solution and added to 20.0 g of mercuric acetate (0.063 moles) in 100 ml of 50:50 - THF:H_2O. A yellow/orange solution resulted which gradually cleared upon stirring for 1 hr. After the dropwise addition of 25

ml of 3N NaOH, the solution regained its yellow/orange appearance. Then, after 5 minutes, 2.5 g (0.066 moles) of $NaBH_4$ were dissolved in 25 ml of 3N NaOH and added dropwise to the solution, liberating free mercury. The reaction was allowed to settle before vacuum filtering through celite. Removal of solvent at reduced pressure yielded 3.89 g (0.027 moles) of the alcohol mixture (52% yield). GC analysis indicates the syn : anti alcohol ratio as 3 : 1.

Methoxymercuration/demercuration of cis-8-oxabicyclo[4.3.0]non-3-ene, [1].

The alkene, [1], (0.435 g, 3.51 moles) was added to a stirring solution of 1.12 g (3.51 moles) of mercuric acetate in 25 ml of methanol to which was added a catalytic amount of nitric acid. After stirring overnight, 0.190 g (3.51 moles) of sodium methoxide was added and the solution was stirred for 1 hr. Then 5 ml of 0.50 M NaOH was added followed by excess $NaBH_4$. The reaction was stirred briefly, resulting in a grey slurry which was allowed to settle and then vacuum filtered through celite. Removal of solvent at reduced pressure afforded 0.484 g (3.10 moles) of a clear liquid (88% yield). GLC (13% DEGS, 8'x1/4", 130°C) showed two peaks for the syn- and anti- methoxy derivatives in the ratio 3 : 1, respectively.

syn-methoxy derivative, [**22**].

^1H NMR: 1.43-1.27 (m, 2H), 1.96-1.56 (methylene envelope, 4H), 2.22- 2.10 (m, 1H), 2.50-2.23 (m, 1H), 3.22-3.10 (m, 1H), 3.40 (s, 3H), 3.70-3.59 (ddd, 2H), 3.86-3.75 (m, 2H).

MS (EI): M+ = 156, 124, 109, 97, 95, 82, 69 (base), 58, 41.

MS (CI): MH+ = 157, 139, 125 (base), 107.

analysis - HRMS calculated for $C_9H_{16}O_2$ = 156.2267; Found = 156.1206.

anti-methoxy derivative, [23].

1H NMR: 1.45-1.35 (m, 1H), 2.75-2.05 (methylene envelope, 4H), 2.20-2.10 (m, 1H), 2.45-2.35 (m, 1H), 3.20 (s, 3H), 3.33-3.25 (m, 1H), 3.65-3.51 (ddd, 2H), 3.88-3.93 (ddd, 2H).

MS (EI): M+ = 156, 141, 124, 109, 97, 79, 64, 58, 41 (base).

MS (CI): MH+ = 157 (base), 125, 107.

analysis - HRMS calculated for $C_9H_{16}O_2$ = 156.1206; Found = 156.1136.

Hydroboration of 8-oxatricyclo[4.3.3.0]ndec-3-ene, [7].

The propellane, [7], (2.00 g, 0.012 moles) was dissolved in 100 ml of dry THF to which was added 4.00 g (0.011 moles) of $NaBH_4$. An argon atmosphere was created and the reaction was cooled to 0°C. Then 1.20 ml,(0.010 moles) of $BF_3O(C_2H_5)_2$ were syringed into the system. The solution was warmed to room temperature and stirred overnight. The reaction mixture was then neutralized with dilute HCl followed by extraction with dichloromethane. The solvent was dried over $MgSO_4$ and the solvent removed at reduce pressure to yield 2.30 g (0.016 moles) of the clear alcohol mixture (80% yield). Capillary GC analysis showed the syn- and anti-alcohol in the ratio 1 : 1.

(syn)-8-oxatricyclo[4.3.3.0]undec-3-ol, [25].

IR: 3350, 2930, 2870, 1453, 1180, 1009, 900 cm-1.

^{1}H NMR: 1.88-1.33 (methylene envelope, 12 H), 3.84-3.58 (m, 6H).

MS (EI): 164 (-H_2O), 146, 133, 119, 109 (base), 93, 91, 79, 67, 55, 41.

MS (CI): 165 (base), 147, 133, 119

analysis - HRMS calculated for $C_{11}H_{18}O_2$ = 182.2542; Found = 182.1540

(anti)-8-oxatricyclo[4.3.3.0]undec-3-ol, [26].

IR: 3350, 2930, 2820, 1460, 1170, 995, 900 cm^{-1}.

^1H NMR: 1.84-1.23 (methylene envelope, 12H), 3.60-3.37 (m, 6H).

MS (EI): M+ = 182, 164, 151, 133, 123, 119, 109, 93 (base), 91, 79, 67, 55, 41.

MS (CI): MH+ = 183, 165 (base), 147, 135, 121, 109.

analysis - HRMS calculated for $C_{11}H_{18}O_2$ = 182.2542; Found = 182.1323.

Epoxidation of 8-oxatricyclo[4.3.3.0]undec-3-ene, [7].

The propellane, [7], (1.11 g, 6.77 moles) and 1.40 g (8.13 moles) of mCPBA were combined with 200 ml of dry chloroform and stirred at room temperature under argon overnight. Then 30 ml of 10% NaS_2O_4 were added to the mixture. The organic layer was separated and washed with saturated sodium bicarbonate followed by an aqueous wash. The organic layer was dried over $MgSO_4$ and the solvent removed at reduced pressure to afford 0.68 g (3.77 moles) of the light yellow epoxide mixture (56% yield). GLC, (10% OVIT, 8'x1/4", 180°C), analysis showed two peaks in the ratio 1 : 1.

To determine the relative stereochemistry of the epoxides, the first peak to elute from GLC was cleanly collected and reduced with a "pinch" of LAH in 5 ml of dry THF. The reaction was stirred under argon overnight and then hydrolyzed with a small amount of water. The salts were filtered off and the solvent removed at reduced pressure to yield only the anti-alcohol as determined by ^1H NMR and GC/MS.

(syn)-3,4-epoxy-8-oxatricyclo[4.3.3.0]undecane, [8].

^1H NMR: 1.70-1.40 (m, 6H), 1.77 (dd, 2H), 2.19 (ddd, 2H), 3.13 (ddd, MS (EI): M+ = 180, 162, 132, 117, 91, 79 (base).

analysis - HRMS calculated for $C_{11}H_{16}O_2$ = 180.1150; Found = 180.1155.

2H), 3.73 (d, 2H).

(anti)-3,4-epoxy-8-oxatricyclo[4.3.3.0]undecane, [9].

^{1}H NMR: 1.65-1.45 (m, 4H), 1.92 (d, 2H), 2.10 (ddd, 2H), 3.14 (ddd, 2H), 3.37 (d, 2H), 3.66 (d, 2H).

MS (EI): M+ = 180, 162, 132, 117, 91, 79 (base).

analysis - HRMS calculated for $C_{11}H_{16}O_2$ = 180.1150; Found = 180.1160.

Preparation of (para)-nitrobenzoate derivatives of (cis)-8-oxabicyclo[4.3.0]non-3-ene, [1].

The mixture of the syn- and anti-alcohols derived from the oymercuration/demercuration of [1] (3.89 g, 0.0274 moles) was dissolved in 50 ml of dry pyridine and an argon atmosphere was created. Then 5.89 g (0.0301 moles) of TsCl, recrystallized from hexane, were dissolved in pyridine and added dropwise to the stirring solution at room temperature. The reaction was then allowed to stir overnight, then the solution was poured over ice water, resulting in the formation of a yellow oil. This mixture was refrigerated for several hours whereupon a solid formed which was filtered off and recrystallized in hexane to yield 6.30 g (0.0208 moles) of the white para-nitrobenzoate mixture (76% yield). Flash separation was employed to cleanly separate the syn- and anti-products.

IR, (mixture): 2930, 2885, 1721, 1717, 1607, 1526, 1349, 1276, 1150, 830, 719 cm^{-1}.

syn-(para)-nitrobenzoate derivative of (cis)-8-oxabicyclo[4.3.0]non-3-ene, [27].

MP: 127-129°C

^{1}H NMR: 1.84-1.63 (methylene envelope, 6H), 2.40-2.30 (m, 2H), 3.71-3.64

(m, 2H), 3.87-81 (m, 2H), 5.04 (m, 1H), 8.26-8.13 (dd, 4H).

MS (EI): M+ = 291, 261, 231, 150 (base), 141, 124, 94, 79, 69, 55, 41, 28.

analysis - HRMS calculated for $C_{15}H_{17}NO_5$ = 291.30867; Found = 291.1107.

anti-(para)-nitrobenzoate derivative of (cis)-8-oxabicyclo[4.3.0]non-3-ene, [28].

MP: 90-93°C

^{1}H NMR: 2.00-1.63 (methylene envelope, 6H), 2.40-2.25 (ddd, 1H), 2.60-2.45 (ddd, 1H), 3.74-3.62 (m, 2H), 3.95-3.83 (m, 2H), 5.32-5.20 (dd, 1H), 8.27-8.13 (dd, 4H).

MS (EI): M+ = 291, 261, 232, 150 (base), 141, 124, 107, 94, 79, 69, 55, 41, 28.

analysis - HRMS calculated for $C_{15}H_{17}NO_5$ = 291.30867; Found = 291.1102.

Preparation of tosylate derivatives of [1].

The syn-(para)-nitrobenzoate derivative of [1] (0.527 g, 1.81 moles) was dissolved in 1 ml of dichloromethane and added to 35 ml of 80% aqueous ethanol that was 0.50% by weight in KOH (2.0 g of KOH in a solution of 200 ml of absolute ethanol and 50 ml distilled water). The reaction was stirred overnight at room temperature. Then, most of the solvent was removed at reduced pressure and 15 ml of dichloromethane were added to the residue. The organic layer was collected, dried of $MgSO_4$, and the solvent removed at reduced pressure yielding 0.169 g (1.91 moles) of the syn-alcohol (66% yield).

The IR, ^{1}H NMR, and MS (EI) spectra of this compound were identical to those of the previously reported syn-alcohol.

In a similar fashion, saponification of the anti-(para)-nitrobenzoate derivative of [1] (1.00 g, 3.44 moles) afforded 0.255 g, (1.80 moles), of the

anti-alcohol (52% yield).

Again, the IR, ^{1}H NMR, and MS (EI) spectra of this compound were identical to that of the previously reported syn-alcohol.

The syn-alcohol, (0.169 g 1.91 moles) was then dissolved in 20 ml of dry chloroform to which was added 0.20 ml (2.4 moles) of pyridine. The solution was cooled to 0°C and 0.340 g (1.79 moles) of TsCl were added in small portions. The reaction was then warmed to room temperature and stirred under argon overnight. A solution of 40 ml of ether and 10 ml of water were added to the reaction mixture, which was then washed with 2 N HCL, 5% sodium bicarbonate, and water, respectively. The organic layer was dried over $MgSO_4$ and the solvent removed at reduced pressure to yielded 0.505 g of the crude product. TLC analysis indicated the presence of TsCl. Flash separation was, therefore, employed to cleanly isolate the syn-tosylate.

The product was crystallized in a solution of hexane : dichloromethane in the relative ratio 50 : 1, respectively.

With the identical procedure reported above, 0.250 g (1.76 moles) to the anti-alcohol were dissolved in 20 ml of chloroform to which was added 0.29 ml (3.52 moles) of pyridine and 0.503 g (2.64 mmoles) TsCl. The anti-tosylate was cleanly afforded 0.44 g (1.5 moles) flash separation.

The anti-product was a clear oil that could not be crystallized.

(syn)-tosylate derivative of (cis)-8-oxabicyclo[4.3.0]non-3-ene, [**19**].

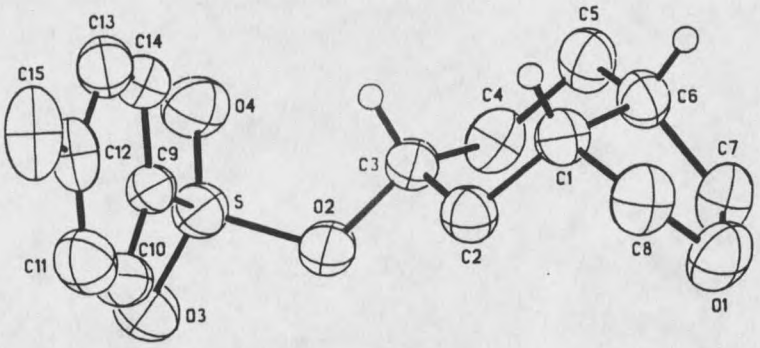

Figure 76. ORTEP drawing of [**19**].

Table 24. Atomic coordinates ($x10^4$) and isotropic thermal parameters ($A^\circ x10^3$) of [**19**].

	x	y	z	U
C(1)	224(4)	3851(2)	4927(3)	78(1)*
C(2)	2641(5)	3901(2)	5392(3)	79(1)*
C(3)	3228(5)	3340(2)	6130(2)	73(1)*
C(4)	2930(6)	2666(2)	5613(3)	88(1)*
C(5)	519(5)	2580(2)	5171(3)	92(2)*
C(6)	-299(6)	3153(2)	4479(3)	80(1)*
C(7)	618(7)	3194(2)	3404(3)	103(2)*
O(1)	644(5)	3888(2)	3132(2)	113(1)*
C(8)	-168(8)	4275(2)	3959(3)	105(2)*
O(2)	5616(4)	3424(1)	6489(2)	93(1)*

(Table 24. continued)

S	6286(1)	3444(1)	7696(1)	83(1)*
O(3)	8675(4)	3483(2)	7745(2)	111(1)*
O(4)	5241(4)	2913(1)	8210(2)	104(1)*
C(9)	5213(5)	4212(2)	8096(2)	70(1)*
C(10)	6304(5)	4799(2)	7913(3)	94(2)*
C(11)	5423(8)	5397(2)	8217(3)	106(2)*
C(12)	3497(7)	5426(2)	8733(3)	97(2)*
C(13)	2452(6)	4831(2)	8903(3)	98(2)
C(14)	3278(6)	4225(2)	8601(3)	85(1)*
C(15)	2536(9)	6069(2)	9086(4)	139(2)*

* Equivalent isotropic U defined as one third of the trace of the orthogonalised U_{ij} tensor.

Table 25. Bond lengths (A°) of [19].

C(1)-C(2)	1.533(5)	C(1)-C(6)	1.529(5)
C(1)-C(8)	1.504(5)	C(2)-C(3)	1.490(5)
C(3)-C(4)	1.503(5)	C(3)-O(2)	1.486(4)
C(4)-C(5)	1.527(5)	C(5)-C(6)	1.505(5)
C(6)-C(7)	1.523(5)	C(6)-H(6)	0.960(7)
C(7)-O(1)	1.428(5)	O(1)-C(8)	1.426(5)
C(9)-C(10)	1.369(5)	C(10)-C(11)	1.373(6)
O(2)-S	1.568(2)	S-O(3)	1.436(2)
S-O(4)	1.419(3)	S-C(9)	1.754(4)
C(12)-C(13)	1.367(6)	C(12)-C(15)	1.490(6)
C(13)-C(14)	1.372(6)		

Table 26. Bond angles (°) of [19].

H(1)-C(1)-C(2)	110.7(17)	H(1)-C(1)-C(6)	113.4(20
C(2)-C(1)-C(6)	111.6(3)	H(1)-C(1)-C(8)	108.3(19)
C(2)-C(1)-C(8)	111.7(3)	C(6)-C(1)-C(8)	100.8(3)
C(1)-C(2)-C(3)	111.7(3)	C(2)-C(3)-H(3)	113.8(20)
C(2)-C(3)-C(4)	112.1(3)	H(3)-C(3)-C(4)	108.4(20)
C(2)-C(3)-O(2)	106.8(3)	H(3)-C(3)-O(2)	106.8(17)
C(4)-C(3)-O(2)	108.6(3)	C(3)-C(4)-C(5)	110.0(3)
C(4)-C(5)-C(6)	113.2(3)	C(1)-C(6)-C(5)	114.8(3)
C(1)-C(6)-H(6)	102.6(22)	C(5)-C(6)-H(6)	112.2(22)
C(1)-C(6)-C(7)	102.2(3)	C(6)-C(7)-C(7)	116.7(3)
H(6)-C(6)-C(7)	106.8(21)	C(6)-C(7)-O(1)	106.5(3)
C(7)-O(1)-C(8)	109.4(3)	C(1)-C(8)-O(1)	105.5(3)
C(3)-O(2)-S	118.7(2)	O(2)-S-O(3)	103.2(1)
O(2)-S-O(4)	110.4(1)	O(3)-S-O(4)	119.8(2)
O(2)-S-C(9)	103.7(1)	O(3)-S-C(9)	109.2(2)
O(4)-S-C(9)	109.3(2)	S-C(9)-C(10)	120.2(3)
S-C(9)-C(14)	119.8(3)	C(10)-C(9)-C(14)	119.9(3)
C(9)-C(10)-C(11)	119.5(4)	C(10)-C(11)-C(12)	121.9(4)
C(11)-C(12)-C(13)	117.0(4)	C(11)-C(12)-C(15)	122.7(4)
C(13)-C(12)-C(15)	120.3(4)	C(12)-C(13)-C(14)	122.5(4)
C(9)-C(14)-C(13)	119.1(4)		

1H NMR: 1.92-1.52 (methylene envelope, 6H), 2.31-2.12 (m, 2H), 2.42 (s, 3H), 3.67-3.52 (m, 2H), 3.85-3.74 (m, 2H), 4.51 (m, 1H), 7.37-7.28 (d, 2H),

7.83-7.75 (d, 2H).

MS (EI): 124 (-TsOH), 106, 93, 91, 79 (base), 69, 54, 41.

MS (CI): MH+ = 297, 173, 141, 125 (base), 117.

analysis - HRMS calculated for $C_{15}H_{20}SO_4$ = 296.3897; Found = 296.1026.

(anti)-tosylate derivative of (cis)-8-oxabicyclo[4.3.0]non-3-ene, [31].

^{1}H NMR: 1.95-1.33 (methylene envelope, 6H), 2.31-2.18 (ddd, 1H), 2.43 (s, 3H), 3.58-3.45 (m, 2H), 3.83-3.73 (m, 2H), 4.67 (m, 1H), 7.36-7.26 (d, 2H), 7.82-7.72 (d, 2H).

MS (EI): 124 (-TsOH), 106, 93, 91, 79 (base), 69, 54, 41.

MS (CI): MH+ = 297, 173, 141, 125 (base), 117.

analysis - HRMS calculated for $C_{15}H_{20}SO_4$ = 296.3897; Found = 296.1159.

Preparation of (para)-nitrobenzoate derivatives of 8-oxatricyclo[4.3.3.0]undec-3-ene.

A mixture of the syn- and anti-alcohols derived from the hydroboration of [7] (2.30 g, 0.0126 moles) was dissolved in 50 ml of dry pyridine to which was added 2.80 g (0.0150 moles) of PNBCl in 25 ml of pyridine. The reaction was stirred under argon at room temperature overnight. The solution was then poured over ice water and a white precipitate formed which was filtered off, yielding 3.5 g of the crude product. TLC analysis indicated the presence the desired para-nitrobenzoates and para-nitrobenzoyl chloride. Flash chromatography was employed to cleanly isolate the isomers.

syn-3-(para)-nitrobenzoate-8-oxatricyclo[4.3.3.0]undecane, [29].

MP: 119-121 °C

^{1}H NMR: 1.83-1.53 (methylene envelope, 10H), 2.08 (m, 2H), 3.87-3.61 (dq, 4H), 5.19 (m, 1H), 8.29-8.15 (ddd, 4H).

MS (EI): M+ = 164 (-PNBOH), 146, 133, 119, 105, 91 (base), 79, 77.

MS (NCI): M+ = 331, 299, 167.

analysis - HRMS calculated for $C_{18}H_{21}NO_5$ = 331.3712; Found = 331.1415.

anti-3-(para)-nitrobenzoate-8-oxatricyclo[4.3.3.0]undec-3-ene, [30].

^{1}H NMR: 1.84-1.59 (methylene envelope, 10H), 2.1 (m, 2H), 3.86-3.63 (dq, 4H), 5.20 (m, 1H), 8.29-8.16 (ddd, 4H).

MS (EI): M+ = 164 (-PNBOH), 146, 133, 119, 105, 91 (base), 79, 77.

MS (NCI): M+ = 331, 299, 167.

analysis - HRMS calculated for $C_{18}H_{21}NO_5$ = 331.3712; Found = 331.2563.

Preparation of tosylate derivatives of [7].

The syn-para-nitrobenzoate derivative of [7] (0.380 g, 1.15 moles) was dissolved in 2 ml of dichloromethane and then added to a 80% aqueous ethanol solution that was 0.5% by weight in KOH. The reaction was stirred overnight. Most of the solvent was stripped, then 10 ml of water was added to the residue. The solution was extracted with dichloromethane, the organics dried, and the solvent stripped to yield 0.20 g (1.09 moles) of the clear alcohol (73% yield). The IR, GC/MS, and ^{1}H NMR of this compound were identical to the previously reported syn-alcohol.

Saponification, reported in the preparation of tosylate derivatives of [1], of the anti- para-nitrobenzoate of [7] (0.450 g, 1.35 moles) resulted in 0.18 g, (1.26 moles) of the anti-alcohol (93% yield).

The syn-alcohol (0.130 g, 0.71 moles) was dissolved in 10 ml of dichloromethane to which was added 0.12 ml (1.4 moles) of pyridine. The solution was cooled to 0°C and 0.16 g (0.84 moles) of TsCl was added in small portions. The reaction was warmed to room temperature and stirred

overnight. After the identical workup reported above, 0.200 g of a yellow oil were obtained. ^{1}H NMR and TLC analysis indicated the presence of the desired para-nitrobenzoate along with a minor amount of TsCl. Flash chromatography was employed to isolate the product. Crystallization of the product was accomplished in hexane : dichloromethane in a relative ratio of 50 : 1, respectively.

In a similar fashion, 90 mg of the anti-alcohol (0.49 moles) were derivatized yielding 0.160 g of a yellow liquid. TsCl was indicated as a minor product by TLC and flash chromatography was employed to isolate the desired product. The isolated product was a clear oil that would not crystallize.

syn-3-tosyl-8-oxatricyclo[4.3.3.0]undecane, [**24**].

^{1}H NMR: 1.90-1.30 (methylene envelope, 12H), 2.42 (s, 3H), 3.72-3.55 (dq, 4H), 4.65 (m, 1H), 7.35-7.30 (d, 2H), 7.82-7.77 (d, 2H).

MS (EI): M+ = 164 (-TsOH), 146, 133, 119, 105, 91 (base), 79, 77.

MS (CI): MH+ = 337, 181, 165 (base), 147, 135, 117.

analysis - HRMS calculated for $C_{15}H_{20}SO_4$ = 336.4259; Found = 336.1465.

X-ray analysis:

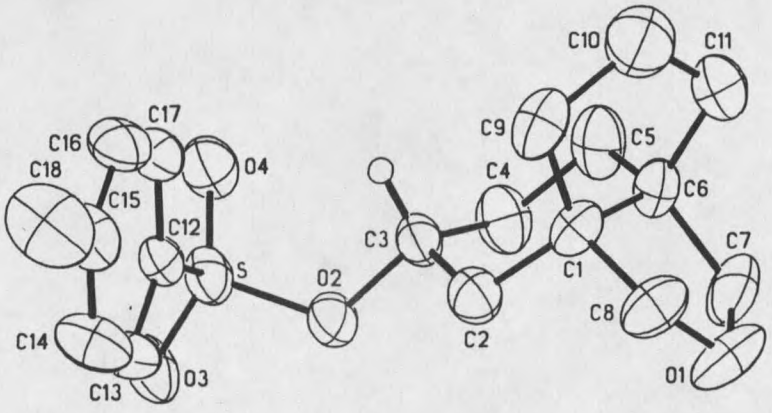

Figure 77. ORTEP drawing of [**24**].

Table 27. Atomic coordinates ($x10^4$) and isotropic thermal parameters ($A^\circ x10^3$) for [24].

	x	y	z	U
C(1)	7888(4)	6234(4)	5984(3)	53(2)*
C(2)	7622(5)	7453(4)	6392(3)	61(2)*
C(3)	7352(4)	7335(4)	7267(3)	49(2)*
C(4)	8504(5)	6696(4)	7896(3)	68(2)*
C(5)	8673(5)	5434(5)	7537(3)	73(2)*
C(6)	8870(4)	5445(4)	6622(3)	53(2)*
C(7)	10217(4)	5896(5)	6520(3)	81(2)*
O(1)	10018(3)	6470(5)	5700(3)	91(2)*
C(8)	8650(4)	6431(5)	5270(3)	73(2)*
C(9)	6618(4)	5516(4)	5682(3)	69(2)*
C(10)	7089(5)	4205(5)	5739(4)	104(3)*
C(11)	8514(6)	4170(4)	6202(4)	86(3)*
O(2)	7279(3)	8563(3)	7607(2)	63(1)*
S	6005(1)	8925(1)	7937(1)	56(1)*
O(3)	6310(3)	101000(3)	8282(2)	73(1)*
O(4)	5688(3)	7993(3)	8476(2)	67(1)*
C(12)	4748(4)	9015(4)	6984(3)	48(2)*
C(13)	4670(5)	10006(4)	6449(3)	66(2)*
C(14)	3692(6)	10059(5)	5699(4)	81(2)*
C(15)	2768(5)	91489(5)	5470(3)	74(2)*

(Table 27. continued)

C(16)	2853(5)	8179(4)	6005(3)	67(2)*
C(17)	3831(4)	8096(4)	6759(3)	58(2)*
C(18)	1705(6)	9227(6)	4632(4)	121(3)*

* Equivalent isotropic U defined as one third of the trace of the orthogonalised U_{ij} tensor.

Table 28. Bond lengths (A°) for [24].

C(1)-C(2)	1.553(6)	C(1)-C(6)	1.529(6)
C(1)-C(8)	1.527(7)	C(1)-C(9)	1.512(6)
C(2)-C(3)	1.473(7)	C(3)-H(3)	0.960(32)
C(3)-C(4)	1.534(6)	C(3)-O(2)	1.477(5)
C(4)-C(5)	1.540(7)	C(5)-C(6)	1.501(7)
C(6)-C(7)	1.5177)	C(6)-C(11)	1.574(7)
C(7)-O(1)	1.414(6)	O(1)-C(8)	1.416(5)
C(9)-C(10)	1.535(7)	C(10)-C(11)	1.481(7)
O(2)-S	1.569(4)	S-O(3)	1.425(3)
S-O(4)	1.424(3)	S-C(12)	1.746(4)
C(12)-C(13)	1.380(6)	C(12)-C(17)	1.382(6)
C(13)-C(14)	1.366(7)	C(14)-C(15)	1.381(8)
C(15)-C(16)	1.360(7)	C(15)-C(18)	1.511(7)
C(16)-C(17)	1.373(6)		

Table 29. Bond angles (°) of [24].

C(2)-C(1)-C(6)	112.5(3)	C(2)-C(1)-C(8)	110.4(4)
C(6)-C(1)-C(8)	101.1(3)	C(2)-C(1)-C(9)	111.8(4)
C(6)-C(1)-C(9)	107.2(4)	C(8)-C(1)-C(9)	113.3(3)
C(1)-C(2)-C(3)	113.5(4)	C(2)-C(3)-H(3)	114.0(28)
C(2)-C(3)-C(4)	111.3(4)	H(3)-C(3)-C(4)	110.1(24)
C(2)-C(3)-O(2)	107.0(3)	H(3)-C(3)-O(2)	107.2(25)
C(4)-C(3)-O(2)	107.0(3)	H(3)-C(3)-O(2)	108.7(3)
C(4)-C(5)-C(6)	113.4(4)	C(1)-C(6)-C(5)	114.9(4)
C(1)-C(6)-C(7)	102.9(4)	C(5)-C(6)-C(7)	115.6(4)
C(1)-C(6)-C(11)	100.8(3)	C(5)-C(6)-C(11)	109.1(4)
C(7)-C(6)-C(11)	112.6(4)	C(6)-C(7)-O(1)	107.5(3)
C(7)-O(1)-C(8)	110.0(4)	C(1)-C(8)-O(1)	105.9(3)
C(1)-C(9)-C(10)	104.3(4)	C(9)-C(10)-C(11)	108.5(4)
C(6)-C(11)-C(10)	107.0(4)	C(3)-O(2)-S	118.3(3)
O(2)-S-O(3)	103.6(2)	O(2)-S-O(4)	109.4(2)
O(3)-S-O(4)	120.2(2)	O(2)-S-C(12)	103.9(2)
O(3)-S-C(12)	109.3(2)	O(4)-S-C(12)	109.2(2)
S-C(12)-C(13)	119.9(3)	S-C(12)-C(17)	120.4(3)
C(13)-C(12)-C(17)	119.7(4)	C(12)-C(13)-C(14)	119.4(4)
C(13)-C(14)-C(15)	121.3(5)	C(14)-C(15)-C(16)	118.6(4)
C(14)-C(15)-C(18)	120.2(5)	C(16)-C(15)-C(18)	121.2(5)
C(15)-C(16)-C(17)	121.3(4)	C(12)-C(17)-C(16)	119.6(4)

anti-3-tosyl-8-oxatricyclo[4.3.3.0]undecane, [32].

^{1}H NMR: 1.91-1.40 (methylene envelope, 12H), 2.43 (s, 3H), 3.75-3.53 (m, 4H), 4.61 (m, 1H), 7.34-7.29 (d, 2H), 7.81-7.76 (d, 2H).

MS (EI): M+ = 164 (-TsOH), 146, 133, 119, 105, 91 (base), 79, 77.

MS (CI): MH+ = 337, 181, 165 (base), 147, 135, 117.

analysis - HRMS calculated for $C_{15}H_{20}SO_4$ = 336.4259; Found = 336.1469.

Mass spectral data on 2-methoxy-8-oxatricyclo[4.3.3.0]undecane, [34].

MS (EI): M+ = 164, 146, 135, 120, 109 (base), 105, 91, 79, 77, 67, 55, 41.

MS (CI): MH+ = 197, 165 (base), 147, 135, 121, 109.

analysis - HRMS calculated for $C_{12}H_{20}O_2$ = 196.2916; found = 196.1462.

Preparation of (cis)-1,6-dicarbomethoxy-3-methyl-8-oxabicyclo[4.3.0]non-3-ene, [37].

A solution of 100 ml of dry THF, 56.0 ml (2.5 equivalents) of 2.6 M n-BuLi and 18.8 ml (1.1 equivalent) of diisopropylamine was stirred under argon at -78° C for 15 minutes. Then 11.4 g (0.0538 moles) of cis-3-methyl-1,6-dicarbomethoxycyclohex-3-ene were added dropwise, creating a bright red solution. After the addition was complete, the solution was stirred for 15 minutes and warmed to -10° C and 6.00 ml (1.1 equivalent) of 1,3-dibromopropane were added dropwise. The reaction was then warmed to room temperature and stirred for 2.5 hours. After workup, a clear liquid resulted which was vacuum distilled to yield 6.24 g (46% yield) of the desired diester.

$BP_{0.5}$ = 108-110° C

IR: 2930, 1732, 1434, 1251, 1232, 1207, 1173 cm^{-1}.

^{1}H NMR: 2.52-1.50 (13H), 3.60 (s, 3H), 3.65 (s, 3H), 5.29 (bs, 1H).

MS (EI): 220 (-MeOH), 192, 161, 133 (base), 105, 91, 77, 59, 41.

Preparation of 3-methyl-8-oxatricyclo[4.3.3.0]undec-3-ene, [**35**].

The diester, [**37**], (5.10 g, 0.0202 moles) was added to 0.92 g (0.0243 moles) of LAH in 50 ml of dry THF. The reaction was stirred under argon overnight and then quenched with a small amount of wet ether. The lithium salts were suction filtered off and most of the solvent was removed at reduce pressure. The residue was extracted with dichloromethane which was dried and stripped yielding 3.37 g (0.0171 moles) of the clear diol. IR analysis confirmed the diol functionality.

The diol (3.37 g, 0.0171 moles) was combined with 50 ml of dry pyridine and heated to reflux under argon. Then 3.58 g (0.0188 moles) of TsCL dissolved in 30 ml of pyridine were added dropwise to the stirring solution. After workup, vacuum distillation afforded 2.10 g (0.0118 moles) of the desired propellane, having a camphor-like fragrance (67% yield).

$BP_{1.5}$ = 67-69° C

IR: 2952, 2927, 2863, 2836, 1446, 1084, 1061, 944 cm^{-1}.

^1H NMR: 1.78-1.40 (methylene envelope), 1.95 (bs, 3H), 3.56-3.43 (m, 4H), 5.47 (t, 1H).

MS (EI): M^+ = 178, 160, 147, 145, 133, 119, 105 (base), 91, 79, 67, 53, 41.

analysis - HRMS calculated for $C_{12}H_{18}O$ = 178.2767; found = 178.1355.

Hydrogenation of 3-methyl-8-oxatricyclo[4.3.3.o]undec-3-ene, [**35**].

100 mg of [**35**] were combined with 10 mg of 5% Pt/Al catalyst and 10 ml of absolute ethanol. The reaction vessel was shaken under 20 psi of H_2 at room temperature for 12 hours. The catalyst was then filtered off and peak integration by GC/MS indicated the reduced products were formed in a ratio of 3 : 1, respectively.

minor product

MS (EI): M+ = 180, 162, 149, 135 (base), 121, 107, 95, 93, 79, 67, 53, 41.

analysis - HRMS calculated for $C_{12}H_{20}O_1$ = 180.2926; found = 180.1524.

major product

MS (EI): M+ = 180, 149, 135 (base), 121, 107, 95, 93, 79, 67, 55, 41.

analysis - HRMS calculated for $C_{12}H_{20}O_1$ = 180.1524; found = 180.1507.

Preparation of (cis)-8-oxabicylo[4.3.0]non-2-ene, [13].

The mixture of tosylates derived from [1] (30 micro l) were repeatedly injected onto a preparatory GC (SE-30, 10' x 1/4 ", column temp. = 150 °C, injection port temp. = 250°C) and the olefins [1] and [13] in the relative ratio of 1 : 4 , respectively, were collected.

^{1}H NMR: 1.78-1.45 (2H, m), 2.05-1.95 (2H, m), 2.41-2.30 (1H, m) 2.73-2.60 (1H, m), 3.63- 3.40 (2H, m), 3.97-3.90 (2H, m), 5.68-5.58 (1H, m), 5.85-5.78 (1H, m).

MS (EI): M+ = 124, 94, 91, 79 (base), 77, 66, 41.

MS (CI): MH+ = 125 (base), 107.

analysis - HRMS calculated for $C_8H_{12}O_1$ = 124.1842; found = 124.0888.

Preparation of 8-oxatricylo[4.3.3.0]undec-2-ene, [33].

A mixture of the tosylates derived from [7] (30 micro l) were repeatedly injected onto a preparatory GC (SE-30, 10' x 1/4", column temp. = 175° C, injection port temp. = 250° C) and the olefins [7] and [33] in the relative area of 1 : 4, respectively, were collected.

^{1}H NMR: 2.00-1.45 (10H, m), 3.75-3.50 (4H, m), 5.70-5.61 (1H, dd), 5.85 (m, 1H).

MS (EI): M+ = 164, 146, 133, 119, 105, 91 (base), 77, 65, 41.

MS (CI): MH+ = 165, 147, 133, 119.

analysis - HRMS calculated for $C_{11}H_{16}O_1$ = 164.1197; found = 164.1208.

Preparation of phthalan, [40].

Phthalic anhydride, [39], (10.0 g, 0.066 moles) was dissolved in 50 ml of dry THF and added dropwise to a solution of 50 ml of THF and 2.81 g (0.074 moles) of LAH at 0° C. The reaction was warmed to room temperature and stirred for 12 hours. After the previously described workup, 7.25 g (0.044 moles) of the diol, as determined by IR, was isolated.

The diol was then dissolved in 50 ml of pyridine and heated to a gentle reflux under argon. Then 10.3 g (0.048 moles) of TsCl in 30 ml of pyridine were added dropwise to the stirring solution. After the previously described workup, 2.02 g (0.017 moles) of phthalan were isolated.

IR: 1696, 1684, 1675, 1489, 1455, 1372, 1219, 1088, 1043, 1015 cm^{-1}.

^1H NMR: 5.10 (bs, 4H), 7.25 (bs, 4H).

MS (EI): M+ = 120, 119, 91 (base), 77, 65, 63, 51.

Preparation of Δ-1,6-Δ-3,4-8-oxabicyclo[4.3.0]nondiene, [41].

To 200 ml of freshly distilled ammonia, 0.146 g (0.020 moles) of lithium were added in small chunks. Immediately the solution turned bright blue. Then 1.1 ml (0.010 moles) of phthalan in anhydrous ether were added dropwise. After addition the solution was allowed to stir for 20 minutes. Absolute ethanol was then added dropwise until the blue color dissipated. Then lithium (2 equivalents) was again added to the solution which regained its bright blue color. The solution was allowed to stir for an addition 20 minutes, at which time absolute ethanol was once again added dropwise to discharge the blue color. The resulting solution was poured over 50 g of crushed ice to which was added 200 ml of diethyl

ether. Most of the ammonia was allowed to evaporate, the solution was neutralized and then extracted with dichloromethane. The solvent was dried and removed at reduced pressure to yield 0.71 g.(5.82 moles) of the desired product (58% yield).

^{1}H NMR: 2.65 (s, 4H), 4.53 (s, 4H), 5.76 (s, 2H).

MS (EI): M+ = 122, 104, 93 (base), 91, 77, 65, 51, 41.

analysis - HRMS calculated for $C_8H_{10}O$ = 124.18424; found = 122.0729.

Preparation of Δ-1,6-8-oxabicyclo[4.3.0]nonene, [**15**].

A solution of 100 ml of absolute ethanol and 0.200 g of 10% Pd/C catalyst were saturated with H_2 gas. After saturation, the H_2 pressure was reduced to one atmosphere and 0.40 ml of the diene, [**41**], were syringed into the reaction vessel and the solution was stirred at room temperature for 15 minutes. The catalyst was filtered off and the solvent removed at reduced pressure to yield the reduced products [**12**] and [**15**] in a 5 : 1 ratio, respectively, as determined by preparative GC (13% DEGS, 10' x 1/4", T= 130° C).

^{1}H NMR: 1.66 (m, 4H), 1.94 (bs, 4H), 4.48 (bs, 4H).

MS (EI): M+ = 124, 95 (base), 93, 91, 81, 77, 67, 65, 55, 53, 41.

analysis - HRMS calculated for $C_8H_{12}O_1$ = 124.0889; found = 124.0889.

Preparation of (cis)-7,7,9,9-tetradeutero-8-oxabicyclo[4.3.0]non-3-ene, [**42**].

Phthalic anhyride (1.50 g, 9.86 moles) was dissolved in 10 ml of dry THF and added at 0° C to 0.66 g (15.8 moles) of LAD. The reaction was warmed to room temperature and stirred under argon overnight.

After the previously described workup, 0.68 g (4.66 moles) of the deuterium labeled diol were obtained (47% yield).

The diol was then dissolved in pyridine and the solution refluxed gently under argon. Then 1.46 g (7.66 moles) of TsCl dissolved in pyridine were added dropwise to the stirring solution. After addition was completed, the reaction was stirred at reflux overnight. After workup, 0.48 g (3.35 moles) of the desired product were isolated (78% yield).

IR: 3024, 2927, 2903, 2839, 1437, 1160, 1036, 818, 852 cm^{-1}.

^1H NMR: 2.16-2.05 (m, 2H), 2.55-2.30 (m, 4H), 5.80 (bs, 2H).

MS (EI): M+ = 128, 110, 109, 95, 79 (base), 72, 68, 54, 39, 27.

Preparation of (cis)-2,2,5,5-tetradeuterophthalic anhydride, [47].

Butadiene sulfone (20.0 g, 0.169 moles) was combined with 50 ml of deuterium oxide and a catalytic amount of metallic sodium. The solution was stirred under argon for 48 hours and then extracted with dichloromethane. The solvent was dried and stripped to yield 19.0 g (0.156 moles) of the desired product (92% yield). ^1H NMR indicated that substitution was achieved in high yield (> 95%).

The deuterium labeled butadiene sulfone (9.1 g, 0.075 moles) was dissolved in 8 ml of dry xylenes and 5.24 g (0.053 moles) of maleic anhyride. The reaction was refluxed at 200° C for 0.5 hrs and then allowed to cool to room temperature. 70 ml of benzene and 1 g of charcoal were added to the solution. The solution was heated to reflux for 10 minutes and then filtered to remove the charcoal. The filtered solution was slightly cooled and then hexane was slowly added until a persistent cloudy solution remained. After further cooling of the solution, 4.64 g of the desired product crystallized out of the solution.

MP = 98-102° C

^1H NMR: 3.88 (s, 2 H), 6.78 (s, 2H).

MS (EI): 128 (-CO), 83, 68, 53, 41.

Preparation of (cis)-2,2,5,5-tetradeutero-8-oxabicyclo[4.3.0]non-3-ene, [43].

The deuterium labeled phthalic anhydride (2.62 g, 0.0170 moles) was dissolved in 25 ml of THF and added dropwise to a solution of 0.66 g (0.0174 moles) of LAH in 20 ml of THF at 0° C. The reaction was warmed to room temperature and stirred under argon overnight. After workup, 2.18 g (0.0149 moles) of the desired product, as determined by IR, were isolated (88% yield).

The diol was then dissolved in 25 ml of pyridine to heated to a gentle reflux under argon. Then 3.13 g (0.0164 moles) of TsCl dissolved in 25 ml of pyridine were added dropwise to the stirring solution. The reaction was stirred at reflux overnight. After workup, 1.60 g (0.0125 moles) of the desired product were isolated (76% yield).

IR: 3024, 2968, 2925, 2857, 1058, 1056, 965, 923, 864, 807 cm^{-1}.

^{H} NMR: 2.32 (bs, 2H), 3.65 (dd, 2H), 3.89 (dd, 2H), 5.65 (s, 2H).

MS (EI): M+ = 128, 110, 109, 96, 93, 84, 82, 69 (base), 56, 41, 29.

Preparation of (cis)-2,2,5,5,7,7,9,9-octadeutero-8-oxabicyclo[4.3.0]non-3-ene, [44].

The deuterium labelled phthalic anhydride, [47], (2.02 g, 0.0129 moles) was dissolved in THF and added to a stirring solution of 0.77 g (0.0184 moles) of LAD in 20 ml of THF at 0° C. The reaction was warmed to room temperature and then stirred under argon at 0° C. After workup, 1.30 g, (8.55 moles) of the deuterium labelled diol, as determined by IR, were isolated (66% yield).

The diol was then dissolved in dry pyridine and heated to reflux under argon. Then 1.79 g (9.41 moles) of TsCl dissolved in pyridine were

added dropwise to the stirring solution. The reaction was stirred at reflux overnight. After workup, 0.67 g (5.10 moles) of the desired product were isolated (60% yield).

IR: 3023, 2926, 2192, 2088, 1778, 1304, 1208, 1183, 1143, 1119, 1096, 1083, 1067, 1059, 1036, 1000, 922 cm^{-1}.

^1H NMR: 2.30 (s, 2H), 5.62 (s, 2H).

MS (EI): M+ = 132, 112, 98, 95, 87, 83, 82, 80, 72 (base), 69, 58, 52, 44, 41, 29.

REFERENCES

1. S. Winstein and R. Buckles, J. Am. Chem. Soc., (1942), 64, 2780.

2. S. Winstein, C. Lindrean, H. Marshall, and L. Ingraham, J. AM. Chem. Soc., (1953), 75, 147.

3. S. Winstein, E. Allred, R. Heck, and R. Glick, Tetrahedron, (1958), 3, 1.

4. A. Streitwieser, Solvolytic Displacement Reactions, McGraw-Hill, New York, (1962).

5. B. Capon and S.P. McManus, Neighboring Group Participation, Vol. 1, Plenum Press, New York, (1976).

6. R.O. Hutchins and L. Rua, Jr. J. Org. Chem., (1975) 40, 2567.

7. T.A. Wnuk and P. Kovacic, J. Am. Chem. Soc., (1975), 97, 5807.

8. G. Grob, W. Kunz, and P.R. Marbet, Tetrahedron Lett., (1975), 2616.

9. R.F. Gratz and P. Wilder, Jr. Chem. Comm., 1449 (1970).

10. P.v.R. Schleyer and C.T. Lancelot, J. Am. Chem. Soc., (1969), 91, 4297.

11. G.T. Kwiatkowski, S.J. Kavarnos, and W.D. Closson, J. Heterocyl. Chem., (1965), 2, 11.

12. L.A. Paquette, I.R. Dunkin, J.P. Freeman, and P.C. Storm, J. Am. Chem. Soc., (1972), 95, 3067.

13. M. Ladika, B. Jursic, and D.E. Sunko, Tetrahedron, (1987), 43, 179.

14. D.S. Tarbell and J.R. Hagen, J. Am. Chem. Soc., (1969), 91, 765.

15. P.G. Gassman, J.G. Schaffhausen, and P.W. Reynolds, J. Am. Chem. Soc., (1982). 104, 6408.

16. R.D. Otzenberger, Pinacol-Tetrahydrophtalans-Frontalin, Ph.D. Thesis, Montana State University, 1971.

17. A.C. Cope and R.W. Gleason, J. Am. Chem. Soc., (1962), 84, 1928.

18. J.C. Hallageas and E. Casadevall, Comptes Rendus, Acad. Sci., (1969), 268C, 449.

19. D.W. Wilkening, A New Regiocontrolled and Stereospecific Total Synthesis of (dl) Modhephene, Ph.D. Thesis, Montana State University, (1984).

20. B.P. Mundy and D. Wilkening, J. Org. Chem., (1984), 49, 8779.

21. P.N. Rylander, Organic Synthesis with Noble Metal Catalysts, Academic Press, New York, (1978).

22. P.N. Rylander, Hydrogenation Techniques, Academic Press, New York, (1985).

23. J.J. Theodore, Heteroatom Influences on Structure and Reactivity, Ph.D. Thesis, Montana State University, (1978).

24. S.B. Glancy, Ethereal Oxygen Influences on Solvermercuration and Hydrogenation Reactions, Ph.D. Thesis, Montana State University, (1983).

25. S. Siegel, Adv, Catal., (1966), 16, 123.

26. H.W. Thompson and R.E. Naipawer, J. Am. Chem. Soc., (1973), 6379.

27. H.W. Thompson, E. McPherson, and B.L. Lences, J. Org. Chem., (1976), 41, 2903.

28. M.J. Gula and T.A. Spencer, J. Org. Chem., (1980), 45, 805.

29. D. Wilkening and B.P. Mundy, Tetrahedron Lett., (1984), 25, 4619.

30. B.P. Mundy, D. Wilkening, and K. Lipkowitz, J. Org. Chem., (1985), 50, 5727.

31. P.N. Rylander, Adv. Chem. Ser., (1971), 68, 150.

32. S. Siegel and B. Dmuchovsky, J. Am. Chem. Soc., (1962), 84, 3132.

33. M. Ando, A. Akahane, H. Yamaoka, and K. Takase, J. Org. Chem., (1982), 47, 3909.

34. R.L. Augustine, F. Yaghmaie, and Jan. F. Van Peppen, J. Org. Chem., (1984), 49, 1865.

35. R.E. Parker and N.S. Isaac, Chem. Rev., (1959), 59, 737.

36. S. Winstein and R.B. Henderson, Heterocyclic Compounds, Vol. 1, Wiley, New York, (1950).

37. J. Sanders and J.D. Mersh, Prog. Nucl. Magn. Reson. Spec., (1983), 15, 353.

38. W.L. Waters and E.F. Kiefer, J. Am. Chem. Soc., (1967), 89, 6261.

39. S.D. Kahn, C.F. Pau, A.R. Chamberlain and W.J. Hehre, J. Am. Chem. Soc., (1987), 109, 650.

40. N.L. Allinger, M.T. Tribble, M.A. Miller, and D.H. Wertz, J. Am. Chem. Soc., (1971), 93, 1637.

41. D.B. Boyd and K.B. Lipkowitz, J. Chem. Ed., (1982), 59, 269.

42. M.J.S. Dewar and W. Thiel, J. Am. Chem. Soc., 99, 1400.

43. W. Davidon, Comput. J., (1968), 10, 406; R. Fletcher, ibid., (1963), 6, 163.

44. M.J.S. Dewar and W. Thiel, J. Am. Chem. Soc., (1977), 99, 4907.

45. S.D. Kahn, C.F. Pau, L.E. Overman, and W.J. Hehre, J. Am. Chem. Soc., (1986), 108, 7381.

46. S.D. Kahn and W.J. Hehre, ibid., (1987), 109, 663; ibid., 666.

47. K.N. Houk, Pure Appl. Chem., (1983), 55, 145.

48. K.N. Houk and N.G. Roddon, Tetrahedron, (1984), 40, 2257.

49. I. Fleming, Frontier Orbital and Organic Chemical Reactions, Wiley, New York, (1975).

50. R.G. Pearson, Hard Soft Acid and Bases, (1973), Dowden, Hutchinson and Ross, Stroudberg PA.

51. T.L. Ho, Hard and Soft Acid and Base Principle in Organic Chemistry, (1977), Academic Press, New York.

52. N.W. Hoffman, Ber. Dtsch. Chem. Ges., (1872), 5, 704.

53. T.W. Bentley and P. von R. Schleger, Adv. in Phys. Org. Chem., (1977), 14, pg. 39.

54. Montana Interface (Huffman Building, Advance Technology Park, Montana State University, Bozeman, MT 59717) has prepared a unique electronic interface that allows the computer to act as one of a number of measuring devices.

55. J. Norlander and T.J. McGrary, J. Am. Chem. Soc., (1972), 94, 5133.

56. J.B. Lambert, G.J. Putz, and C.E. Mixan, (1972), J. Am. Chem. Soc., 94, 5132.

57. J.B. Lambert and G.J. Putz, J. Am. Chem. Soc., (1973), 95, 6313.

58. J.M. Harris Prog. in Phys. Org. Chem., (1974), 11, 89.

59. T.H. Lowery and K.S. Richardson, Mechanisms and Theory in Organic Chemistry, Second Addition, Harper and Row, New York, (1981) pg 374.

60. I. Horiuti and M. Polanyi, Trans. Faraday Soc., (1934), 30, 1164.

61. W.F. Maier and P.v.R. Schleyer, J. Am. Chem. Soc., (1981), 103, 1891.

62. A.B. McEwen and P.v.R. Schleyer, ibid., 108, 3951.

63. Z.H. Li and M. Jones, Tetrahedron Lett., (1987), 28, 753.

64. Y. Tobe, T. Kishimura, T. Kakuichi, Y. Odaira, J. Org. Chem.

65. Y. Odaira, Y. Sakai, Y. Tobe, Tetrahedron Lett., 91982), 23, 537.

66. A. Akhorema and Y. Titov, Total Steroid Synthesis, Plenum, New York, (1970).

67. L. Fieser and M. Fiester, Steroids, New York, (1959).

68. P. Warner, Tetrahedron Lett., (1983), 24, 4169.

MONTANA STATE UNIVERSITY LIBRARIES
3 1762 10051943 6

AMERICAN BINDERY
TOPEKA KANSAS